CANADIAN THESES

THÈSES CANADIENNES

NOTICE

The quality of this microfiche is heavily dependent upon the quality of the original thesis submitted for microfilming. Every effort has been made to ensure the highest quality of reproduction possible.

If pages are missing, contact the university which granted the degree.

Some pages may have indistinct print especially if the original pages were typed with a poor typewriter ribbon or if the university sent us an inferior photocopy.

Previously copyrighted materials (journal articles, published tests, etc.) are not filmed.

Reproduction in full or in part of this film is governed by the Canadian Copyright Act, R.S.C. 1970, c. C-30.

AVIS

La qualité de cette microfiche dépend grandement de la qualité de la thèse soumise au microfilmage. Nous avons tout fait pour assurer une qualité supérieure de reproduction.

S'il manque des pages, veuillez communiquer avec l'université qui a conféré le grade.

La qualité d'impression de certaines pages peut laisser à désirer, surtout si les pages originales ont été dactylographiées à l'aide d'un ruban usé ou si l'université nous a fait parvenir une photocopie de qualité inférieure.

Les documents qui font déjà l'objet d'un droit d'auteur (articles de revue, examens publiés, etc.) ne sont pas microfilmés.

La reproduction, même partielle, de ce microfilm est soumise à la Loi canadienne sur le droit d'auteur, SRC 1970, c. C-30.

THIS DISSERTATION HAS BEEN MICROFILMED EXACTLY AS RECEIVED

LA THÈSE A ÉTÉ MICROFILMÉE TELLE QUE NOUS L'AVONS REÇUE

A Feasibility Study on an Electronically Controlled Hydrogen Gas Injector

Theodore Giannacopoulos

A Thesis

in

The Department

of

Mechanical Engineering

Presented in Partial Fulfillment of the Requirements
for the Degree of Master of Engineering at
Concordia University
Montréal, Québec, Canada

March 1986

ISBN 0-315-30653-X

ABSTRACT

A Feasibility Study on an Electronically Controlled Hydrogen Gas Injector

Theodore Giannacopoulos

A new electronically controlled gas injection system was developed in order to investigate the feasibility of high pressure hydrogen gas injection in a high speed diesel engine. The injector prototype had a variable area orifice and it was actuated with a solenoid under microprocessor management. The system was able to operate with power supplied directly from a 12 V car battery without any amplification. Its maximum operating frequency corresponded to 2000 RPM of a four stroke diesel engine and the gas supply pressure was 20 MPa. A mathematical model was developed to simulate the hydrogen gas injection process which could be used to optimize the gas flow rate characteristic. The prototype system was first tested on an experimental set-up where the pressure in the injector, the needle lift and the gas dose were measured. Moreover, an attempt was made to measure the gas discharge flowrate by recording the amplitude of a pressure wave created in a special long pipe. Finally, ignition feasibility tests were performed in a high speed

diesel engine supported by spark ignition. The results indicated that such a gas injection system with electronic control is feasible and it is recommended for further development. Two improved injector designs were suggested which incorporate recently invented compact and powerful solenoids. In addition, these designs might reduce the gas leakage and needle seizure hazards. Other suggestions included improvements in the electronic control circuit and in the ignition of hydrogen in the diesel engine.

ACKNOWLEDGEMENTS

The author wishes to express his gratitude to his supervisor Dr. T. Krepec for his constant encouragement and advice throughout the course of this study.

Thanks are directed to the technical staff of this University for the construction of the experimental devices and in particular to the electronics technician Mr. P. Favreau for his technical assistance in the design of the switching circuit. The author is also thankful to Dr. R.M.H. Cheng for the use of the microprocessor as well as to all his professors and colleagues in the Department of Mechanical Engineering for their valuable discussions and suggestions. Special thanks are also directed to his friends A. Georgantas, S. Athitakis and C.H. To as well as to his sister in law A. Papathanasopoulos for their help during the final stages of preparation of this manuscript.

Furthermore, the author wishes to express his gratitude to his family members for their support, encouragement and understanding. He is particularly indepted to his wife Bessy, for the great number of hours she spent for typing, proofreading and generally for helping in the preparation of the final version of this thesis.

Finally, the author is very thankful to the "Fonds pour la Formation et l''Aide a la Recherche" (Bourses d' Etudes et de Recherche dans le Domaine des Transports) and to the Natural Sciences and Engineering Council of Canada, for their financial support without which the present work would not have been possible.

TABLE OF CONTENTS

CHAPTER 5

COMPUTER SIMULATION OF THE GAS INJECTION SYSTEM

CHAPTER 6

HYDROGEN INJECTION IN A DIESEL ENGINE

CHAPTER 7

RECOMMENDATIONS FOR FUTURE WORK

CHAPTER 8

SUMMARY

LIST OF FIGURES

LIST OF PLATES

NOMENCLATURE

a_c -acceleration of the needle during closing period, m/s^2.

A_e -effective critical flow area of nozzle, m^2.

A_n -geometric critical nozzle flow area, m^2.

a_o -acceleration of the needle during opening period, m/s^2.

A_p -cross sectional area of pipe, m^2.

A_{pr} -area under the pressure curve, Pa.s.

A_{12} -flow area at metering or control valve, m^2.

A_{23} -flow area at needle seat of injector, m^2.

A_{34} -flow area between pintle and nozzle-hole of injector, m^2.

C_d -coefficient of discharge.

C_m -mass flow coefficient, $(s\sqrt{K/m})$.

c -speed of sound, m/s.

D_f -damping coefficient, N.s/m.

D_H -nozzle hole diameter, m.

d_i -needle core diameter, m.

d_p -needle pintle diameter, m.

d_{si} -needle seat diameter at inlet, m.

FA_{actual} -actual fuel/air ratio.

F_d -damping force, N.

F_e -solenoid force, N.

F_{eff} -effective force, N.

F_g -gas force acting on needle seat, N.

F_h -force acting along the needle axis, N.

f_i -cross sectional area of needle corresponding to d_i, m^2.

F_p -gas force acting on needle differential area, N.

f_{po} -cross sectional area of pintle, m^2.

F_{ps} -spring preload, N.

F_r -friction force, N.

F_s -spring force, N.

f_{so} -cross sectional area of needle corresponding to d_{so}, m^2.

FA_{stoich} -stoichiometric fuel/air ratio.

h -actual needle lift, m.

H_2 -hydrogen (chemical formula).

K_s -spring constant, N/m.

L -needle length, m.

m_a -mass of air, kg.

m_e -armature mass, kg.

m_f -mass of fuel, kg.

$\dot{m}_l$ -mass flow rate of hydrogen leakage, kg/s.

m_n -needle mass, kg.

m_s -spring mass, kg.

m_t -total moving mass, kg.

$\dot{m}_{12}$, $\dot{m}_{23}$, $\dot{m}_{34}$ -mass flow rate through A_{12}, A_{23}, A_{34} respectively, kg/s.

m_2, m_3 -mass of gas in volumes V_2 and V_3 respectively, kg.

N -engine speed, RPM.

N_2 -nitrogen (chemical formula).

O_2 -oxygen (chemical formula).

P -pressure, Pa.

P_c -critical pressure at the throat of nozzle, Pa.

P_d -pressure in engine cylinder at the time of injection- (downstream or back pressure).

P_e -atmospheric pressure, Pa.

P_f -forward propagating pressure wave, Pa.

$P_{f\ avg}$ -mean pressure wave, Pa.

P_u -upstream pressure of gas supplied, Pa.

P_1 -supply gas pressure ($P_1=P_u$), Pa.

P_2 -pressure in chamber between metering or control valve, Pa.

P_3 -pressure in chamber between needle seat and pintle, Pa.

P_4 -back pressure corresponding to engine cylinder pressure, Pa.

$\dot{Q}_l$ -volumetric flow rate of hydrogen leakage, m^3/s.

R -gas constant, J/kg.K.

S -effective pintle length, m.

T -gas temperature, K.

t -time, s.

t_c -valve closing time, s.

t_o -valve opening time, s.

T_u -upstream temperature of gas supplied, K.

T_1, T_2, T_3 -gas temperature corresponding to P_1, P_2, P_3, K.

U -needle velocity, m/s.

u -velocity of fluid, m/s.

u_f -gas flow velocity in the long pipe, m/s.

u_{23}, u_{34} -velocity of gas flowing through A_{23}, A_{34}, m/s.

V -volume, m^3.

GREEK SYMBOLS

α	-valve angle (90 -θ) , degrees.
β	-angle of pintle tip, degrees.
γ	-ratio of specific heats, C_p/C_u.
δ	-gap between needle and needle holder, m.
θ	-angle of needle seat with respect to needle axis, degrees.
μ	-viscosity of gas, N.s.
ρ	-density of gas, kg/m^3.
ρ_{23}, ρ_{34}	-gas density corresponding to A_{23}, A_{34}, kg/m^3.
τ_{yx}	-shear stress applied on yx plane, Pa.
ϕ	-equivalence ratio.
ψ	-crank shaft angle, degrees.

CHAPTER 1

INTRODUCTION

1.1 GENERAL

Despite all controversies as to how much crude oil is left on our planet, all scientists agree that crude oil deposits are limited and according to the most optimistic estimates, the beginning of their exhaustion will come approximately in the year 2040 [1]. This fact has forced engineers and scientists to search for other sources of energy for automotive use with four main objectives:

1. To be easily stored in automotive fuel tanks
2. To have high energy density
3. To provide engine-fuel compatibility
4. To be safe

A large number of alternative nonpetroleum fuels in either liquid or gaseous form is being considered with increasing interest [2]. Some alternative fuels such as hydrogen, natural gas, propane and some alcohols have already been used in internal combustion engines, especially with spark ignition, to power commercial vehicles. Figure 1.1 shows how the energy densities of several candidate fuels compare with the energy density of gasoline [3]. As it can be seen from this figure, the most promissing alternative fuels are propane, methane

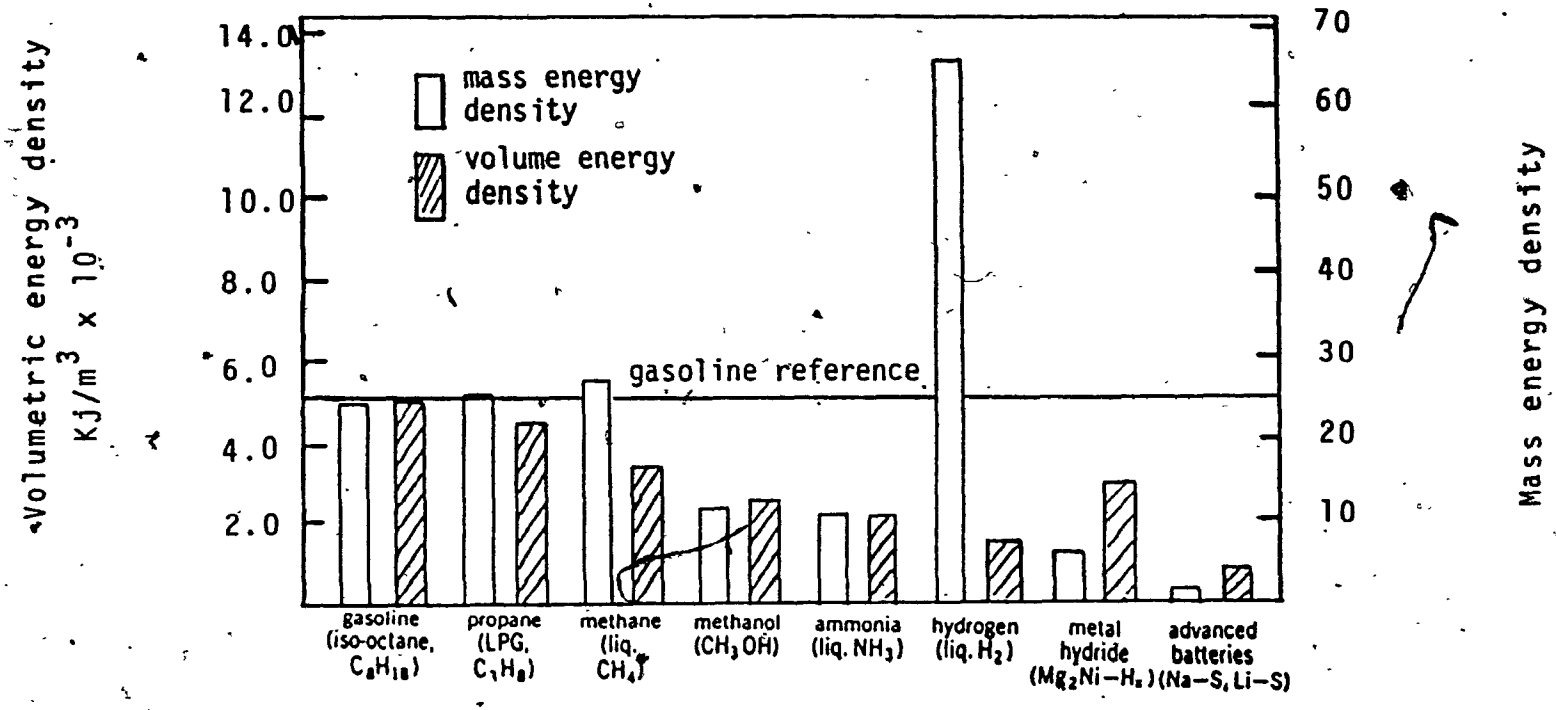

Fig. 1.1 Energy densities of some candidate alternative fuels as compared to gasoline (3)

and hydrogen. However, although propane and methane fulfill the conditions which have been set above, they lack a very important factor: they are limited in quantities. Thus, the energy problem might be solved only for a short period of time. However, the hydrogen fuel not only meets the above objectives, but it also has some unique advantages as compared to the fuels which are mentioned above. It is available in vast quantities, since its main source is water, it is recyclable, the only pollutant to the environment may be limited NO_x emissions, and it has the potential to be used with high efficiency in almost every suggested application. In addition, it may be produced by using any energy source such as solar, nuclear, hydro, geothermic, etc.

Hydrogen, as automotive fuel has already been used for spark ignition engines in some applications and is also presently utilized for rocket propulsion [4]. Recently, hydrogen became the subject of broad investigation concerning applications on different types of combustion engines utilizing Otto, Diesel, Brayton, Stirling and other combined thermodynamic cycles. During the latest years, due to the progress which has been made in the development of hydrogen fuel systems, some new possibilities have emerged regarding hydrogen storage in vehicles and its supply to the engine. The competition between metal hydrides storage and liquid hydrogen tank (cryogenic) storage seems to have been won by the well

insulated low temperature liquid hydrogen (LH_2) tanks, due to the use of vacuum insulation and to the special insulating materials, like rigidly closed cell foam. Even with insulation weight penalty, the LH_2 tanks are much lighter than the hydrides with equivalent storage capacity [5,6].

The combustion of hydrogen in internal combustion engines presents several problems which have not been solved completely yet. Misfire, knock, flashback and pre-ignition mainly occuring in spark ignition engines, are some of these problems. Methods to avoid undesirable combustion phenomena include exhaust gas recirculation, water injection, elimination of hot spots in the engine cylinder and cooling of the intake charge. Therefore, as suggested by some researchers, the best way to avoid these problems is by direct hydrogen injection into the combustion chamber of a diesel engine [7,8]. In addition, it is well known that compression ignition engines offer higher fuel economy than spark ignition engines due to their higher compression ratio. Unfortunately, direct hydrogen injection presents a number of other problems which must be overcome. The most serious of these problems are related to the required high injection pressure, rapid mixing of hydrogen with air, long ignition delay period and hydrogen leakage. Therefore, a new approach is needed for the design of hydrogen-gas injectors based on gas

dynamics theory and intensive research work has to be done in the area of fuel control systems in order to allow further development of efficient hydrogen fuelled engines, particularly those working on the compression ignition cycle.

Modern microprocessor technology allows the development of efficient gas injection systems with electronic control. Applied already in conventional engines [9,10,11,12], it offers outstanding opportunities for efficient control of the fuel supply system in the hydrogen fuelled diesel engines, as will be discussed in this thesis.

1.2 SCOPE OF THE THESIS

Although attempts to use hydrogen in internal combustion engines are dated as early as 1920's [13,14], intensive feasibility studies are being carried out only during the last decade when it became apparent that the best option which seems to solve the problems of pollution and renewable energy sources is hydrogen [15,16,17,18].

The scope of this study is to investigate the possibility of hydrogen gas injection in compression ignition engines with microprocessor control. A hydrogen fuel injection system with electronic control has been proposed by Krepec [19]. In his proposal, he suggests a hydrogen gas injector, equipped with a solenoid actuator which is under microprocessor management. This technology affects radically the design of the fuel supply components and one has to assume that the new generation of hydrogen fuelled engines must be equipped with advanced fuel control systems. To provide sufficient hydrogen gas flow rate to the engine, high pressure should be maintained in order to assure chocked flow conditions through the metering valve (injector) at all times without effect on fuel delivery from back pressure (cylinder pressure) variations. The pressure and temperature of hydrogen gas should be sensed and

monitored by the computing unit. Based on these data, as well as on other engine information, the on-board microcomputer will adjust the opening of the metering valve, in order to provide the engine with the required gas supply.

For the feasibility study of this project, a prototype hydrogen injection system will be built and the problems associated with its design will be discussed. A mathematical model will also be developed in order to simulate the dynamic response of this system. Next, the feasibility of gas injection will be tested on a diesel engine. Finally, a new injector design will be proposed on the basis of the experience acquired from this work.

1.3 PRESENTATION OF THESIS

The presentation of this study has been divided in six chapters. Chapter 2 presents a brief historical background on the development of fuel injectors. Then the research related to the hydrogen fuel supply systems is discussed in the next three chapters. Thus, in chapter 3 the design of the prototype hydrogen gas injector is discussed. Following that, the results of the experimental work are presented and discussed in chapter 4. Chapter 5 deals with the development of the mathematical model, with the problems associated with the solution of the differential equations and with the comparison between predicted and experimental results. In chapter 6, the difficulties associated with the hydrogen injection in a diesel engine are discussed. Finally, suggestions for future improvements on the gas injection system, along with a proposed hydrogen gas injector, are given in chapter 7.

CHAPTER 2

LITERATURE REVIEW

2.1 FUEL INJECTION SYSTEMS FOR INTERNAL COMBUSTION ENGINES

A fuel injection system is designed to inject the required quantity of fuel at a predetermined rate and at a specified time into the combustion chamber of an engine. In addition, the system must atomize the fuel (if it is in liquid form) and distribute it throughout the combustion chamber. Consequently, the performance of engines equipped with fuel injection depends, to a large extent, upon the quality of the fuel injection system [20].

The idea of fuel-gas injection is not new. It was first attempted one hundred years ago by Rudolph Diesel under the name of air injection and remained in use until about 1930 [21]. Then, the liquid fuel injection systems were used, almost exclusively, in all diesel engines because these systems offered better fuel delivery control, better injection efficiency and lower cost. The fact that the conventional fuels, such as diesel-oil and gasoline, were available in liquid form became another important factor for the development of liquid fuel injection systems only. Burman [21] gives a very good description with illustrations of the most significant patents granted to various inventors until 1960. According to Burman, most types of injectors such as

poppet, pintle and hole types were invented around 1900. Later, they simply underwent modifications to provide the engines with better efficiency and fuel metering. An extensive survey on liquid injection systems is beyond the scope of this work. However, literature on early developments of these systems, as well as description of the various injector nozzles may be obtained from source books such as Lichty[20], Judge[22], Polson[23] and Taylor[24]. Particularly, Taylor cites about one hundred publications related to developments on fuel injection in both diesel and gasoline engines which cover the period from 1930 to 1965. Literature on early developments in fuel injection may also be found in the Proceedings of the Institute of Mechanical Engineers (I. Mech. E.) and in NACA reports. Research on fuel injection systems after 1965 can be mainly found in the transactions and proceedings of the Society of Automotive Engineers (SAE).

Until mid-sixties gasoline engines were used mainly for light carriers (passenger cars, airplanes) where diesel engines were used for heavy equipment such as heavy trucks, ships, locomotives, off-highway vehicles, etc. According to the existing literature, the fuel injection systems were developed mainly for diesel engines and popular carburators were used exclusively in spark ignition engines. However, during the last twenty five years this philosophy has changed, mainly due to increasingly stringent laws concerning exhaust emissions

control and to the demand for better fuel economy [25,26]. Then the superiority of both, the diesel engines and the fuel injection systems over the gasoline engines and carburators respectively, became more apparent [27,28,29]. As a result, intensive research conducted all over the world, especially during the last decade, led to the development of precise fuel injectors and sophisticated fuel control systems for both diesel and gasoline engines [30]. Some of the latest developments include concepts for electronic fuel management [11,12,31,32] and solenoid actuated injectors [9,33,34,35]. In addition, the expansion of electronic control of fuel injectors resulted in the development of extremely fast acting solenoid actuators and highly accurate sensing elements [36,37,38,39,40].

Some of the concepts of electronic fuel management as well as solenoid actuators and sensing elements can also be applied in fuel gas injection systems. Such gas injection systems are being developed during the last five years mainly for hydrogen fuelled engines. These developments will be discussed, in more detail, in the next section.

2.2 HYDROGEN USE IN INTERNAL COMBUSTION ENGINES

Current research on the potential use of hydrogen as fuel involves three major areas: production, storage and application in automotive propulsion. In this section, the work of other researchers on the application of hydrogen as fuel in automotive propulsion will be reviewed, as well as the problems associated with it. Then, the new possibilities of applications for hydrogen will be considered with the employment of electronic control.

2.2.1 Hydrogen Supply Systems.

The hydrogen supply system greatly depends on the storage form of hydrogen and on the type of application. Several supply systems have been investigated. In general, the combustible mixture formation is divided in two categories [41].

1. External mixture formation in the intake manifold,
2. Internal mixture formation in the combustion chamber.

These two types of mixture formation in combination with the liquid hydrogen (cryogenic) or metal-gas (hydride) storage forms offer four alternative systems of fuel supply.

i) LH_2 cryogenic storage unit + high pressure hydrogen injection.

ii) Ti-Fe hydrogen storage unit + high pressure hydrogen injection.

iii) LH_2 cryogenic storage unit + external mixture formation

iv) Ti-Fe/Mg(Ni) hydride unit + external mixture formation.

The feasibility of metal hydrides for on-board installation in automobiles is currently under extensive investigation [42,43,44,45]. However, the systems consisting of LH_2 cryogenic storage tanks with high pressure gas injection seem to be the most promissing fuel supply systems for hydrogen fuelled vehicles. Such a system has been already employed by some researchers during the last decade with quite satisfactory results in engine operation [46,47,48,49].

2.2.2 Problems Related to Hydrogen Combustion in I.C. Engines.

The combustion of hydrogen in internal combustion engines presents several problems which have not been

solved completely yet. Misfire, knock, flashback, and pre-ignition are some of these problems especially occuring in spark ignition engines. A very good review of previous work on hydrogen-fuelled internal combustion engines is given by deBoer [50] covering the period from 1923 (Ricardo's first hydrogen engine) until 1976. In his review deBoer puts special emphasis on undesirable combustion and on remedies that can be taken to avoid it. Such remedies for undesirable combustion include mainly exhaust gas recirculation, water injection, elimination of hot spots in the engine cylinder, cooling of the intake charge, restriction for maintaining low fuel/air ratio and direct cylinder injection.

The potential effectiveness of the direct injection method for hydrogen fuelled engines has already been suggested by Erren and Campbell more than fifty years ago [4]. Lately, analytical and experimental studies concluded that pure compression ignition of hydrogen-air mixtures is hard to achieve [51,52,53,54]. Despite these difficulties, however, direct hydrogen injection is gaining popularity because it offers several unique advantages, as compared to other methods, like better volumetric efficiency, higher power output, higher thermal efficiency and reduction of NO_x emissions. Homan [8] has suggested a scheme called LIRIAM (Late Injection, Rapid Ignition and Mixing) as a method to avoid undesirable combustion and to reduce NO_x emissions.

Peschka [7] has also recommended direct hydrogen injection as a better method to eliminate backfire, flashback, need for water injection etc., provided that a LH_2 storage tank and a high pressure LH_2 pump would be developed. Among all researchers working on hydrogen engine, the most successful seems to be Furuhama and his team who have succeeded in developing a complete hydrogen supply system with cryogenic LH_2 tank and direct hydrogen injection for two engines, one two-stroke and one four-stroke [46,48,49]. Moreover, Furuhama has developed a special high pressure LH_2 pump and a special glow plug to support the hydrogen ignition [47].

2.2.3 Proposed Hydrogen Supply System

In the literature reviewed, it was noted that all the hydrogen-gas injectors were actuated either mechanically, by using a cam mechanism, or hydraulically, by using a conventional high pressure diesel injection pump and piston actuators. A new concept on fuel control systems for hydrogen fuelled automotive combustion engines was suggested by Krepec [19]. This concept assumes application of modern electronic control on hydrogen injection systems. Specifically, Krepec proposes the use of a microprocessor controller utilizing analog actuators (solenoids) and digital actuators (stepper motors) for three types of internal combustion engines: gas turbine engines, spark ignition engines and

compression ignition engines. The hydrogen supply system for all these types would consist of a cryogenic storage tank, a liquid hydrogen high pressure pump, a hydrogen preheating system and a metering system. The microprocessor will adjust the opening of the injector to provide the engine with the required amount of fuel according to the engine operating parameters (temperature, pressure, torque, etc.).

Based on this concept, a new electronically controlled gas injection system was developed by Tebelis [55] which was able to operate conventional solenoid actuators with power supplied directly from a 12 V car battery without any amplification. In addition, the system was able to operate with a frequency corresponding to 2000 RPM of a four stroke diesel engine and at a gas supply pressure of 20 MPa. Finally, further developments on electronically controlled hydrogen injection systems are discussed by Giannacopoulos[56] and Krepec[57].

Although this review may not be complete, it is representative of all the research performed in the field of hydrogen utilization for automotive applications.

CHAPTER 3

NEW HYDROGEN GAS INJECTION SYSTEM WITH ELECTRONIC CONTROL

3.1 INTRODUCTION

A hydrogen gas injection system cannot be operated in the same way as conventional liquid fuel systems, due to the compressibility of the combustible. The bulk modulus of elasticity, E, for liquids is very high (in the order of 10^3 MPa), whereas for gases it is much lower and depends directly on the pressure. For example, the bulk modulus of elasticity of a perfect gas can be expressed by the formula $E = nP$, where n is the polytropic exponent and depends on the compression process. Hence, if the supply pressure is 20 MPa (pressure used in the proposed system) and the process is isothermal ($n = 1$), then $E = 20$ MPa for all perfect gases. This represents a value which is almost two orders of magnitude smaller than the bulk modulus of liquid fuels. Hence, the use of an injection system similar to that for a conventional diesel engines is rendered impractical.

Based on this fact, it is clear that the needle of a gas injector must be lifted by an external force rather than by the gas pressure which might contribute only partly to the injector opening process depending on the needle geometry.

The proposed hydrogen-gas injection system consists of an electrical and a mechanical part. The

role of the first is to control the latter. The electrical part consists of the electronic control unit, the switching circuit and the solenoid actuators, whereas the mechanical part consists of all moving parts of the injection system. The overall performance of the present fuel-gas injection system depends on the particular performances of both the electrical and the mechanical components. In this chapter, three hydrogen-gas injection concepts will be described. Then, the design of both the electrical and the mechanical part will be discussed.

3.2 HYDROGEN GAS INJECTION CONCEPT

The concept of this fuel-gas injection system for hydrogen fuelled automotive engines assumes microprocessor control in connection with solenoid actuated injectors for direct gas injection in a diesel engine. The full supply system consists of a cryogenic liquid hydrogen storage tank, a high pressure pump to bring the liquid hydrogen to high pressure level, a hydrogen preheating system to change it into a gaseous phase and a metering system (Fig. 3.1). The microprocessor controls the fuel metering system by adjusting the opening time of the injector in order to supply the engine with the required amount of fuel according to the engine operating parameters (temperature, pressure, torque, etc.), as shown in figure 3.2.

The adaptation of compression ignition engines to the hydrogen fuel supply creates several problems due to three major factors:

1. It requires a special high pressure pump to deliver LH_2 at the extremely low temperature of approximately 20 K.

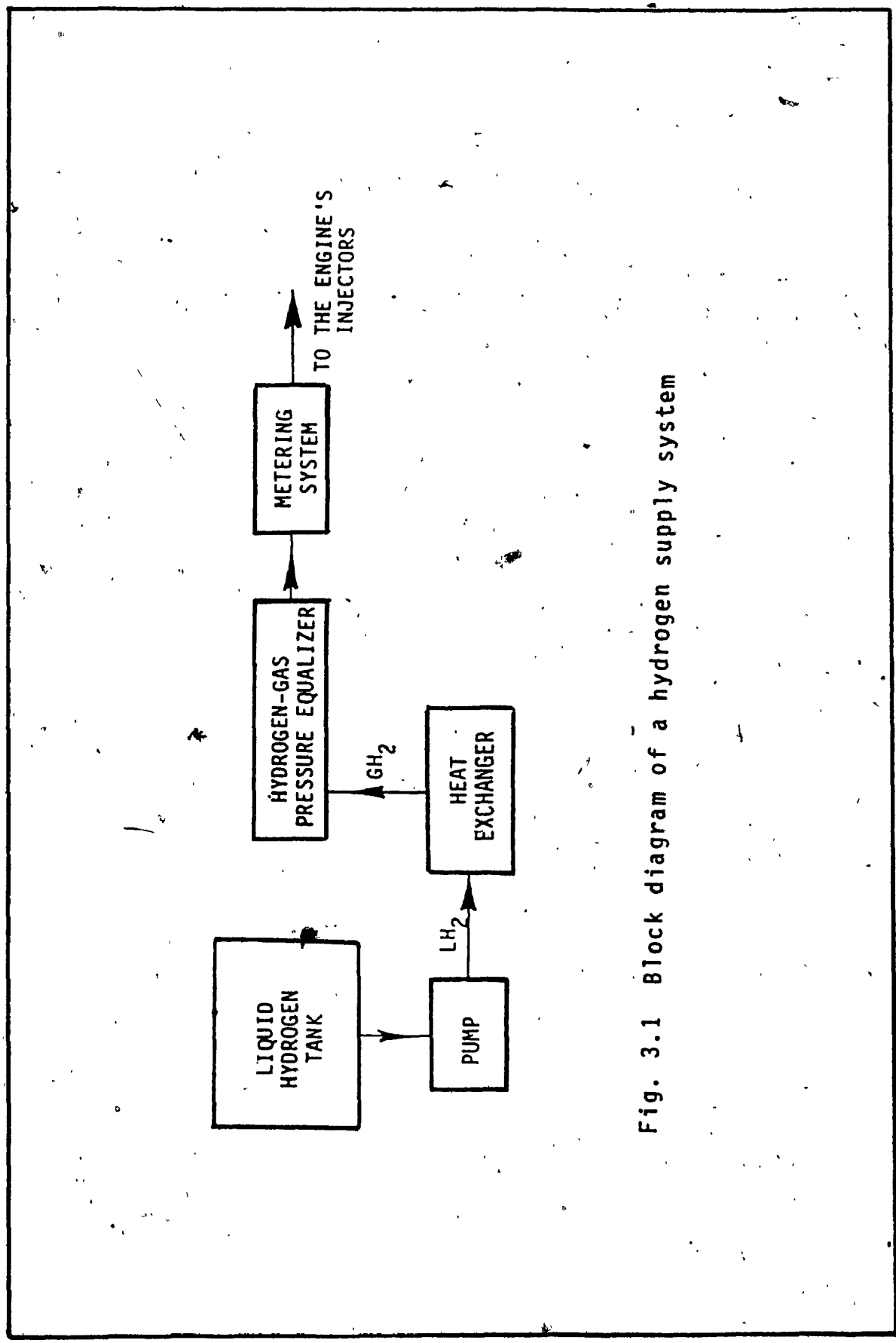

Fig. 3.1 Block diagram of a hydrogen supply system

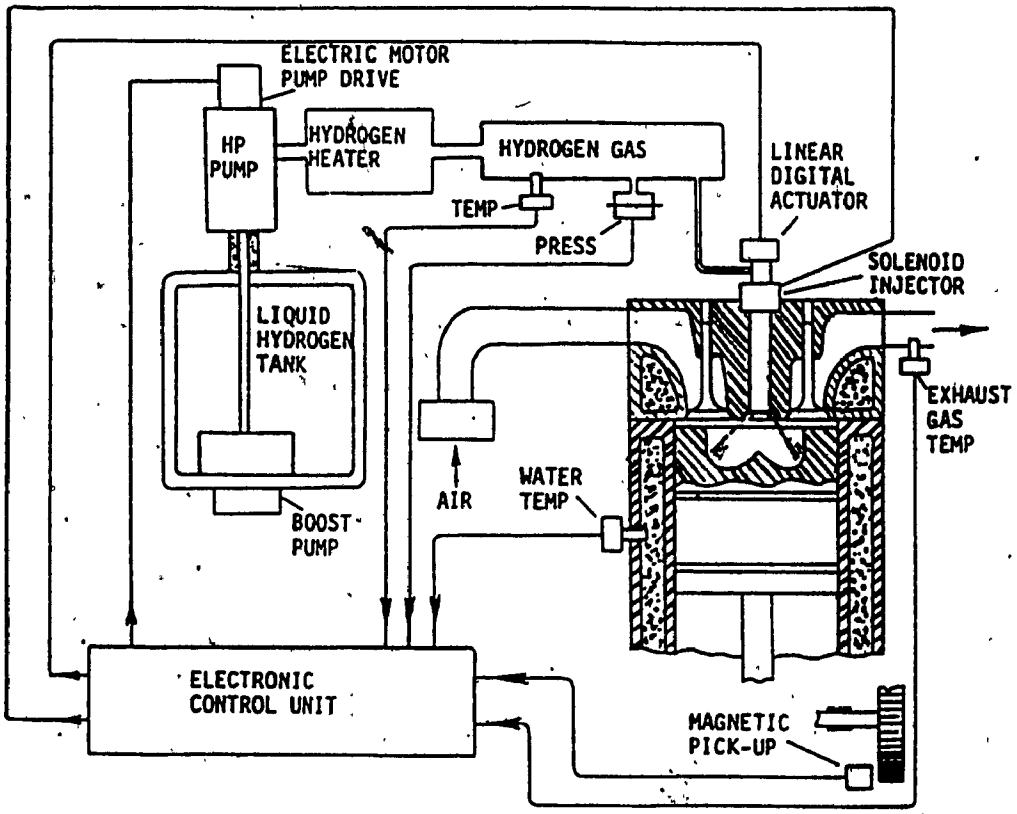

Fig. 3.2 Schematic of proposed hydrogen injection system for a diesel engine

2. It requires to overcome the difficulties with precise timing of the injector's opening and closing.

3. It requires to provide reliable ignition of hydrogen inside the combustion chamber.

The aforementioned difficulties could be overcome if accurate solenoid operated injectors are developed, in order to be integrated with a system required to control the timing and the exact amount of hydrogen which must be injected into the cylinder of a diesel engine. To provide the required hydrogen flow rate to the engine, high pressure is maintained in the supply system in order to assure sonic flow conditions through the metering system. Therefore, the back pressure variations do not affect the fuel delivery. The pressure and the temperature of hydrogen are sensed and monitored by the computing unit. Based on these data, the on-board computer can calculate the hydrogen gas mass flow rate in order to adjust the opening time of the metering valve (injector) and to provide the engine with the required fuel supply. This system is somehow similar to the speed density concept applied a long time ago for the computation of air mass flow in supercharged aircraft engines [21] and revived recently in the throttle body fuel systems for spark ignition engines [31].

To fullfil the metering requirements for the diesel engine operation, the hydrogen-gas injection concept proposes three optional configurations of an electronic injection system which differ in the required flexibility of control, size, cost, etc. In all three versions, a modified pintle nozzle type injector, similar to one used for a conventional diesel engine, is being used (Fig. 3.3).

The operating principle of each configuration of the injection system will be described separately.

3.2.1 Injector Only System (I.O.S.).

This system, shown schematically in figure 3.4, is assumed to operate with constant supply pressure. The injector's needle is lifted by a solenoid actuator and is closed by a spring. Such a system is not very complicated and requires a quite simple interface circuit and software for its operation. However, it needs a powerful solenoid in order to overcome the force of the spring. This creates some problems with proper injection timing because solenoids tend to have longer response time as the power requirements increase.

3.2.2 Metering Valve-Injector System (M.I.S.).

This injector operates in a similar manner as the I.O.S., but it is equipped with a metering valve, as shown in figure 3.5. The metering valve provides a

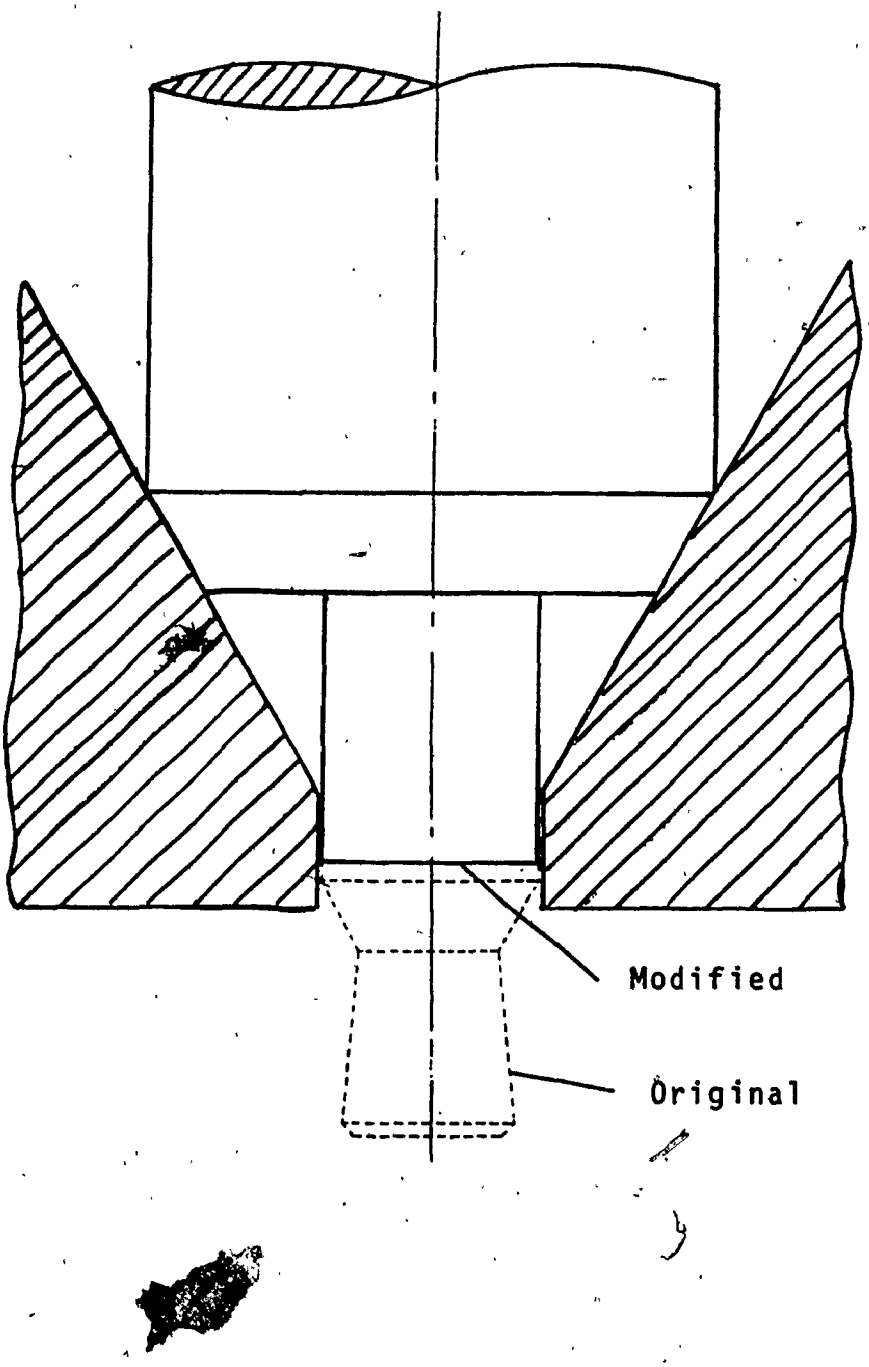

Fig. 3.3 Modified and original pintle nozzle

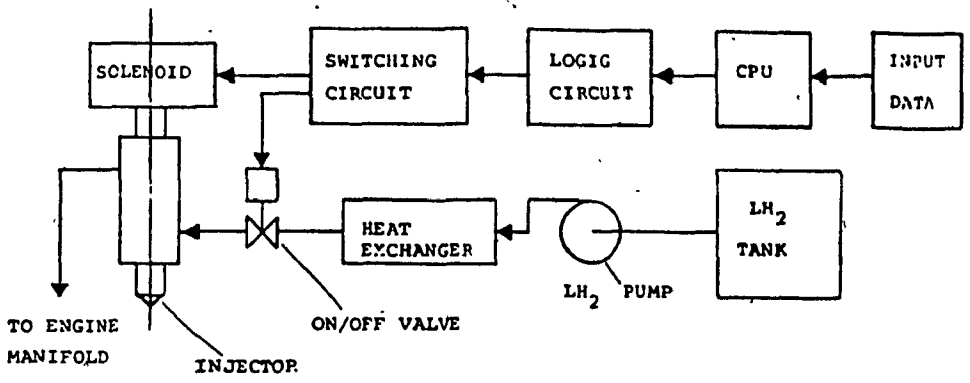

Fig. 3.4 Schematic of I.O.S option

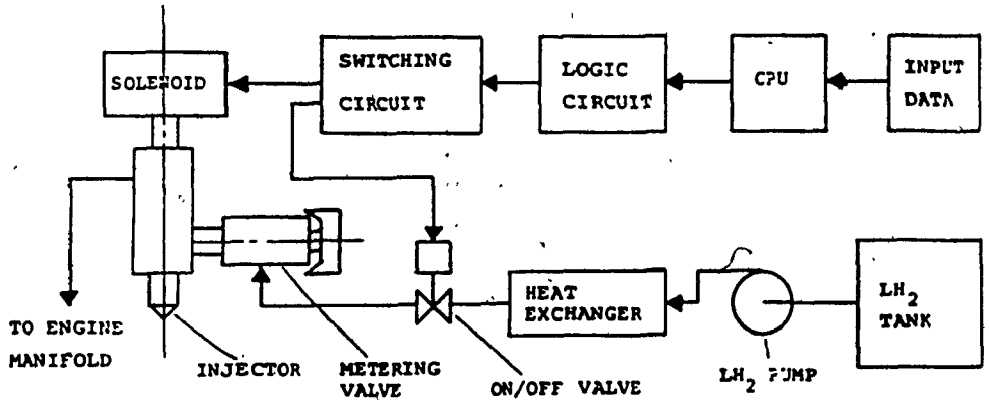

Fig. 3.5 Schematic of M.I.S option

variable area orifice which throttles the gas flow to the injector inlet. Consequently, the pressure in the chamber between the metering valve and the needle seat of the injector, drops significantly during gas injection. The positive effect of the pressure drop is faster closing of the needle as well as smaller injector spring preload required, which reduces the weight and the size of the solenoid. The microprocessor control interface circuit remains the same as for the injector only system.

3.2.3 Control Valve-Injector System (C.I.S.).

This type of fuel injection system consists of an injector and of a fuel control valve as shown in figure 3.6. The purpose of the control valve is to cut-off the fuel supply in order to cause a large pressure drop at the time of the injector's needle closing. This system is the most complex among the three described above, but it enables maximum flexibility in providing the required fuel discharge characteristic. Since both solenoids (for injector and for control valve) are actuated independently by the microprocessor-based controller, the relative motion of the two needles provides enough flexibility in obtaining a short fuel injection period which is essential for high speed diesel engines.

The fuel injection cycle for this system consists of five phases. To start the cycle it is assumed that both the injector and the control valve are in closed

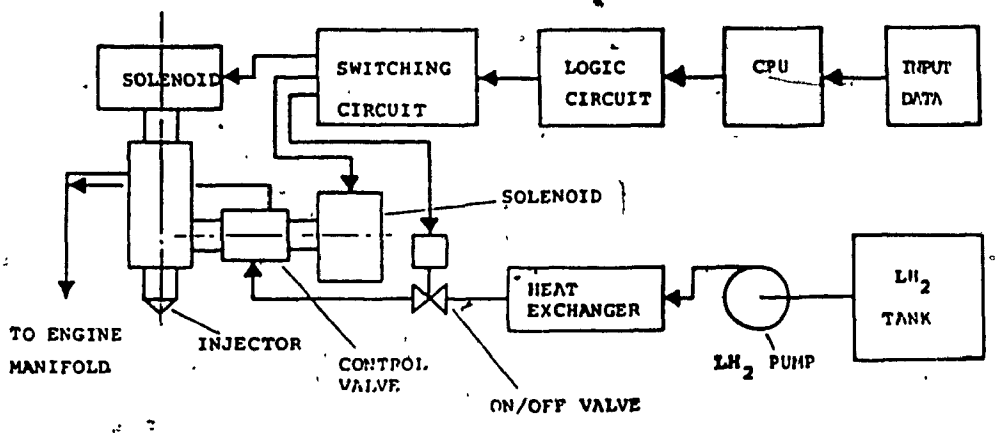

Fig. 3.6 Schematic of C.I.S. option

position. Thus, the maximum gas pressure exists only in the control valve chamber. However, there is also some residual pressure in the duct connecting the control valve with the injector and in the injector's chamber. The phases of the fuel injection cycle are as follows (Fig. 3.7):

1. Opening of control valve (preparation for injection). Shortly before the injection process begins, the fuel control valve opens, letting hydrogen gas (GH_2) at maximum pressure to fill the volume between the control valve and the injector. The control valve remains open during the first part of the injection period in order to allow the fuel to pass through at the required flow rate without throttling.

2. Opening of injector (Injection process begins). At the scheduled crankshaft position, the injector's solenoid is actuated and it moves the needle up. At this time, the gas pressure in the injector's chamber almost balances the preload of the spring. While the needle is accelarating towards the open position, the gas pressure extends to the needle seat area and the growing pressure force helps to lift the needle.

3. Fuel injection. This is the main injection process.

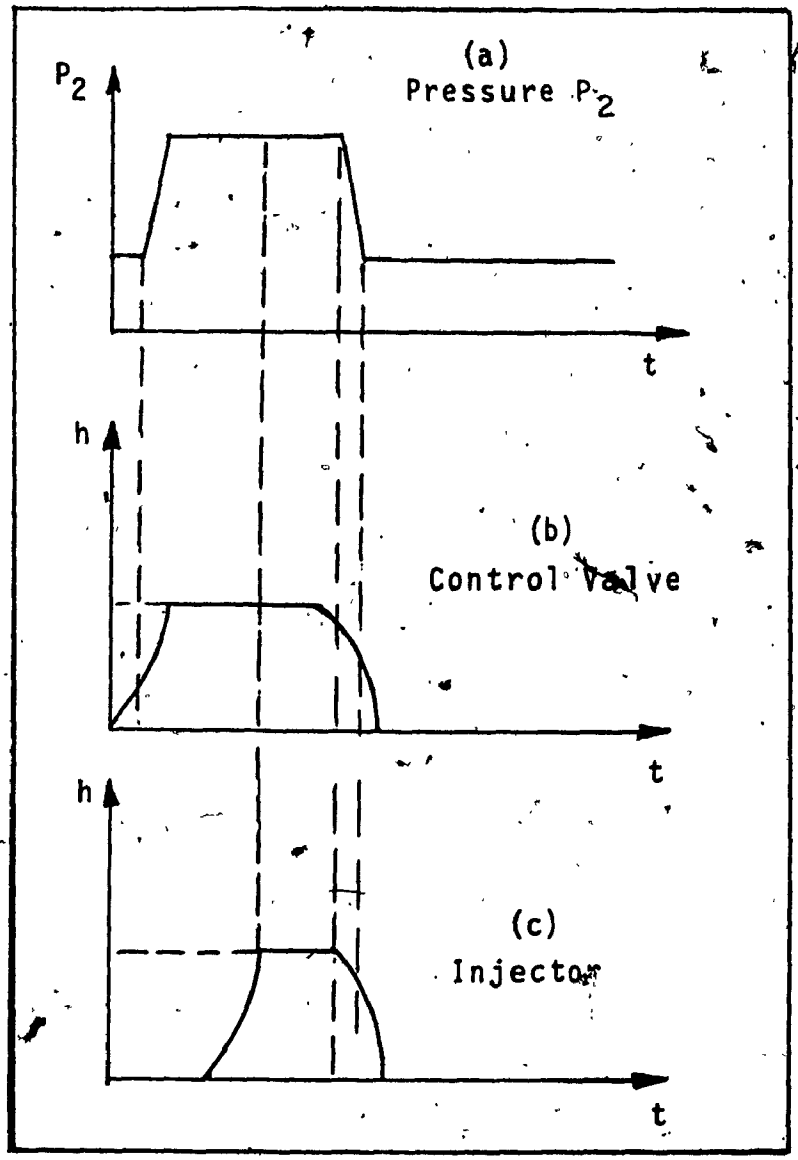

Fig. 3.7

(a) Characteristic of injector pressure of C.I. option
(b) Needle lift characteristic of control valve
(c) Needle lift characteristic of injector

millimeter. Finally, the armature mass and the possible acceleration of HELENOID and COLENOID actuators as compared to the conventional 'E' type solenoids are shown in figure 3.26 a and b.

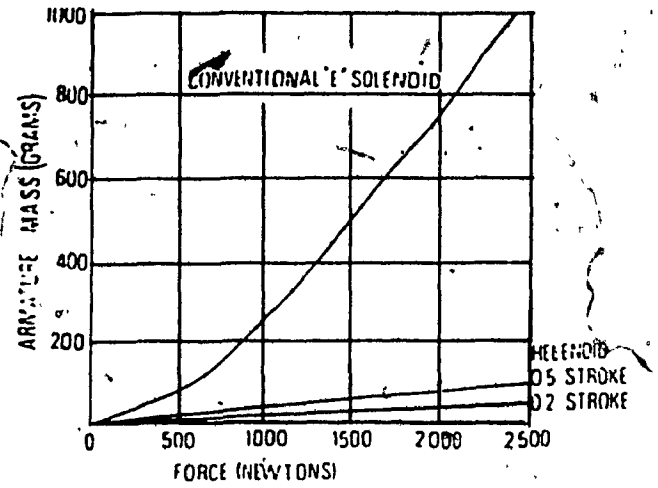

(a) Increase of armature mass vs. force

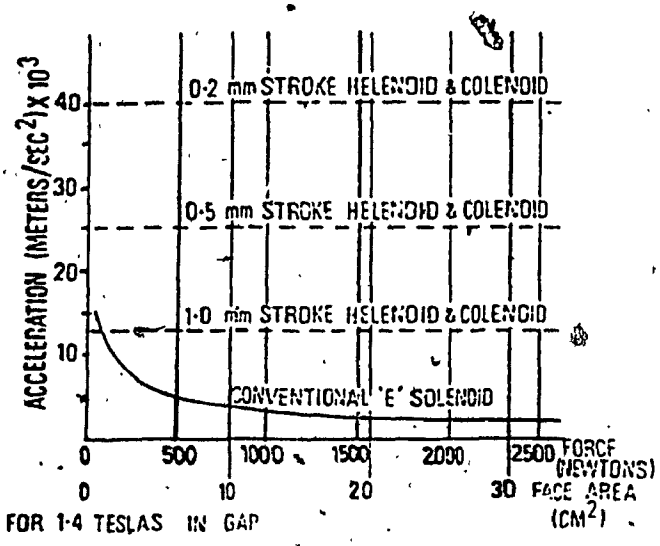

(b) Armature mass acceleration for flat working faces

Fig. 3.26 (Courtesy of Seilly (37))

3.5 HYDROGEN LEAKAGE

The fuel leakage through the needle guide is a very serious problem in the design of hydrogen injectors. In liquid fuel injectors, the leaking fuel is easily collected and returned back to the fuel tank. However, in a hydrogen-gas injection system the gas cannot be returned to the cryogenic fuel tank. A possible solution would be to introduce this fuel in the engine with the air through the intake manifold. This, however, would require the gas leakage to be small enough so as not to cause the typical backfire phenomenon.

In order to calculate the hydrogen leakage through the annulus flow area between the nozzle body and the needle consider figure 3.27. Since the gap is very small and $\delta << d_i$, the gas flow through the annulus should be assumed to be laminar flow between two parallel plates [66]. Then, the volumetric flow rate of the gas is given by Poiseuille's equation as

$$\dot{Q}_1 = -\left(\frac{\pi D_e \delta^3}{12 \mu}\right) \frac{dP}{dy} \qquad (3\text{-}14)$$

where

$$D_e = d_i + \delta$$

since

$$\dot{m}_1 = \rho \dot{Q}_1$$

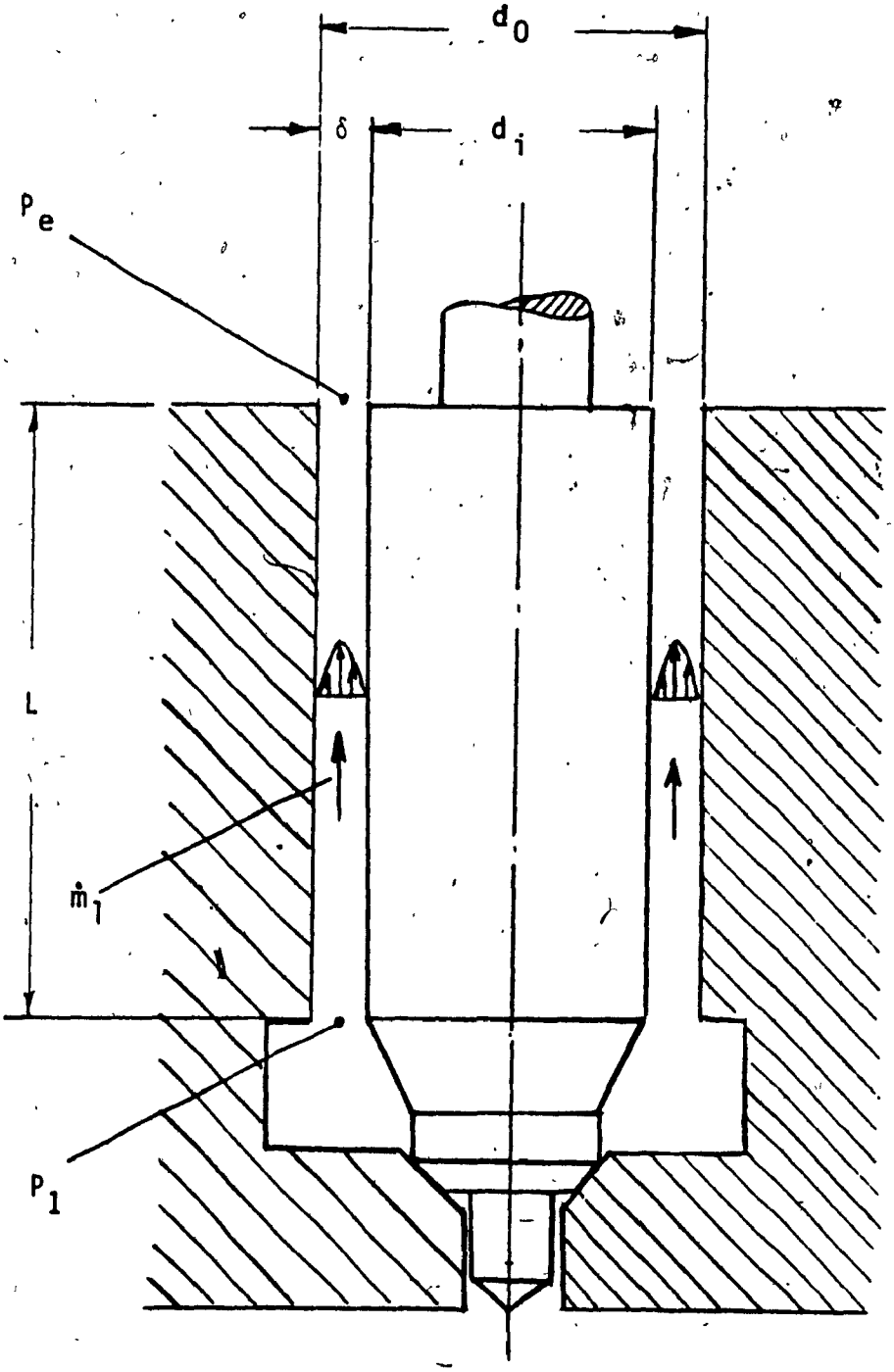

Fig. 3.27 Schematic of gas leakage through the needle guide

and for perfect gases

$$\rho = P/RT$$

equation 3-14 becomes

$$\dot{m}_l = \left(\frac{\pi \delta^3}{24 \mu RT}\right)\left(\frac{D_e}{L}\right)(P_1^2 - P_e^2). \qquad (3\text{-}15)$$

It can be seen, according to equation 3-15, that the clearance δ, between the valve needle and its guide, which appears in the third power in the equation, is a very critical factor in controlling the fuel leakage. The magnitude of the supply pressure also plays a critical role, but since it is one of the requirements in the gas injection system, it should be assumed constant. Finally the ratio of the needle diameter to its length is quite important. If the fuel leakage is sufficiently small, then it can be introduced into the engine through the intake manifold.

In order to find out how the clearance δ, and the ratio D_e/L affect the fuel leakage some values were assumed and the results are plotted in figure 3.28.

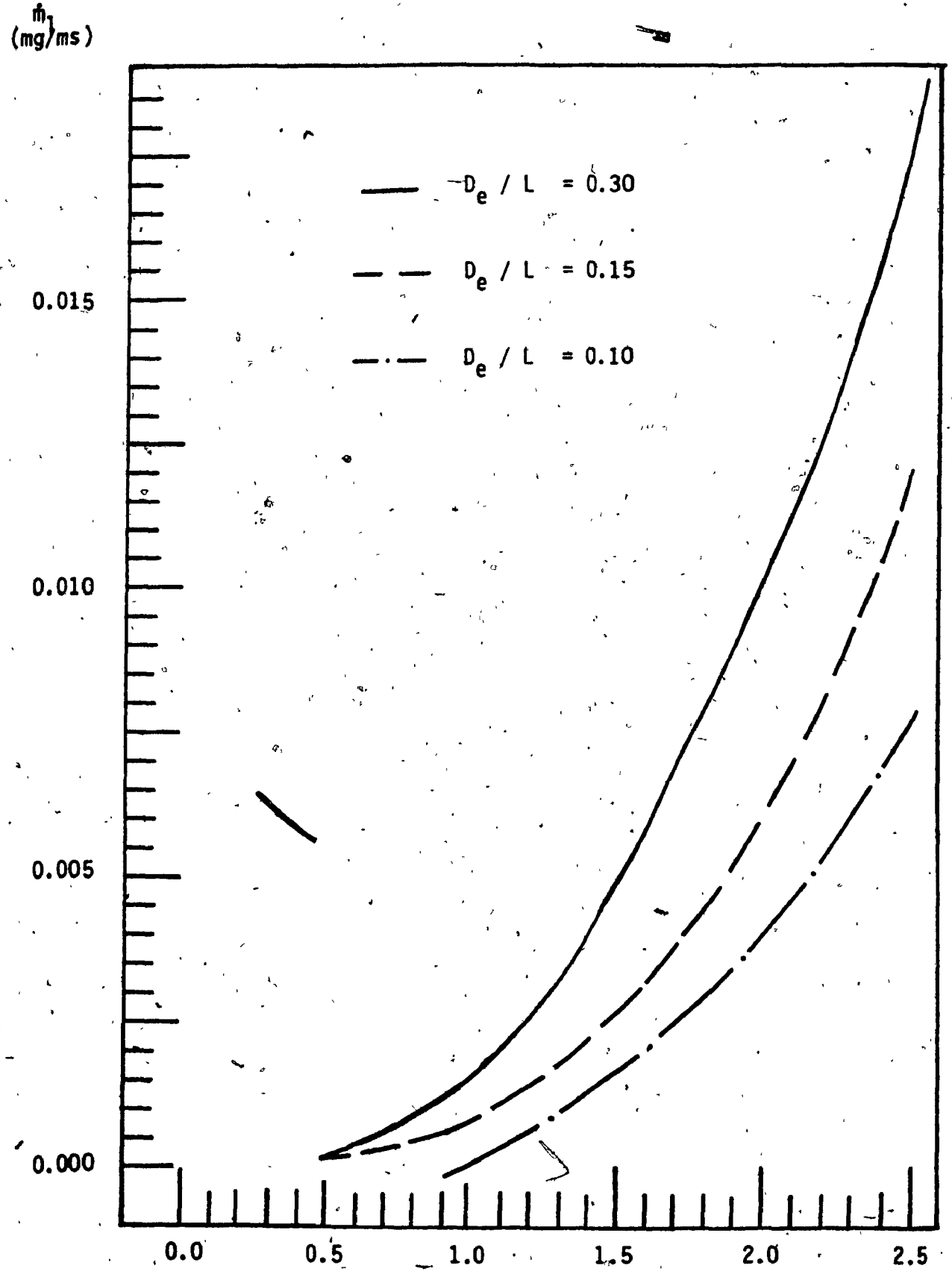

Fig. 3.28 Calculated fuel leakage plots for various D_e/L ratios

CHAPTER 4

EXPERIMENTAL RESULTS AND DISCUSSION

4.1 EXPERIMENTAL APPARATUS

The general experimental apparatus is shown in figure 4.1 with option I.O.S. istalled. The other two options are shown in figures 4.2 and 4.3. The injector was provided with a constant pressure supply of 20 MPa available from a bottle containing compressed hydrogen gas at 40 MPa. At the inlet of the injector either a metering valve or a control valve was installed in order to obtain the three options of the injection system as discussed in chapter 3.

For this feasibility study, all tests were performed with a modified conventional diesel pintle nozzle (CAV BDN12SD12) as is shown in figure 3.3. The actual shape and size of the valve needle has been determined by measurements on a toolroom microscope (shadowgraph) and it has been reproduced in figure 3.3. The reason for selecting this particular model and type of injector is that it could be installed on the cylinder head of such engines as Perkins diesel engine (model 4:99) and Peugeot diesel engine (model 2L) which are both available at this University, hence the injector could actually be tested. Both of these engines are four stroke, water cooled and have four cylinders in line. The control valve in the C.I.S. option was equipped with another pintle nozzle of the same type but without the

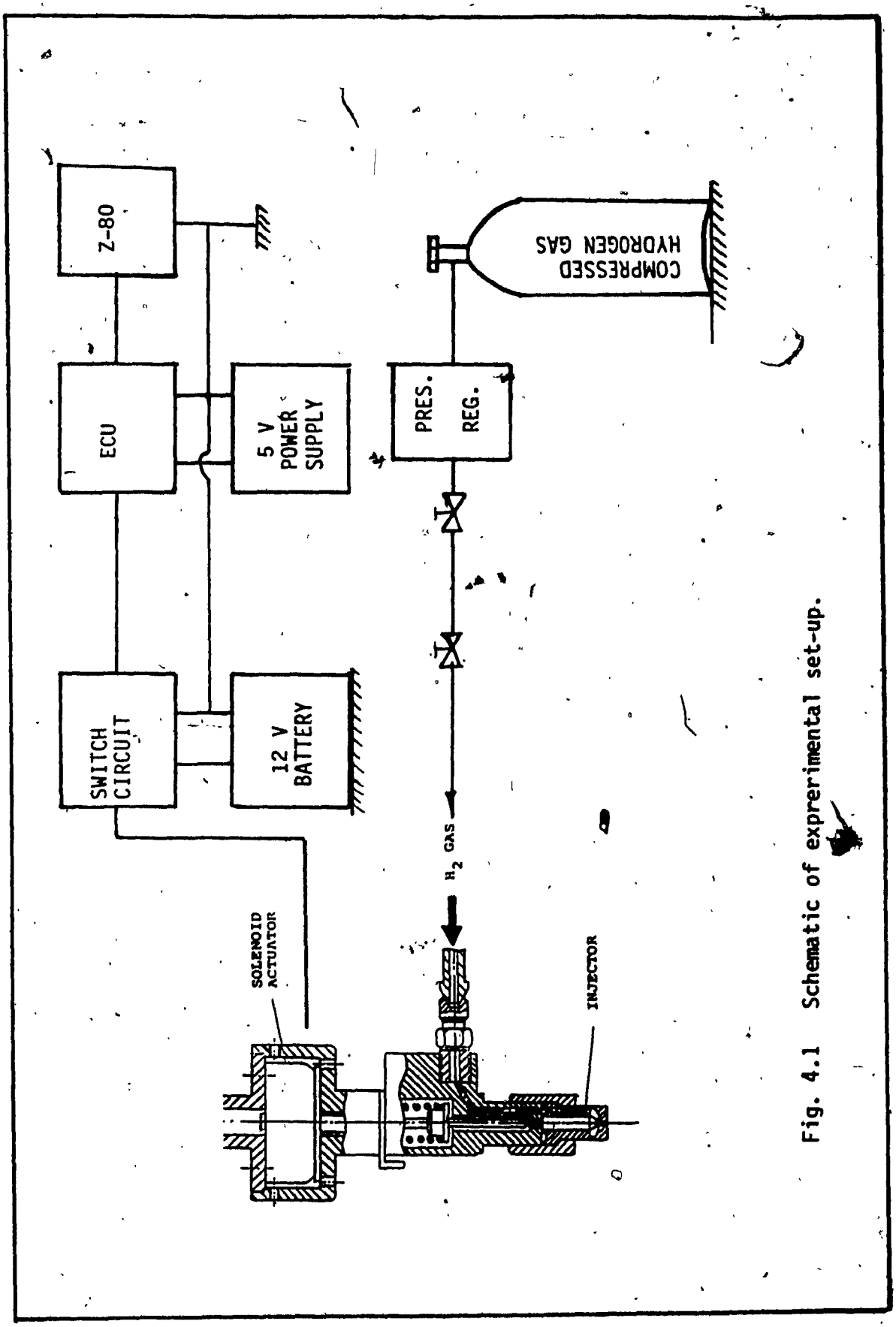

Fig. 4.1 Schematic of experimental set-up.

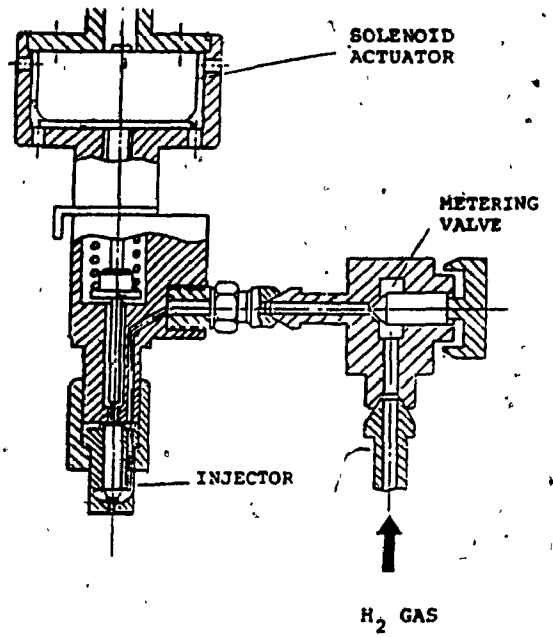

Fig. 4.2 Injector with metering valve

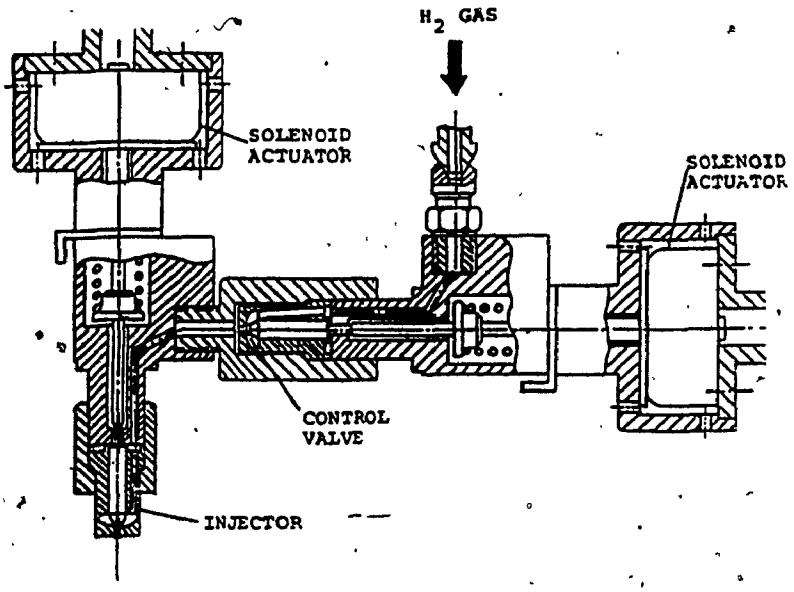

Fig. 4.3 Injector with control valve

pintle.

The injector was operated by a conventional linear solenoid actuator made by LENDEX, INC. (Model 5-SF, PUSH/PULL). The push rod of the injector was extended and connected to the armature of the solenoid by a screw-nut arrangement in order to be able to adjust the armature stroke and consequently the needle stroke. An especially made housing, mounted on the nozzle holder, accomodated the solenoid actuator as shown in figure 4.4. The original spring of the injector was replaced by a much stiffer one with a spring constant of 300 N/mm. In order to balance the force due to the gas pressure acting on the needle, as well as to provide the necessary acceleration during valve closing, the spring was preloaded with a 618 N force. The solenoid was energized by a 12 V_{DC} power supply available from an ordinary car battery. The current supply to the solenoid actuators was controlled by a Z-80 microprocessor via an electronic circuit and a switching circuit.

Although all components in the apparatus were selected to withstand the high pressure involved, there was still a risk of gas leakage due to possible defects. This risk was highest at the connections of the components in the system. Therefore, during the initial pressurization of the system, extreme care was taken to control gas leakage and avoid possible explosion. For this reason, nitrogen was first used in order to avoid

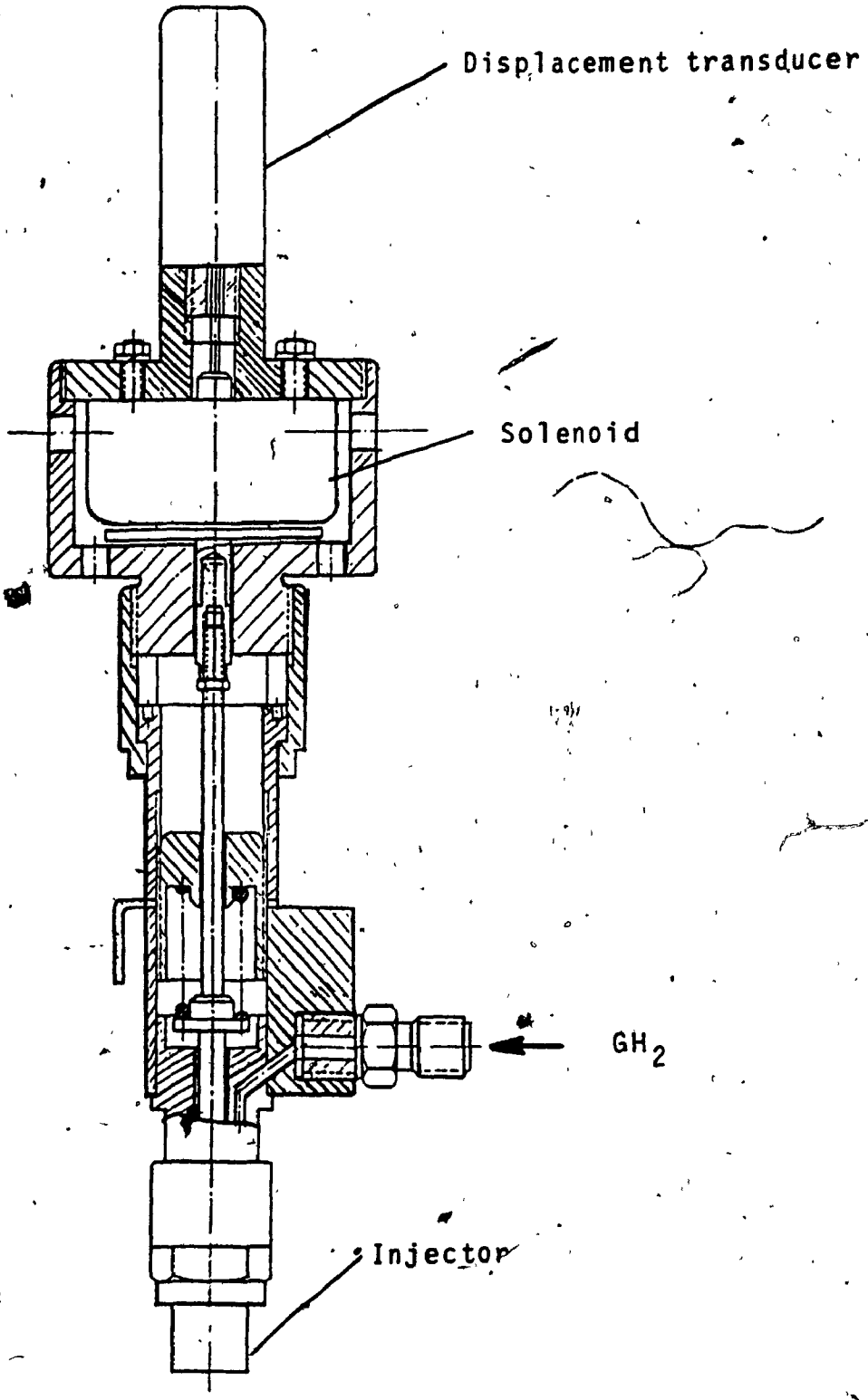

Fig. 4.4 Details of solenoid installation on the diesel injector

the fire hazard in case of malfunction. The pressure in the system was being increased very slowly above the 10 MPa and all connections were checked for leakage as well as for cracks. Then, the same procedure was followed with hydrogen gas, because it was expected that there might still be some leakage through the fittings. However, it was found that no leakage occured except of that through the needle guide and needle seat. In order to reduce the fire hazard, the experiments were performed in a well ventilated laboratory.

Since hydrogen does not have any lubricating properties, there was a possibility that the needle would not be able to open and to close freely. This possibility was tested by adjusting the injector to open at 20 MPa and to close at 18.5 MPa and by observing the pressure rise and fall in the chamber of the injector during the needle oscillations by using an oscilloscope (fig. 4.5). The experimental set-up for these tests is shown figure 4.6 and in plates 4.1a and 4.1b. It was noted that no problems were encountered concerning needle seizure. However, although the same nozzle was used throughout all experiments without any seizure problems, no definite answer can be given about the long term reliability of such an injector which was originally made to inject liquid fuel for diesel engine operation.

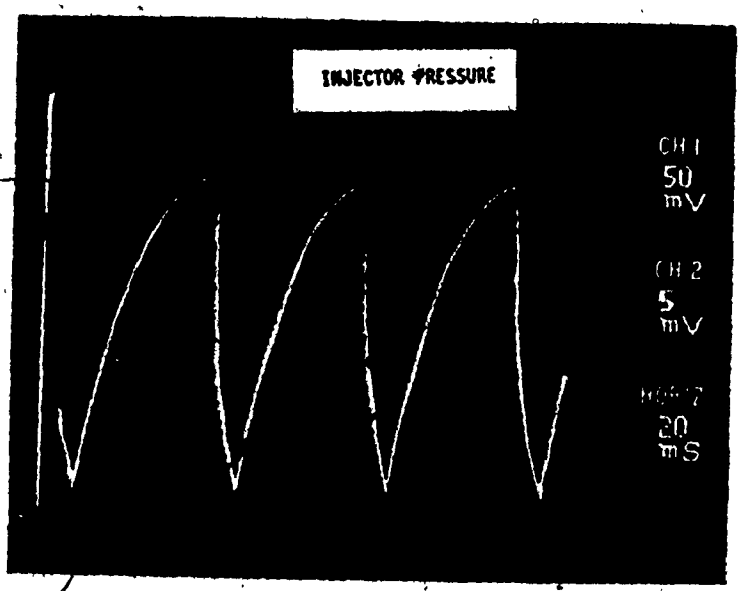

Fig. 4.5 Valve needle oscillations during seizure tests

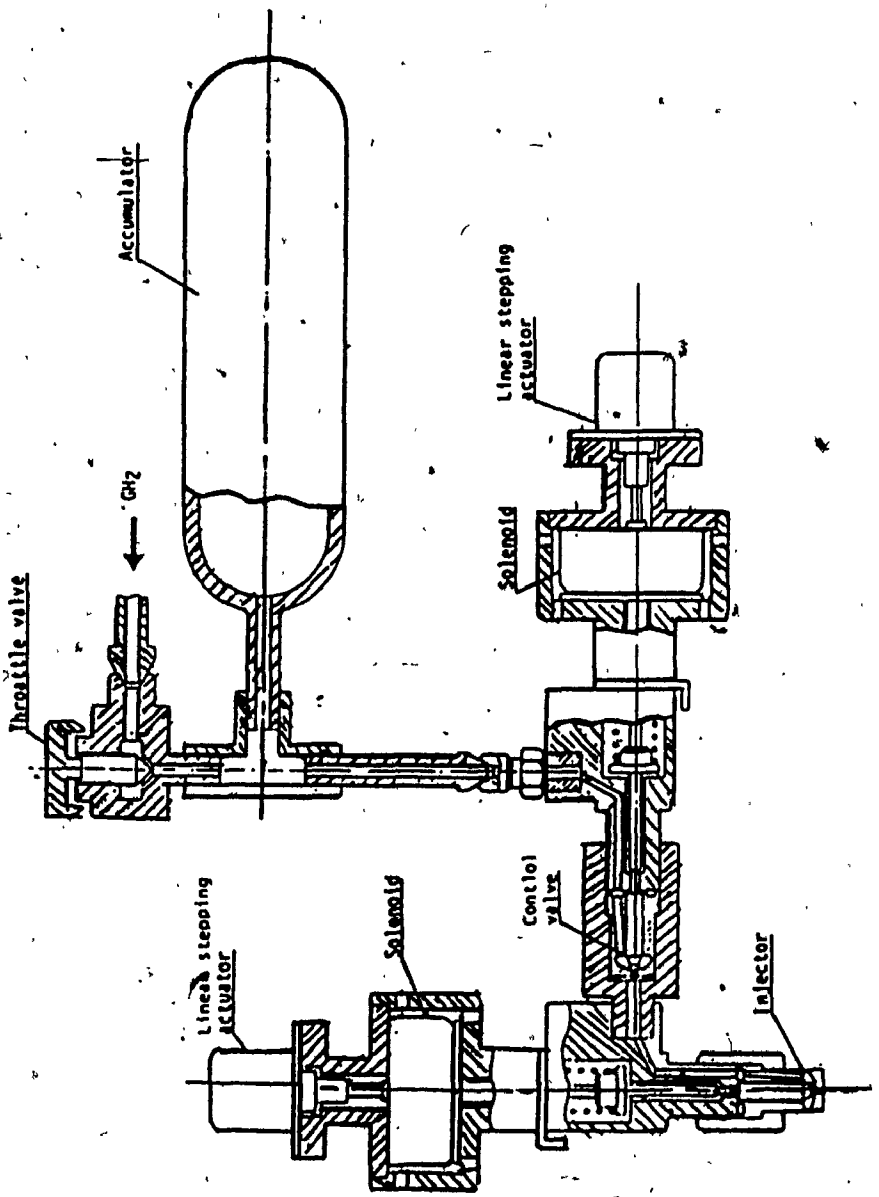

Fig. 4.6 Schematic of experimental apparatus during preliminary tests

Plate 4.1(a) Experimental set-up for needle seizure tests

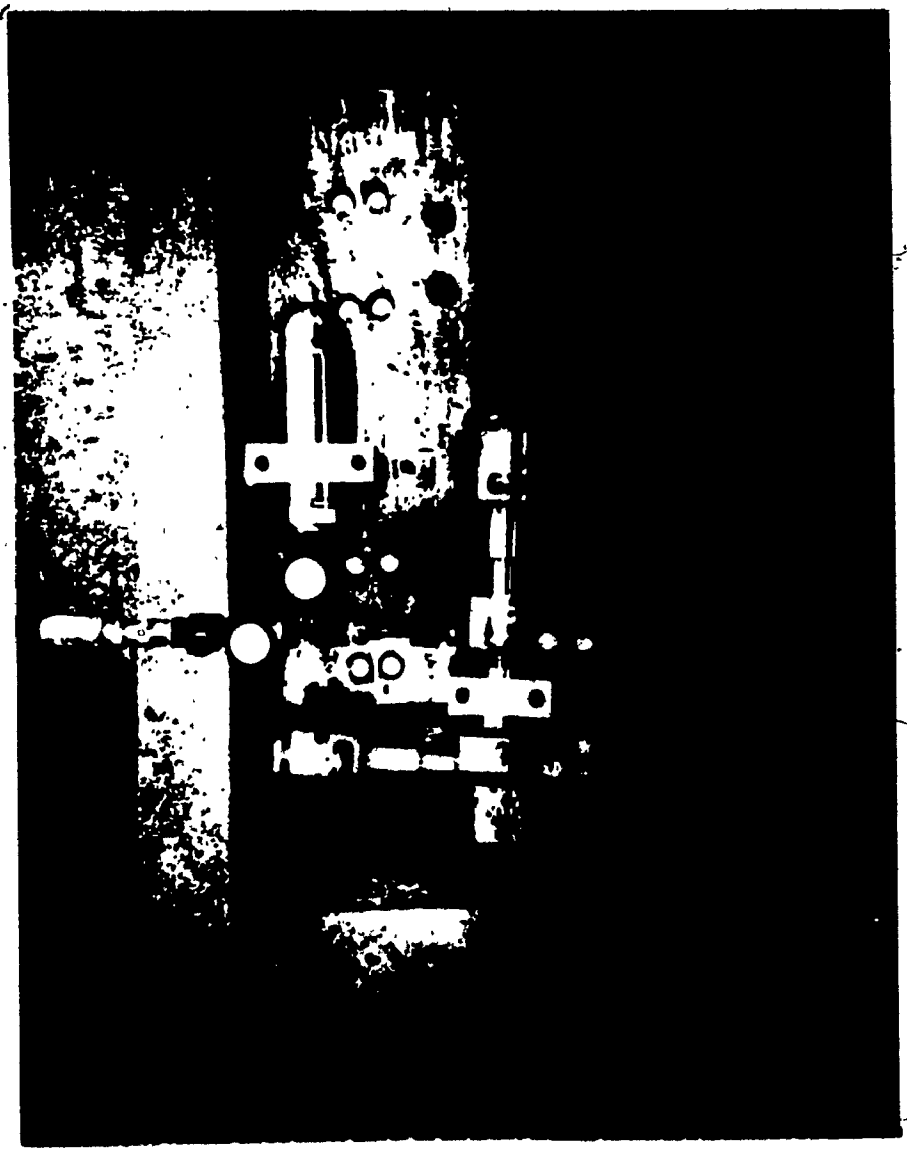

Plate 4.1(b) Top view of the experimental set-up shown in 4.1(a)

4.2 TESTING OF THE INJECTION SYSTEM

All the instrumentation used for testing of this injection system is shown in figure 4.7. With this instrumentation the following measurements were made.

1. Electric current through the solenoid actuator.
2. Hydrogen gas pressure in the chamber of the injector.
3. Movement of the valve needle.
4. Total fuel dose delivered per injection.
5. Fuel leakage through the needle guide.
6. Fuel discharge rate characteristics.

The significance of the electric current characteristic through the solenoid actuator has been explained in chapter 3 in the discussion of performance of the switching circuit.

The gas pressure in the chamber of the injector was measured by a miniature transducer manufactured by Kistler Instrument Corporation (Model 603B2). This model is an acceleration compensated piezoelectric pressure transducer with high impedance charge signal output and it is suitable for extremely rapid pressure changes. The exact mounting position of this pressure transducer is shown in figure 4.8. Using this transducer, the pressure of gas in the injector was recorded for the three injection system options (Fig. 4.9, 4.10 and 4.11).

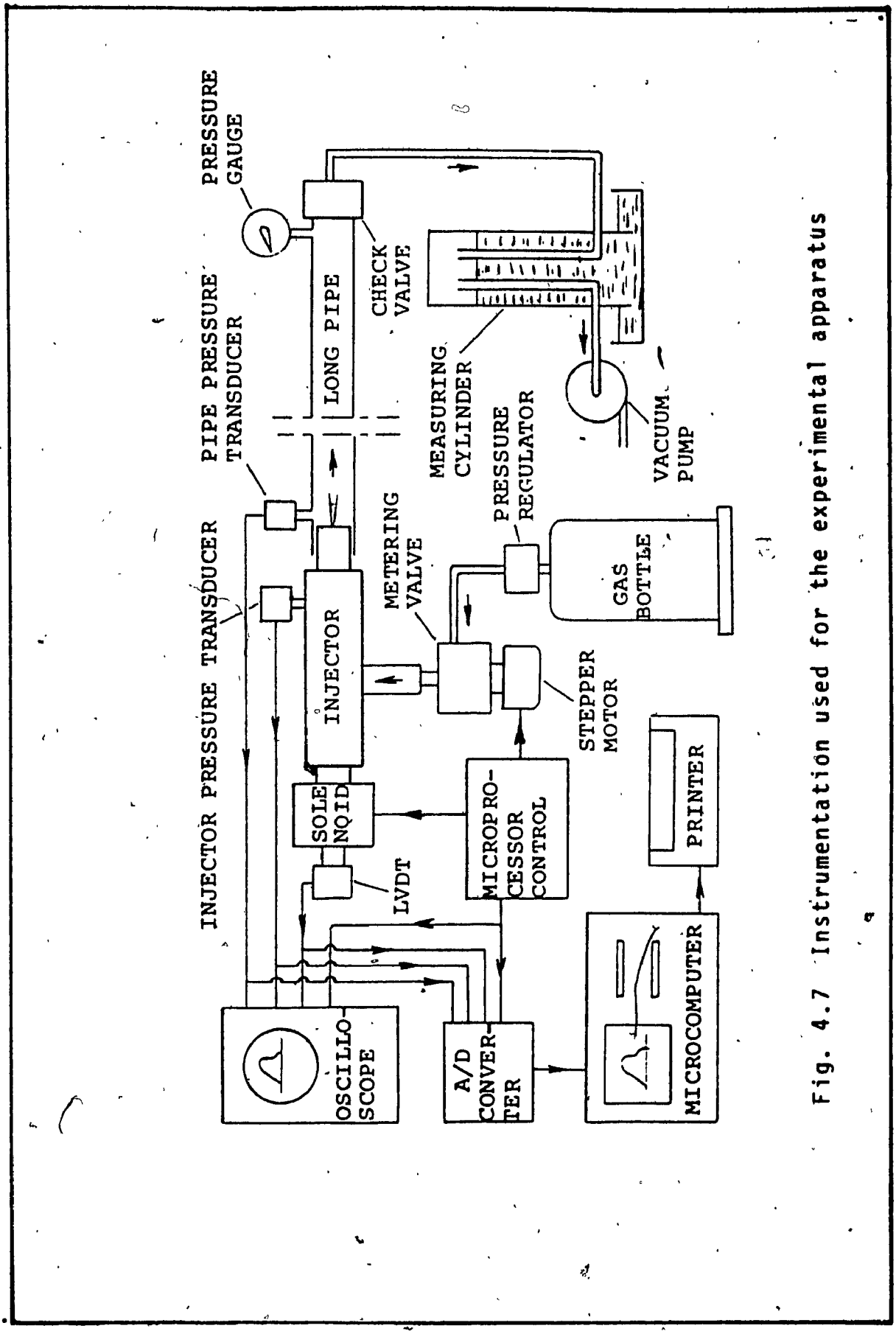

Fig. 4.7 Instrumentation used for the experimental apparatus

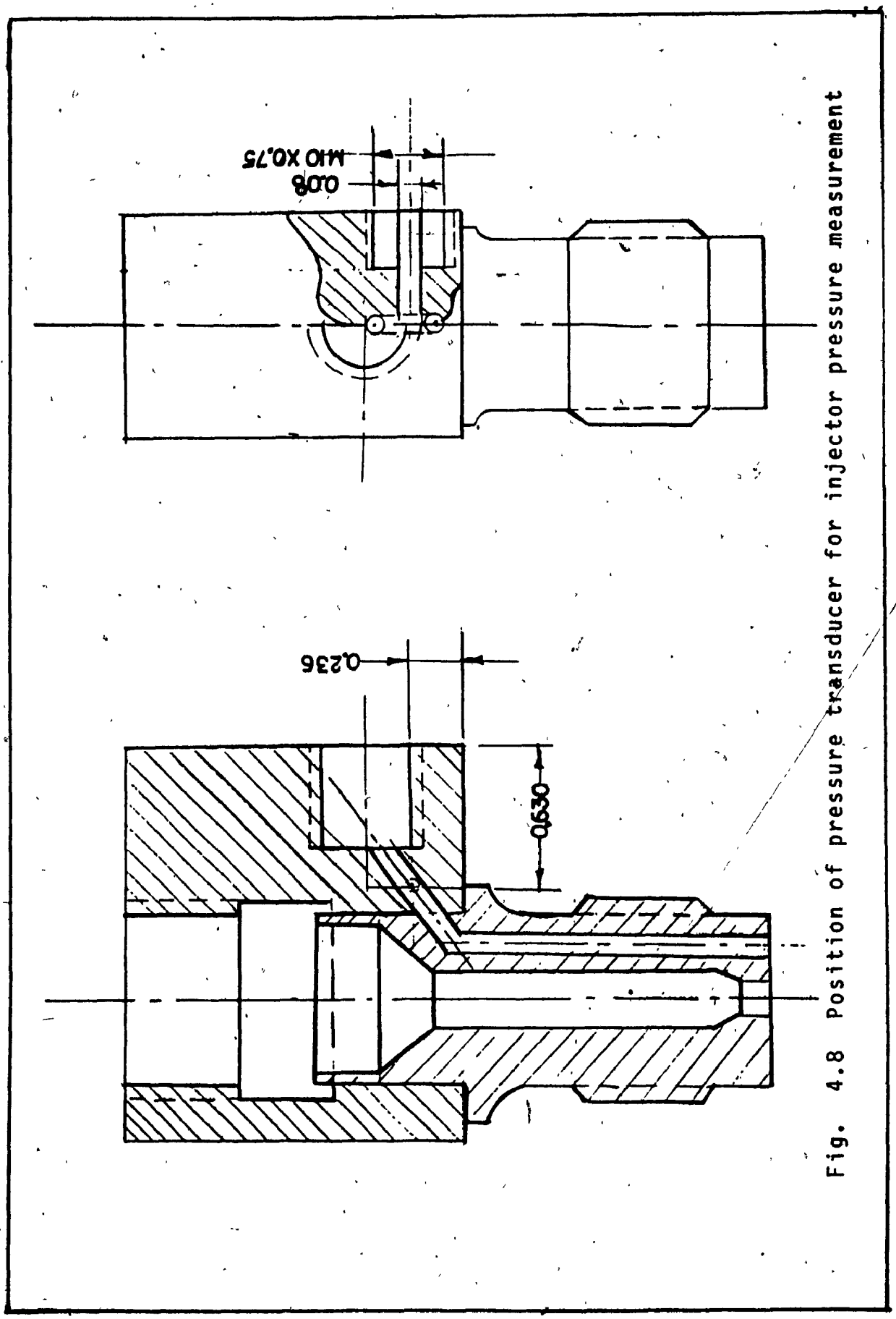

Fig. 4.8 Position of pressure transducer for injector pressure measurement

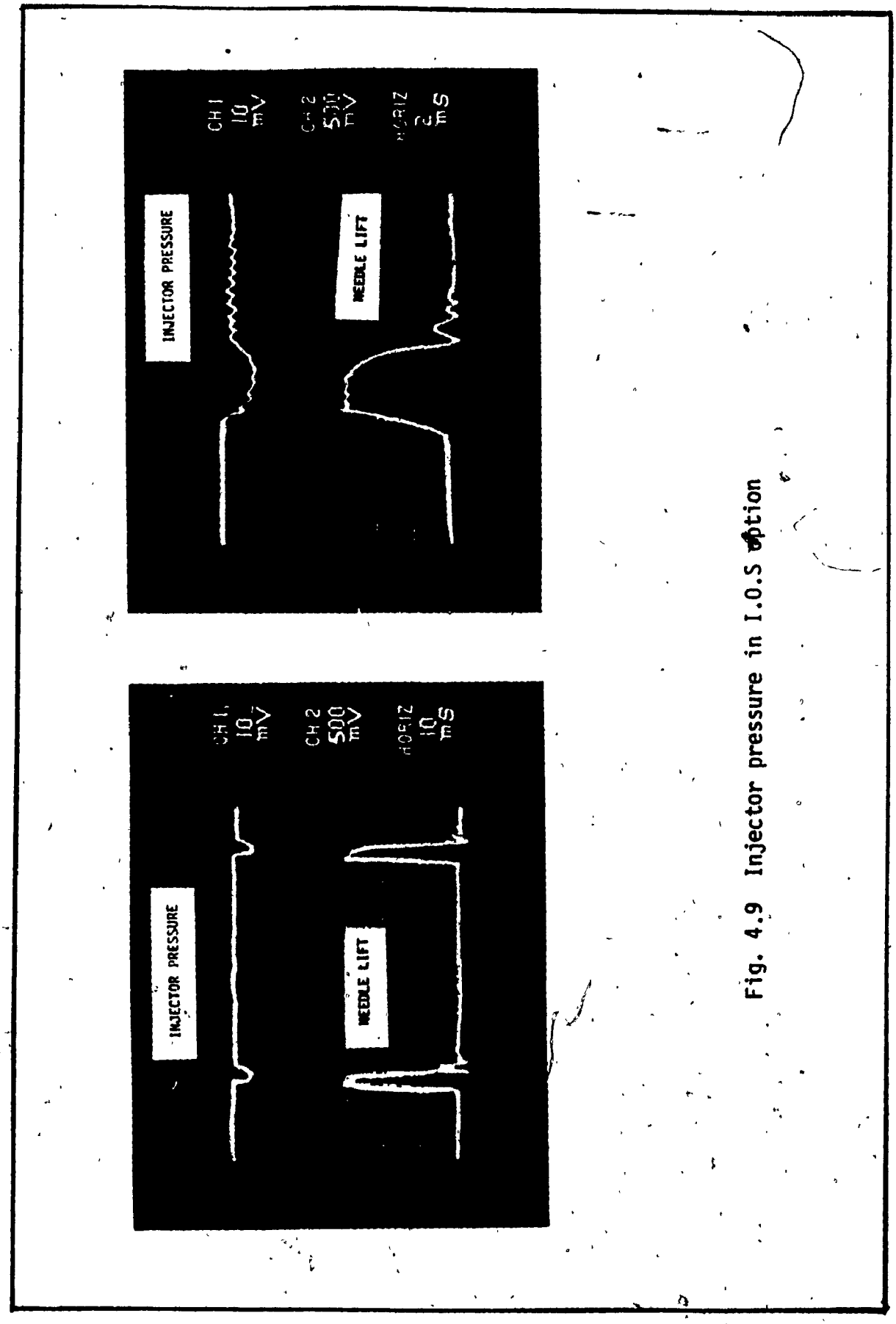

Fig. 4.9 Injector pressure in I.O.S option

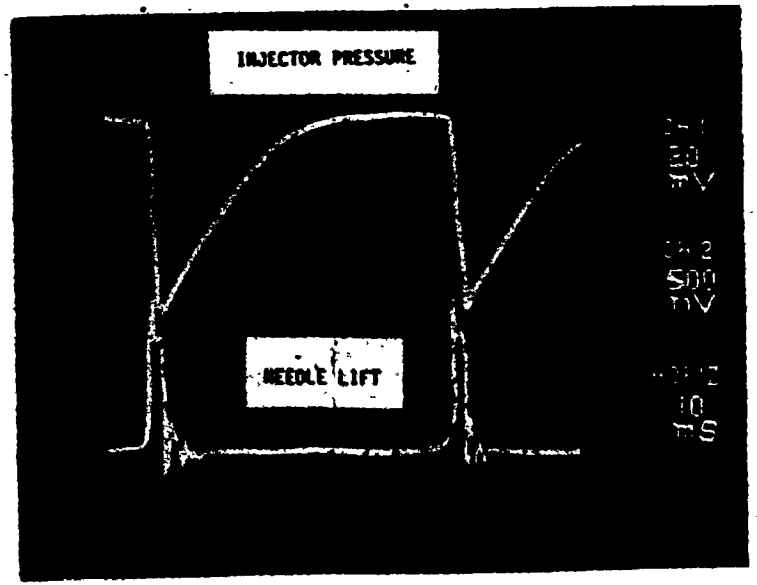

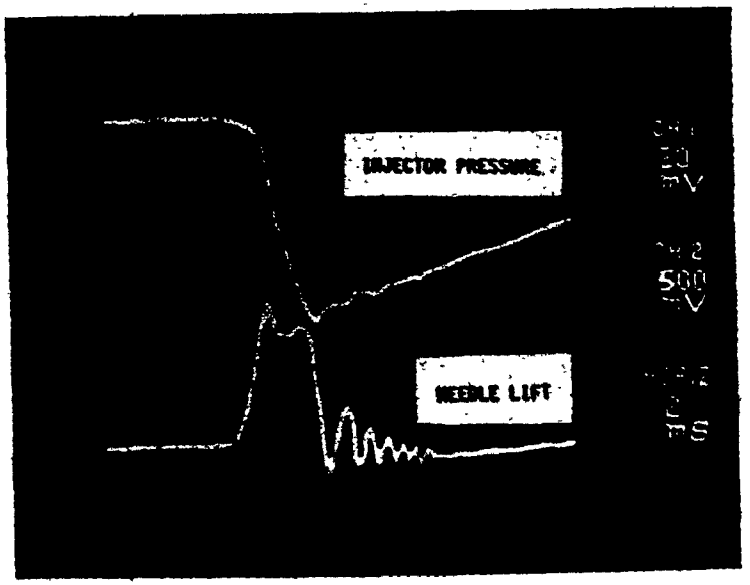

Fig. 4.10 Injector pressure in M.I.S option

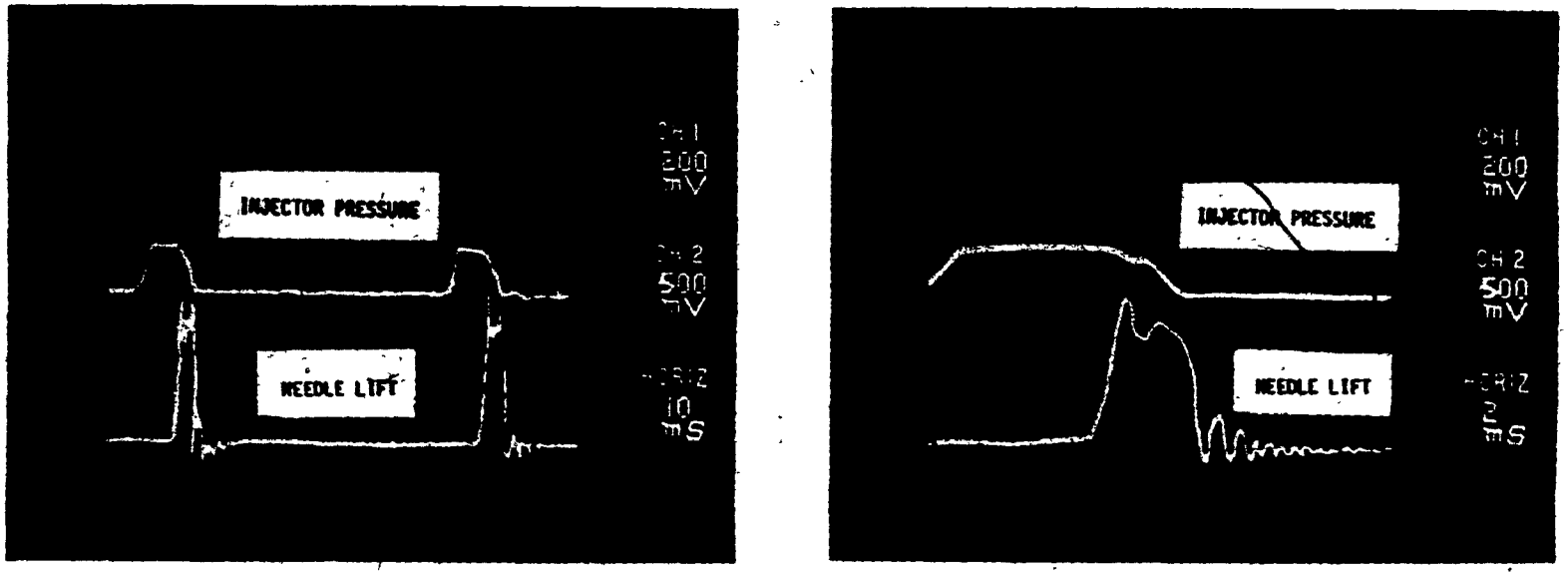

Fig. 4.11 Injector pressure in C.I.S. option

The needle lift was recorded by a linear displacement transducer, produced by AVL model 421 which is a variable inductance type. According to these results the performance of both the nozzle and the solenoid could be evaluated because it indicated the time of opening and closing of the needle (fig. 4.9b, 4.10b, 4.11b).

The total mass of hydrogen gas discharged during each injection was measured by collecting the fuel from several consecutive injections at the top of an inverted graduated cylinder as shown in figure 4.7. This apparatus was manufactured for this project and the method of measurement is as follows: the water level is brought to a reference point by removing the gas from the cylinder with the help of a vacuum pump. Next, the injector performs a known number of injections and the gas displaces the water as it accumulates at the top of the cylinder. Then, the mass of gas per injection can be calculated by dividing the volume, occupied by the gas, by the number of injections and by using the perfect gas law.

In order to see how the shape of the valve needle affects the ability of the injector to deliver a certain fuel dose, measurements were made with two nozzles in which the pintle shape was modified as shown in figure 4.12. Measurements were also made with the original pintle shape for comparison purposes. The changes of the

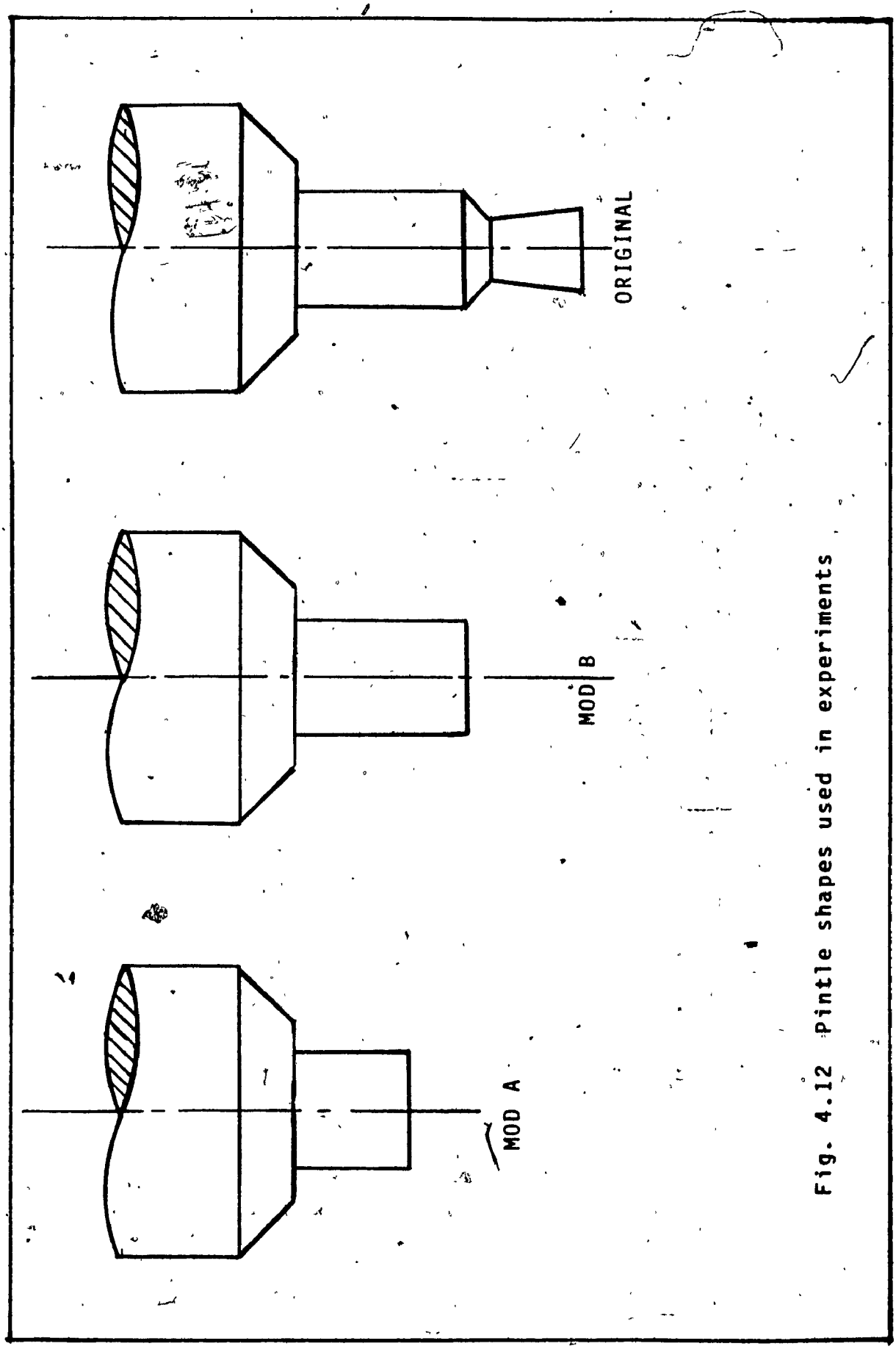

Fig. 4.12 Pintle shapes used in experiments

orifice flow area characteristic due to these modifications are shown in figure 4.13 and the results are plotted in figure 4.14. The fuel dose measurement was repeated several times for each injection period and the average gas dose was recorded to increase the accuracy of measurement. Therefore, the results plotted in figure 4.14 represent the average fuel dose injected during a given injection period. Figure 4.14 also shows how the fuel dose varies with duration of injection. As can be seen from this figure, MOD.B nozzle had the best fuel dose characteristic among the three nozzles that were tested. Thus, MOD.B nozzle was selected for further experiments including engine tests.

The fuel leakage through the needle holder was measured with the same apparatus used for measuring of the total fuel dose. However, since the fuel leakage was continuous, the reading was taken after a certain period of time by using a stopwatch. It was found that the fuel mass flow rate leaking through the needle holder was 0.02 mg/msec. At an engine speed of 2000 RPM the cyclic period is 60 ms and the theoretical injection period is 2.5 ms. During the 60 ms period, the mass of fuel leakage was found to be 1.2 mg. Since the total fuel dose required is 8.4 mg, the percentage of fuel leakage was 14%.

It has to be mentioned that 14% of the actual dose, will be approximately 7% of the stoichiometric

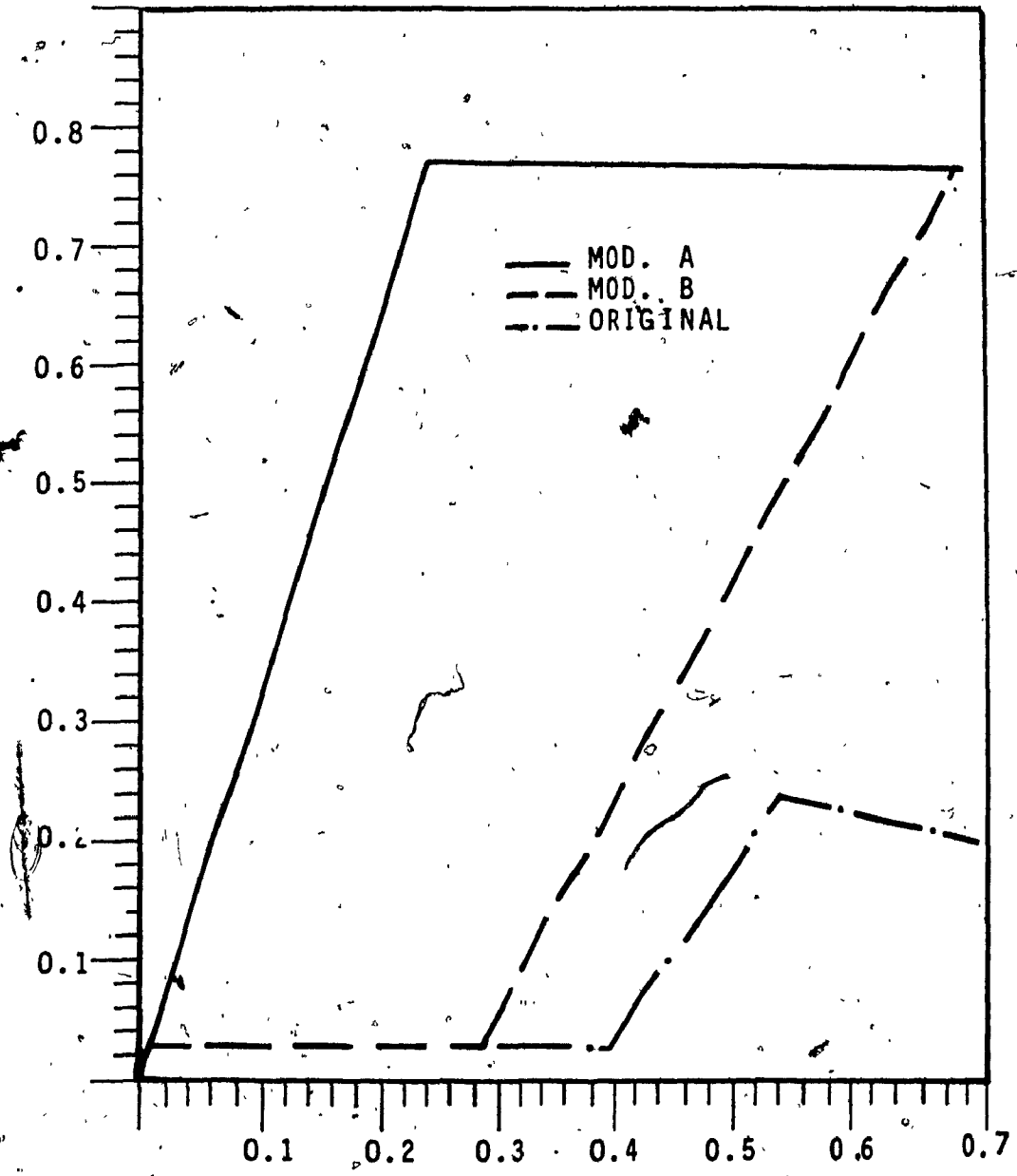

Fig. 4.13 Critical flow area characteristics for the pintle shapes shown in figure 4.12

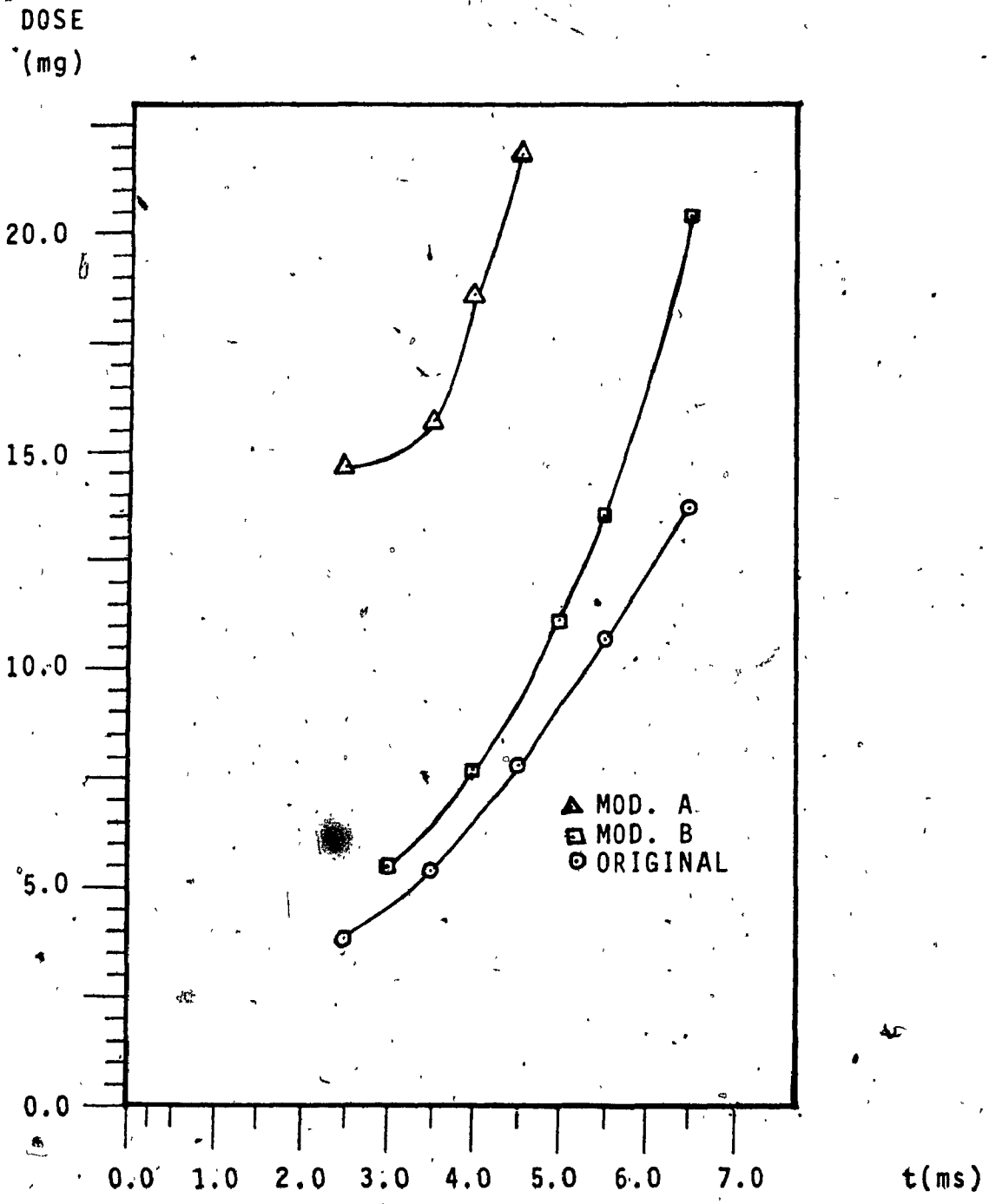

Fig. 4.14 Hydrogen injection dose for the pintle shapes shown in figure 4.12

dose. This should allow the introduction of hydrogen to the manifold of the engine without backfire hazard.

4.3 FUEL DISCHARGE RATE CHARACTERISTIC

In this section, an attempt to measure the instantaneous gas discharge rate from the injector is described. The gas was injected into a long tube of constant diameter equipped with a pressure transducer at the inlet. The amplitude of the pressure wave, measured by the transducer was found to be proportional to the mass flow rate of the injected gas as will be discussed later. The pressure wave was recorded by using an oscilloscope and also a computer controlled data acquisition system.

It is well established in the diesel engine technology that knowledge of the fuel discharge rate plays an important role in shaping the combustion process in a diesel engine during its development. There are several methods of measuring this process for liquid fuels but the most advanced was invented by Bosch [67]. His method was based on the unsteady flow theory which states that the amplitude of the pressure wave is proportional to the amplitude of the velocity wave, as pointed out by Pischinger [68]. Bosch used an extraordinary long pipe, in which the diesel fuel was discharged from an injector, in order to protect the recorded pressure wave against distortion from the returning pressure wave reflected at the end of the pipe.

Knowing the amplitude of the forward propagating pressure wave and the pipe cross section, the volumetric flow rate of the liquid fuel could therefore be calculated.

In the case of gaseous fuel injection into the combustion chamber of a compression ignition engine, the knowledge of the fuel discharge rate is needed as well. Therefore, several attempts have been made by different investigators to determine the gas injection process. Schlieren photography was used by Takahashi [53] to visualize the hydrogen injection process. An ingenious new method called Fast Response probe was invented by Tanabe [69] to investigate the dynamics of the hydrogen jet. In this thesis, a procedure is proposed to calculate the mass flow rate of gas from the injector. Finally, the direct measurement of gas discharge rate has been performed as described below.

4.3.1 Mathematical Formulation.

An attempt was made to modify the method used by Bosch for liquid fuels and to adopt it for measurement of the gas discharge rate characteristic. The mathematical model will describe the gas injection process which takes place in a pipe of constant diameter (fig. 4.7). This process is highly transient with mass flow varying from zero to a very high flow and it returns to zero within few milliseconds. Such a process can be described mathematically for one-dimensional unsteady flow with two

partial differential equations which were derived initially by Allievi [70].

1. Continuity Equation

$$\frac{\partial u}{\partial x} = -\left(\frac{1}{\rho c^2}\right)\frac{\partial P}{\partial t} \qquad (4\text{-}1)$$

2. Momentum Equation

$$\frac{\partial u}{\partial t} = -\left(\frac{1}{\rho}\right)\frac{\partial P}{\partial x} \qquad (4\text{-}2)$$

When equations (4-1) and (4-2) are solved, an expression relating the forward propagating pressure wave with the corresponding flow velocity in the pipe can be obtained. Thus,

$$u_f = P_f/\rho c \qquad (4\text{-}3)$$

Since the pressure wave generated by the injection, travels along the pipe with the speed of sound, the pipe is made very long in order to avoid the disturbance of the readings obtained from the pressure transducer by the reflected pressure wave. Combining equation (4-3) with the mass flow equation

$$\dot{m}_f = \rho A_p u_f \qquad (4\text{-}4)$$

the resulting equation becomes

$$\dot{m}_f = KP_f \qquad (4\text{-}5)$$

where $K = A_p/c$

Therefore, the mass flow rate of gas is directly proportional to the generated pressure wave. The ratio A_p/c can be considered constant if the pressure variations in the pipe are low and the sound velocity in the pipe does not change significantly.

4.3.2 Test Set-Up and Calibration

In order to measure the fuel discharge rate, the hydrogen gas was injected into a 5 m long pipe with a 6 mm diameter. At the pipe entry, a pressure transducer was installed (model KP-15 made by Validyne) which measured the amplitude of the pressure wave. This pressure wave was recorded by an oscilloscope or a data acquisition system. At the end of the pipe, a check valve and a pressure gauge were installed. The former was maintaining a residual pressure of approximately 0.07 MPa in the pipe and the latter was confirming that pressure. The hydrogen gas leaving the pipe was collected in a transparent graduated cylinder where the

gas volume could be measured (fig. 4.7). The actual experimental set-up is shown in plate 4.2.

Several tests have been made by using this method. Figure 4.15 shows an oscillogram of a pressure wave and the corresponding injector needle lift. Note also the returning pressure wave approaching the recorded forward propagating wave. If the scales for both coordinates are known, the area under the pressure time can be computed, hence, the mass dose of the injected gas can be determined. The oscillogram shown in figure 4.15 is translated into a pressure scale and then the mass of the fuel dose is calculated according to the following procedure:

SCALES

Pressure scale : 68947.6 Pa/Div

Time scale : 2 msec/Div

Therefore,

Total duration of injection : t = 2.6 ms

Area under pressure curve : A_{pr} = 275.8 Pa.s

Mean pressure : $P_{f,avg}$ = 106077 Pa

The velocity of sound in hydrogen gas, at 0.07 MPa is 1300 m/s and the cross section area of the 6 mm pipe diameter is

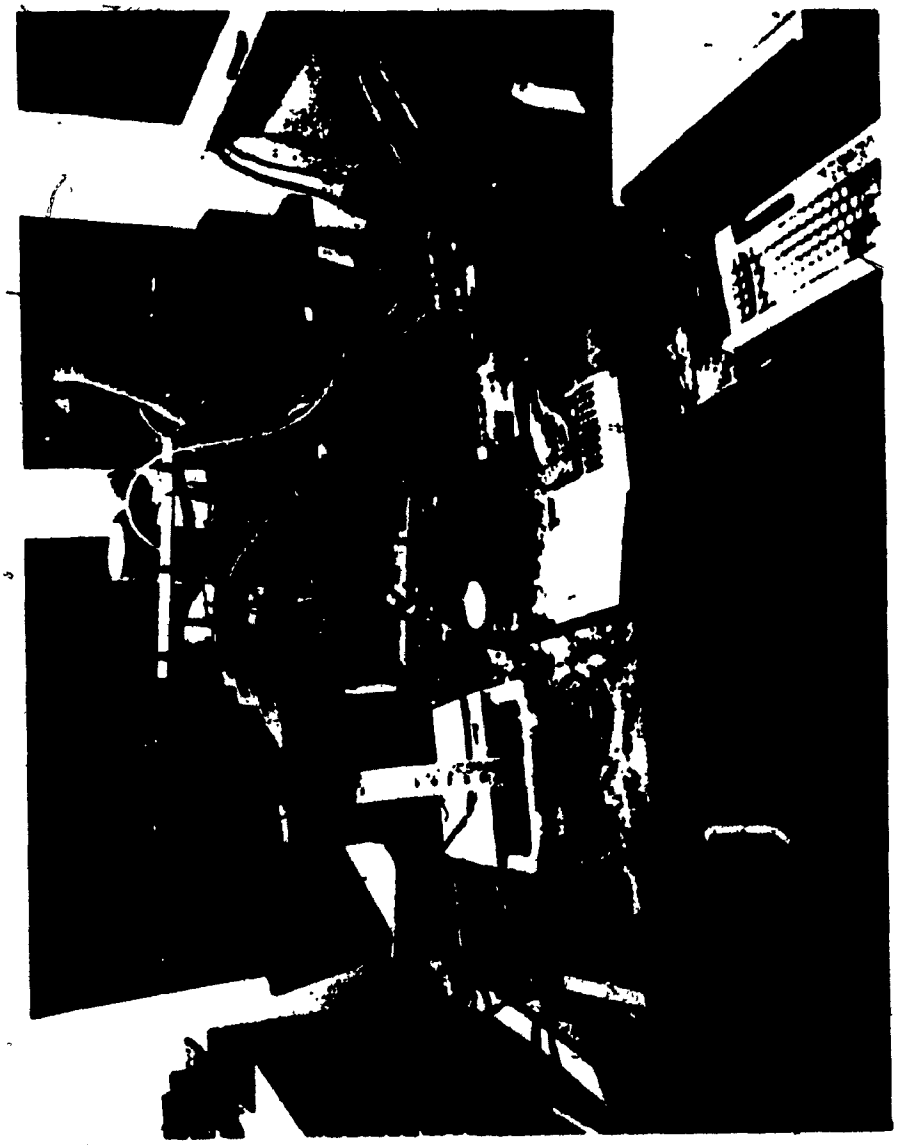

Plate 4.2 Experimental set-up for measurement of discharge characteristic

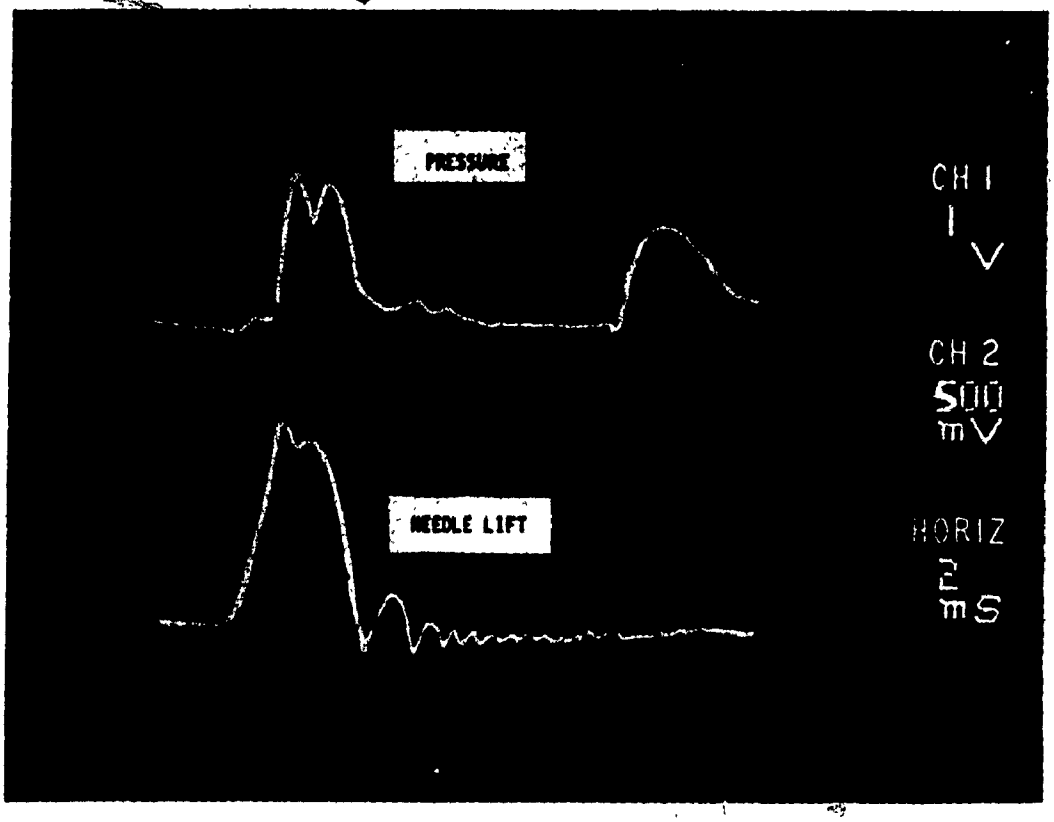

Fig. 4.15 Oscillogram showing the pressure wave created in the long pipe by the gas injection

$$A_p = 2.83 \times 10^{-5}\ m^2$$

Then, from equation (4-5)

$$\dot{m}_{avg} = 2.31\ g/s$$

Therefore, the injected dose is calculated as:

$$m = \dot{m}_{avg} t = 6\ mg$$

The gas dose measured by the graduated cylinder, shown in figure 4.7, was found to be 6.2 mg. This result is very close to the one obtained from the callibration.

Despite the good correlation obtained between these two measurements, there are still several problems which have to be solved before this method can be considered as a reliable tool in the development of diesel engines with hydrogen injection. These problems can be specified as follows:

1. Optimization of the residual pressure in the long pipe and development of a better relief valve which would maintain a constantly repeating residual pressure after every injection.

2. Optimization of the diameter and the length of the

pipe in order to obtain a correct pressure wave shape without interference between the pressure wave remaining from the previous injection with the measured one.

3. Selection of the best pressure transducer in terms of sensitivity and dynamic response, including the use of filters.

4. Selection of the optimal location for installation of the transducer.

5. Use of a computer controlled data acquisition system which allows the direct calculation of the fuel dose as well as the immediate scalling and printing of the graph.

The pressure wave was also recorded by an IBM personal computer by using a data aquisition system having 16 KHz sampling rate. A pressure wave obtained from this method is shown in figure 4.16. This graph, while not fully elaborated, was made as a first step towards the use of data aquisition system as suggested above. Note that the shape of the pressure wave obtained by the data aquisition system is very similar to the one obtained by the oscilloscope. It has to be noted that

the sampling rate of the data aquition system is critical in this case of a very fast process.

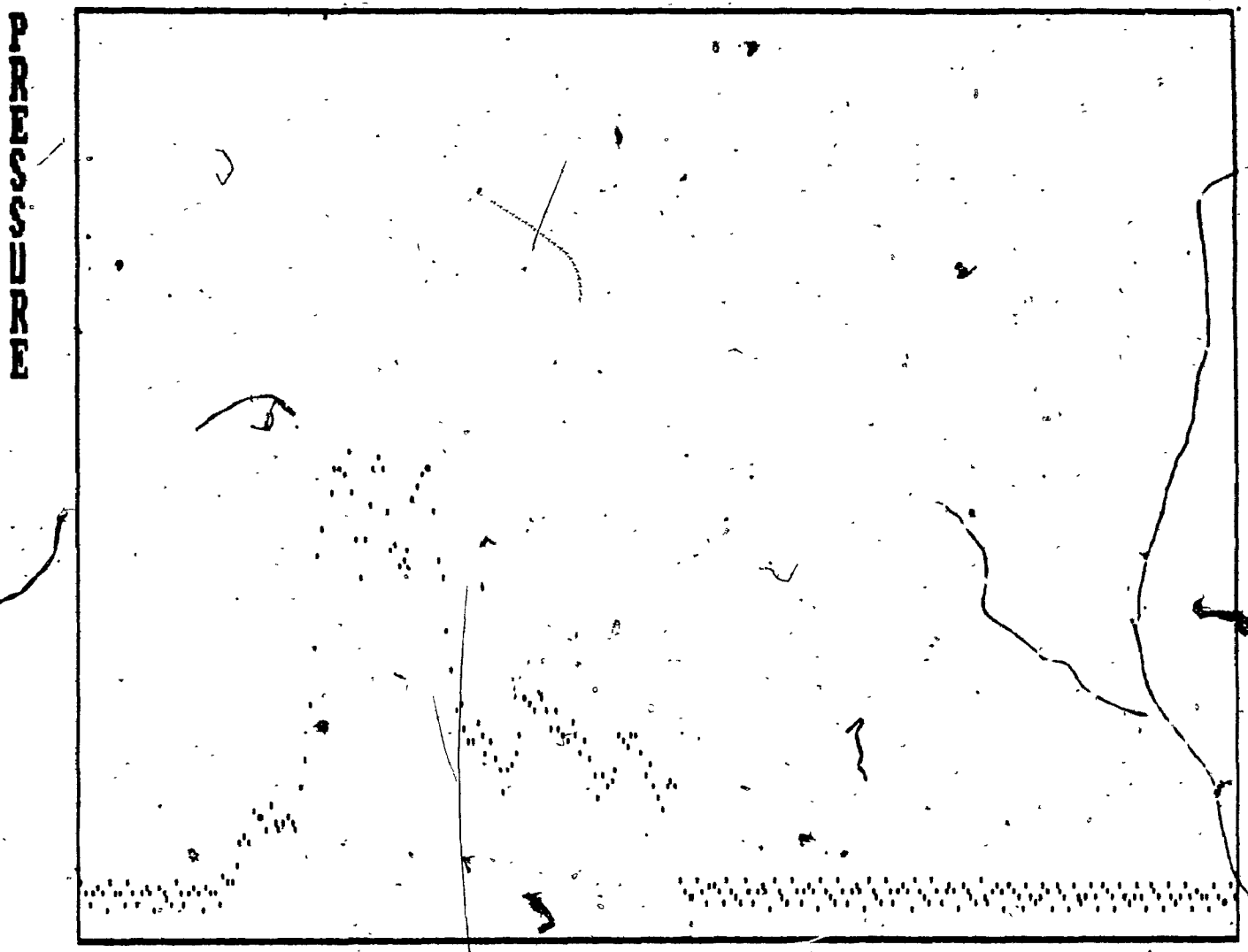

Fig. 4.16 Pressure wave obtained by the IBM data aquisition system

CHAPTER 5

COMPUTER SIMULATION OF THE GAS INJECTION SYSTEM

5.1 INTRODUCTION

The fuel injection system responds to the input action of two forces: an electrical, produced by a solenoid actuator and a hydraulic caused by gas pressure. The hydraulic force acts constantly at the bottom area of the needle whereas the solenoid force acts only when the actuator is energized at the beginning of each injection process. The attempted mathematical model will simulate the gas injection process at all operating conditions of the engine, since the gas flow is assumed to be always choked in the injector orifice area between the pintle and the nozzle hole.

In this chapter, the formulation of the mathematical model describing this system will be presented firstly. Then, since the system of equations is stiff and nonlinear, a brief discussion will be made concerning the numerical solution of such equations. Finally, the computed results will be compared with experimental data.

5.2 FORMULATION OF THE MATHEMATICAL MODEL

5.2.1 Objective.

The equations governing solenoid actuated fuel injectors consist of three components:

1. Electromagnetic component. It relates the electrical and mechanical energies, in other words, it converts the current and the voltage applied to the actuator into the exerted electromagnetic force (energy balance).

2. Mechanical component. It describes the dynamic behavior of the injector by balancing the forces acting on the needle (momentum balance).

3. Fluid Dynamics component. It calculates the instantaneous mass flow rate of the fuel (mass balance). In this component the fuel flow is also integrated to produce the total fuel dose for one injection.

Thus, the complete mathematical model of the gas injection system should include all three components in

order to be able to optimize its performance. A general model which describes a complete fuel injector dynamics has been attempted by Smith [71] for a gasoline injector. However, since in this feasibility study the objective is to simulate only the gas flow through the orifice, the equations describing the electromagnetic component will not be developed. The force exerted by the solenoid actuator will be assumed as a step input function and it will be taken into account in the force balance equation.

The mathematical model, which consists of one force equation and two mass flow equations, is an initial value problem with initial conditions assumed when the needle is seated. The computer program will solve this set of equations for very small time increaments, beginning from the initial conditions and terminating when the needle returns to rest at the seat. These are well known techniques and are used in numerical solutions of initial value problems.

5.2.2 Basic Assumptions

The gas injection model consists of four volumes and three orifices in series as shown in figure 5.1. The flow area A_{12} corresponds to the injector inlet and may be either set manually at a fixed position as in the metering valve, or may vary from zero (closed position) to a maximum, as in the control valve. The other two flow areas, namely A_{23} and A_{34}, are always variable and

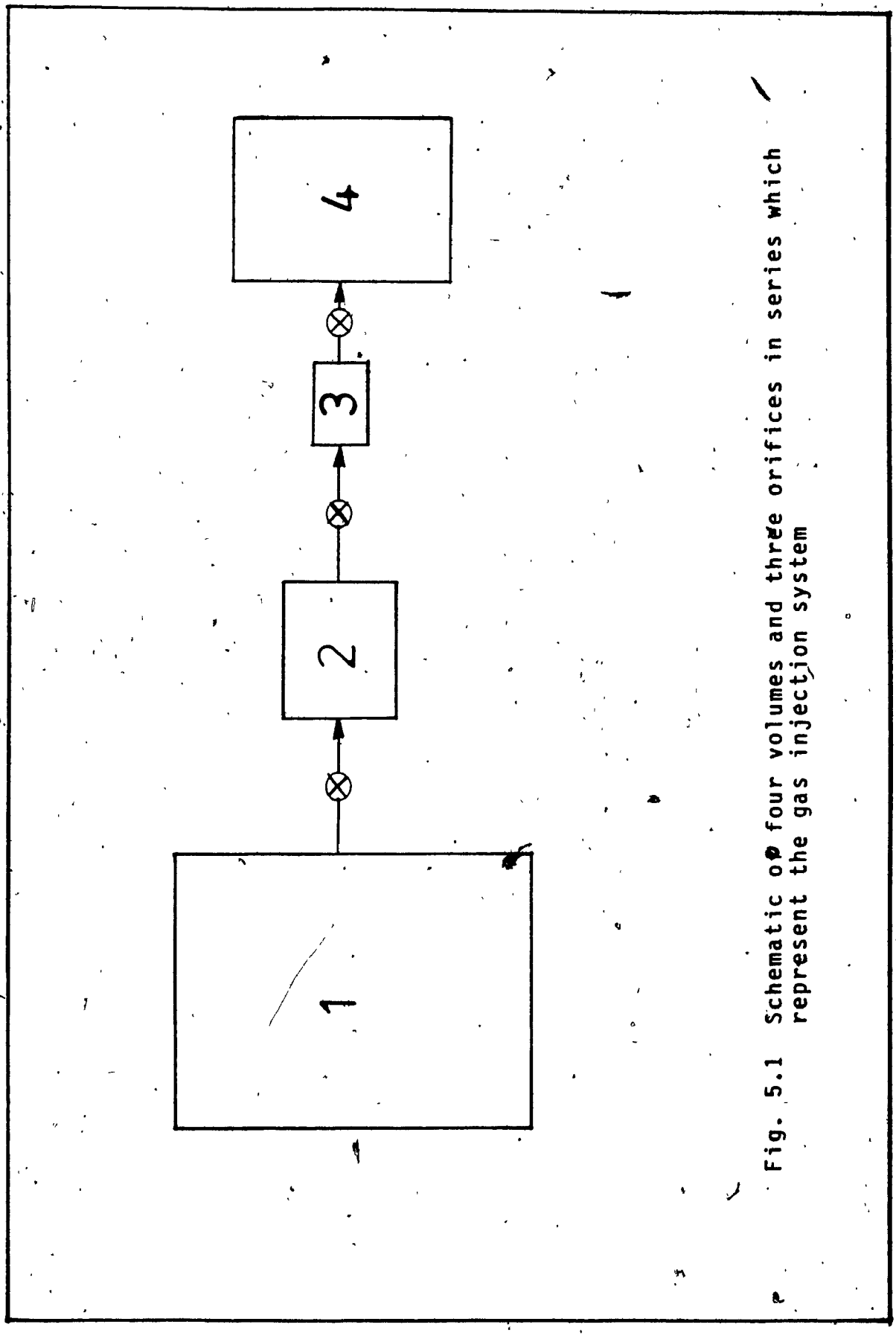

Fig. 5.1 Schematic of four volumes and three orifices in series which represent the gas injection system

depend on the needle lift of the injector. A_{23} is related to the needle seat flow area and A_{34} is related to the nozzle orifice flow area. The mathematical model for this system is derived according to the following assumptions:

1. The impact of the pressure waves can be neglected because of the proximity of all components of the model.

2. The pressure under the needle seat has a uniform distribution when the nozzle opens.

3. Pressures P_1 and P_4 remain constant during injection due to the corresponding large volumes.

4. The injection process occurs under isothermal conditions.

5. The volume change of each chamber due to the movement of the needle does not affect significantly the change of pressure.

6. The flow of gas through the orifices is isentropic.

The differential equations describing this injection system consist of two parts. One part describes the change of pressure in each chamber and the other describes the motion of the needle. The change of pressure is determined from the continuity equation whereas the needle motion is determined from the conservation of momentum. For such formulation, the injection system is assumed to have a fully opened metering valve in order to reduce the computation time. If a control valve were used, then another equation for its needle motion would be required.

5.2.3 Conservation of Mass. The conservation of mass law states that the rate of change of mass within the control volume must be equal to the rate of mass that crosses the control surface.

That is, for chamber volume V_3

$$\frac{dm_3}{dt} + \dot{m}_{34} - \dot{m}_{23} = 0 \qquad (5\text{-}1)$$

Since hydrogen is a perfect gas, the mass in the chamber is obtained from the equation of state.
Hence,

$$m_3 = P_3V_3/RT_3 \qquad (5\text{-}2)$$

where R is the gas constant for hydrogen.

If we differentiate equation (5-2), with respect

to time, we will have:

$$\frac{dm_3}{dt} = \frac{1}{R}\frac{d}{dt}\left(\frac{P_3V_3}{T_3}\right) = \frac{1}{R}\left(\frac{dZ_3}{dt}\right) \quad (5\text{-}3)$$

where

$$Z_3 = P_3V_3/T_3$$

The mass entering and leaving the chamber is given by

$$\dot{m}_{23} = \rho_{23}U_{23}A_{23} \quad (5\text{-}4)$$

$$\dot{m}_{34} = \rho_{34}U_{34}A_{34} \quad (5\text{-}5)$$

where ρ and u are the density and velocity of the gas at the corresponding points in figure 5.2.

The density and velocity terms in equations (5-4) and (5-5) can be expressed in terms of upstream temperature, pressure and a factor N [62]. The factor N is the ratio of the actual flow to the critical flow through the orifice. N is a function of the ratio of specific heats γ and of the downstream to upstream pressure ratio.

Thus,

$$\dot{m}_{23} = BP_2A_{23}N_{23}/\sqrt{T_2} \quad (5\text{-}6)$$

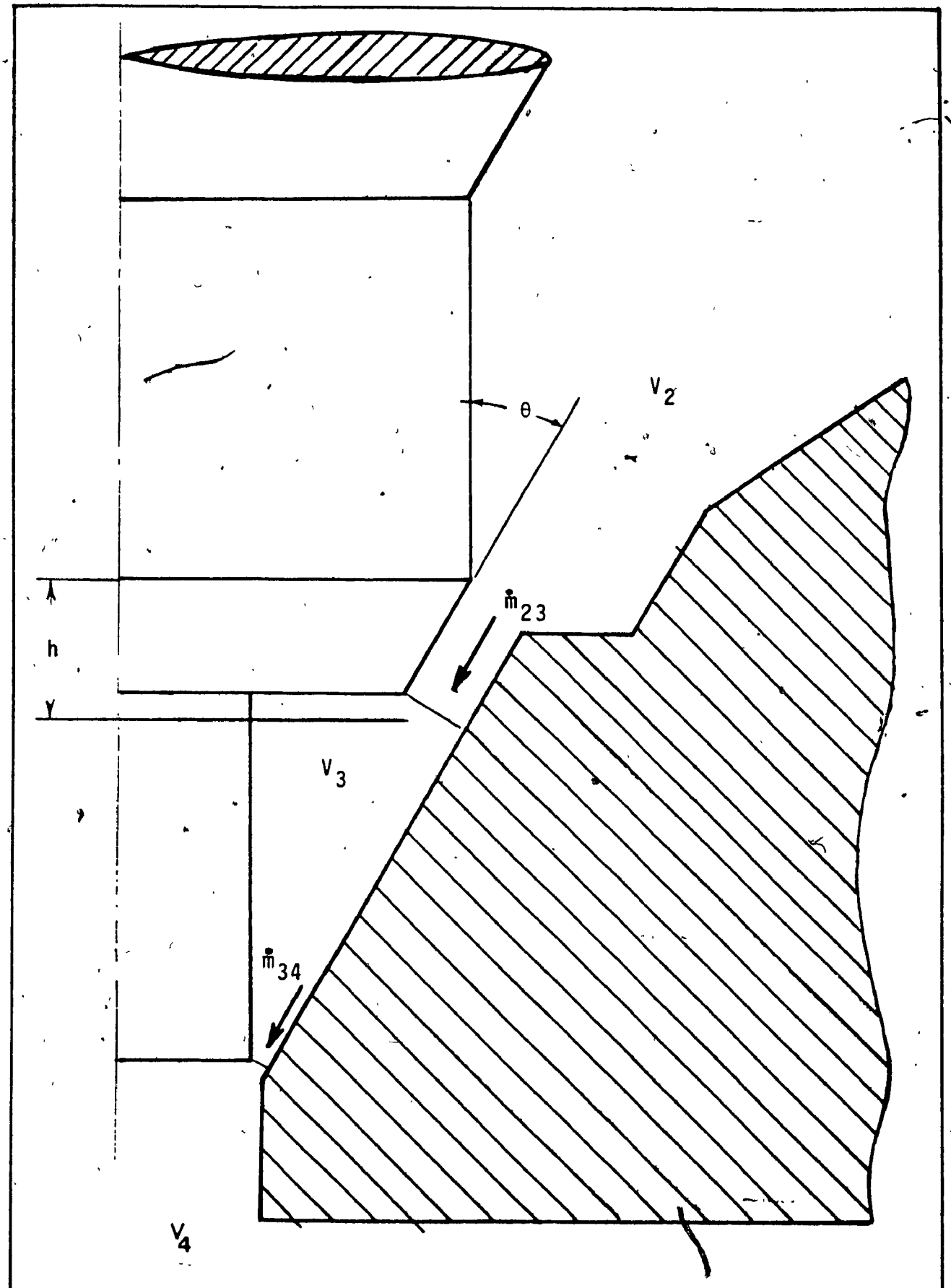

Fig. 5.2 Actual flow areas between volumes V_2, V_3 and V_4

and

$$\dot{m}_{34} = BP_3A_{34}N_{34} / \sqrt{T_3} \qquad (5\text{-}7)$$

where

$$B = \left[\frac{\gamma}{R}\left(\frac{2}{\gamma+1}\right)^{(\gamma+1)/(\gamma-1)}\right]^{1/2}$$

$$N_{23} = G^{-1}\left[\left(\frac{P_3}{P_2}\right)^{2/\gamma} - \left(\frac{P_3}{P_2}\right)^{(\gamma+1)/\gamma}\right]^{1/2}$$

$$N_{34} = G^{-1}\left[\left(\frac{P_4}{P_3}\right)^{2/\gamma} - \left(\frac{P_4}{P_3}\right)^{(\gamma+1)/\gamma}\right]^{1/2}$$

$$G = \left[\left(\frac{\gamma-1}{2}\right)\left(\frac{2}{\gamma+1}\right)^{(\gamma+1)/(\gamma-1)}\right]^{1/2}$$

Substituting equations (5-3), (5-6), and (5-7) in equation (5-1) an expression of the rate of change of the parameter Z is obtained as follows:

$$\frac{dZ_3}{dt} = \frac{BR}{\sqrt{T_2}}\left[P_2A_{23}N_{23} - \left(\frac{T_2}{T_3}\right)^{1/2} P_4A_{34}C_{34}\right] \qquad (5\text{-}8)$$

where

$$C_{34} = P_3 N_{34}/P_4$$

For the injection system under discussion, the process is assumed to be isothermal. Therefore, equation (5-8) becomes

$$\frac{dZ_3}{dt} = \frac{BR}{\sqrt{T_2}}\left(P_2 A_{23} N_{23} - P_4 A_{34} C_{34}\right) \qquad (5\text{-}9)$$

Since N_{23} and C_{34} are functions of P_3, equation (5-9) is nonlinear and it requires numerical integration. With this formulation the change of mass in the chamber is integrated as a unit in terms of the parameter Z. Then, the pressure is calculated from this parameter. This was found to work better than expressing the differential equation in terms of pressure ratio.

Similarly, for the chamber volume V_2, the conservation of mass yields:

$$\frac{dZ_2}{dt} = \frac{BR}{\sqrt{T_1}}\left(P_1 A_{12} N_{12} - P_3 A_{23} C_{23}\right) \qquad (5\text{-}10)$$

where

$$C_{23} = P_2 N_{23}/P_3$$

and

$$N_{12} = G^{-1}\left[\left(\frac{P_2}{P_1}\right)^{2/\gamma} - \left(\frac{P_2}{P_1}\right)^{(\gamma+1)/\gamma}\right]^{\frac{1}{2}}$$

5.2.4 Conservation of Momentum.

The rate of change of the flow areas in equation (3-3) depends on the rate of displacement of the injector's needle. In turn, the needle motion is affected by a number of forces which act as depicted in figure 5.3.

This system has one degree of freedom and its differential equation will be established on the basis of Newton's law of motion [72].

The generalized model representing this type of systems is shown in figure 5.4a. The displacement h(t), of the mass m_t, is measured from the static equilibrium position. Displacement h(t), velocity dh/dt and acceleration d^2h/dt^2 are positive in upward direction and a positive force on the mass m_t will produce a positive acceleration of the mass and vice versa. Refering to the free-body diagram, in figure 5.4b, the forces acting on the mass are:

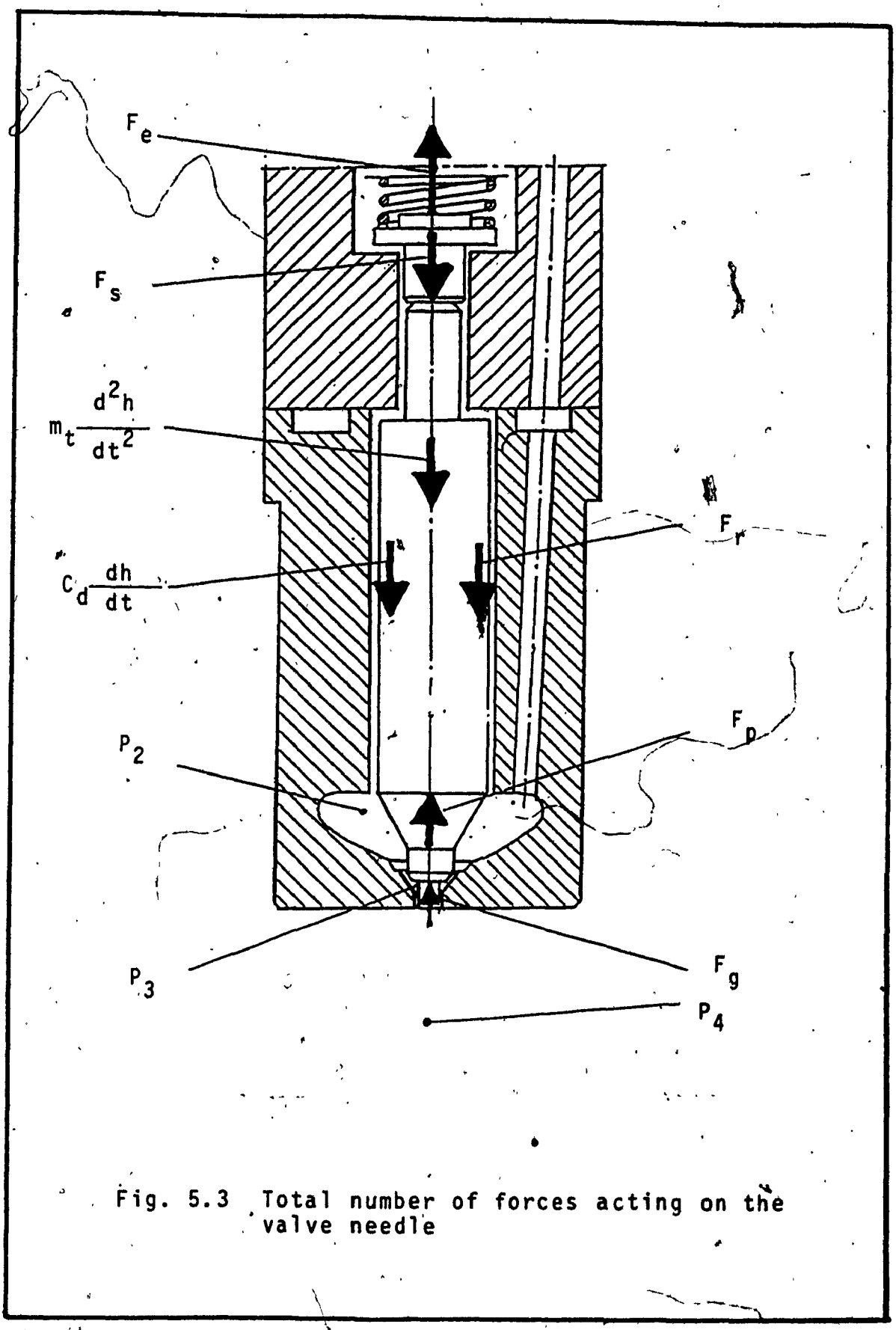

Fig. 5.3 Total number of forces acting on the valve needle

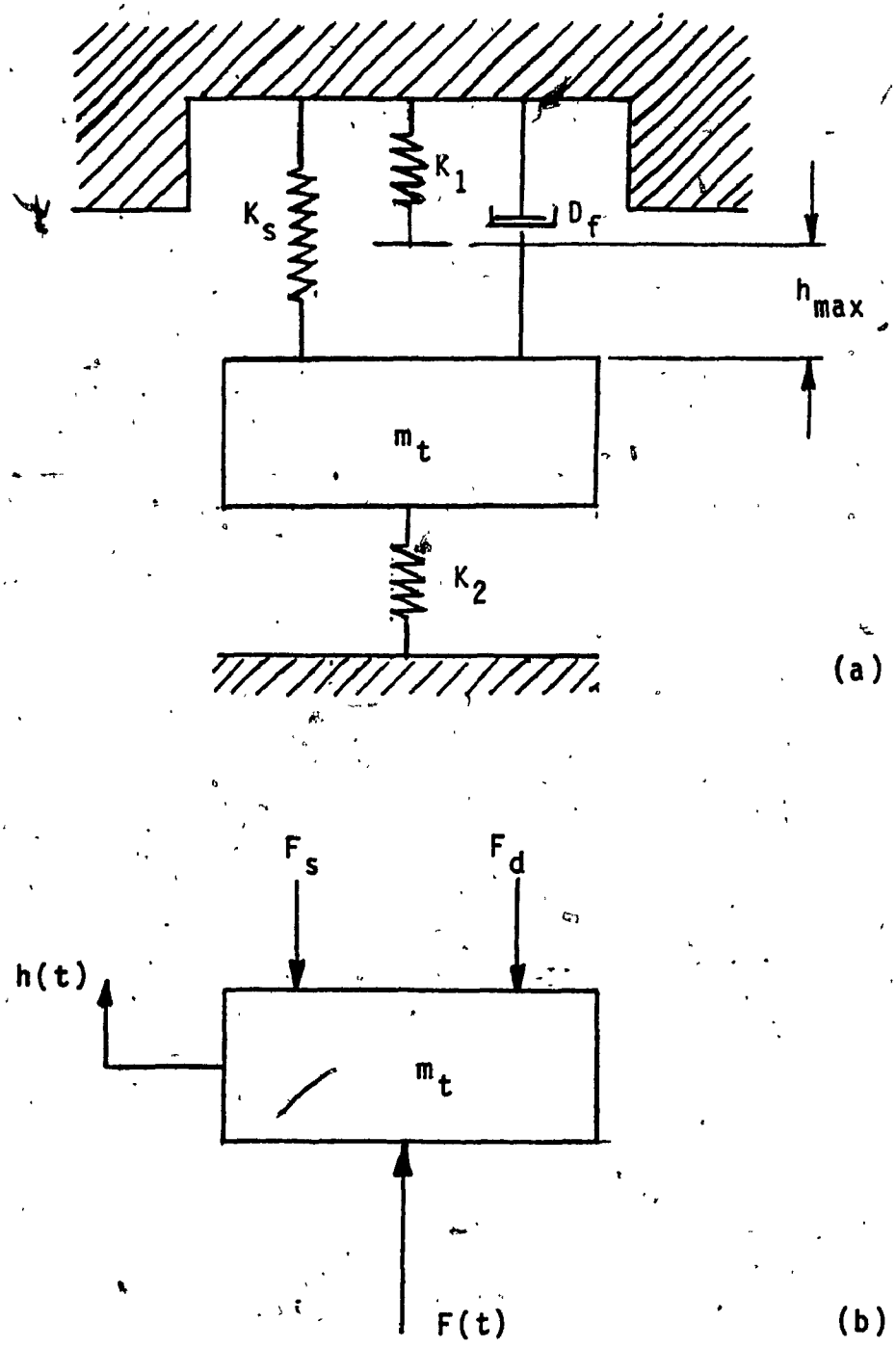

Fig. 5.4 Generalized model of the valve needle dynamics

1. The spring force F_s which always opposes the displacement of the mass.

2. The damping force F_d which is given by equation (A2-5) (see Appendix 2)

$$F_d = \frac{\pi d_i}{2}\left(P_1 - P_e \right)$$

3. The excitation force F(t), which is a function of time and is expressed as the sum of pressure forces F_g, Coulomb friction F_r, electrical force F_e and spring preload force F_{sp}.

Since the pressure forces and the electrical force are periodic functions of time, it follows that the excitation force is also a periodic function of time.

According to Newton's second law, the rate of change of linear momentum is proportional to the applied force and assumes the direction in which the force acts. Thus, from the free-body diagram, the equation of motion of this system is

$$m_t \frac{d^2 h}{dt^2} = \sum F_h \qquad (5\text{-}11)$$

Using d' Alembert's principle, equation (5-11) can be expressed as

$$m_t \frac{d^2h}{dt^2} - \sum F_h = 0 \qquad (5\text{-}12)$$

where the quantity $m_t (d^2h/dt^2)$ is called the inertia force [73]. Hence, introducing the appropriate inertia force, it can be said that the applied force on the mass is in equilibrium with the inertia force and that the dynamic problem is reduced to an equivalent problem of statics.

In explicit terms equation (5-12) becomes

$$m_t \frac{d^2h}{dt^2} + K_s h = F(t) \qquad (5\text{-}13)$$

where

$$F(t) = F_e + F_g - F_s - F_d \pm F_r$$

and

$$F_g = P_3(f_{so} - f_{po}) + p_4 f_{po}$$

The total moving mass m_t, of the system is given by equation (3-11). Therefore, the needle motion is described by a second order differential equation.

5.3 NUMERICAL SOLUTION OF THE DIFFERENTIAL EQUATIONS

It is not always possible to obtain an analytical solution to every differential equation encountered in practice. Especially, the study of pneumatic systems requires the consideration of both nonlinearity and compressibility. These factors make the analysis of pneumatic systems very complicated and require the use of numerical methods for their solution.

A great number of numerical methods have been developed for the solution of differential equations [74,75]. The application of a particular method depends on the type of the problem under consideration. Many physical situations yield initial value problems involving ordinary differential equations which exhibit a phenomenon which is known as "stiffness" [76,77]. Such problems arise from the study of pneumatics, heat and mass transfer, chemical reactions, electrical circuits and many others. Any attempts to use classical methods and techniques to solve such problems encounter substantial difficulties and may lead to high cost of computation and poor accuracy due to round-off errors. This necessitates the careful examination of the special features of stiff systems of equations [78,79].

The problem associated with stiff systems of ordinary differential equations is two-fold: stability

and accuracy. A numerical method is said to be stable if, for a given step size, an error introduced at a particular step does not have a large effect on the computed numerical solution. On the other hand, a method is said to be accurate if at a certain step, the local trancation error does not exceed a certain bound. For non-stiff problems, the accuracy requirement dictates the magnitude of the step size, whereas for stiff problems the stability requirement dictates it. Shampine [80] gives many valuable suggestions on how to handle the stability and accuracy requirements for the solution of stiff ordinary differential equations. Finally, several important theorems on the stability of numerical methods are given by Lapidus [81] and Lambert [82].

In the presented pneumatic system, the equation of motion (eq. 5-13) is linear and non-stiff, whereas the equations of gas flow (eq. 5-9 and 5-10) are both nonlinear and stiff. This makes the whole system of equations to be considered as a system of stiff and nonlinear ordinary differential equations. In addition, the system has a discontinuity at the initial conditions which makes its solution even more difficult. The initial conditions of this system are the following:

For $t = 0$ $\quad h = 0.0$

$\quad U = 0.0$

$\quad P_2 = P_1$

$$P_3 = P_4$$

The computer simulation of the hydrogen injection process is terminated when the valve needle has returned to the closed position.

A solver from the International Mathematical and Statistical Library (IMSL) has been used to obtain the numerical solution of this system of equations [83]. The code uses a pair of fifth and sixth order explicit Runge-Kutta formulas and is very efficient for handling nonstiff differential equations. However, since the stability region of these methods increases as their order increases, stiff problems can also be handled if the step size is sufficiently small.

5.4 DISCUSSION OF THE CALCULATION RESULTS

There is no doubt about the usefulness of the computer model for predicting the dynamic behaviour of a solenoid injector. However, one must be able to know how well the predicted response can approximate the actual dynamic behaviour of an injector.

To compare the calculated results with those obtained experimentally, the needle movement and the pressure in the injector were recorded as is discussed in chapter 4. In addition, all data that were used for the computer simulation of the injection process are given in appendix 4. As is shown in figure 5.5, the predicted needle movement almost coincides with the experimental data. In order to obtain this needle movement characteristic, the solenoid force was assumed to vary as is shown in figure 5.6. This force characteristic was assumed according to the following criteria:

1. When the solenoid was energized, the traction force increased extremely fast and the needle began to move only when this force exceeded the preload force. For this prototype injector the spring preload was found in chapter 3 to be F_{sp} = 152 N. In the computer calculations, the solenoid force for needle opening

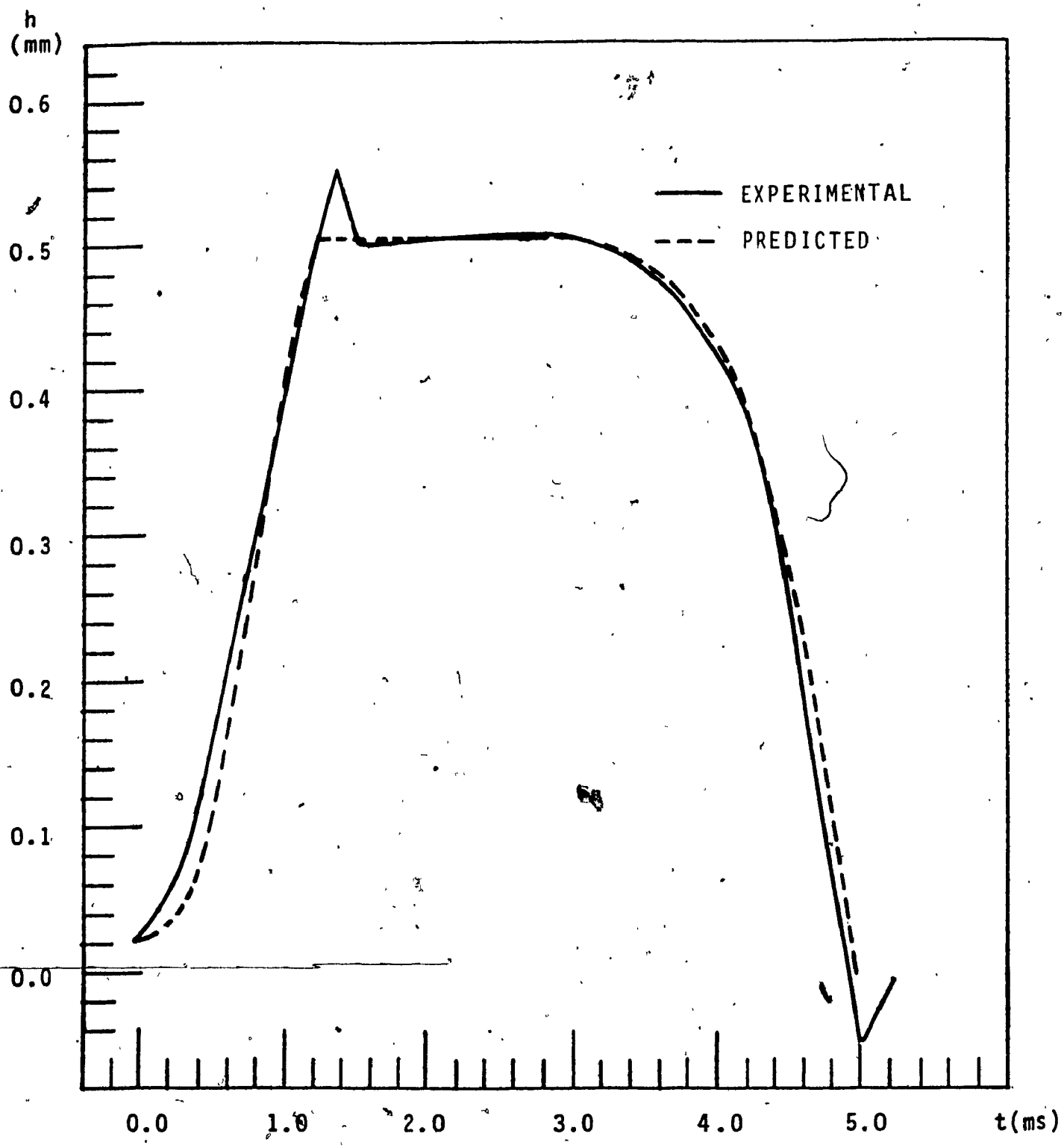

Fig. 5.5 Injector needle lift characteristics

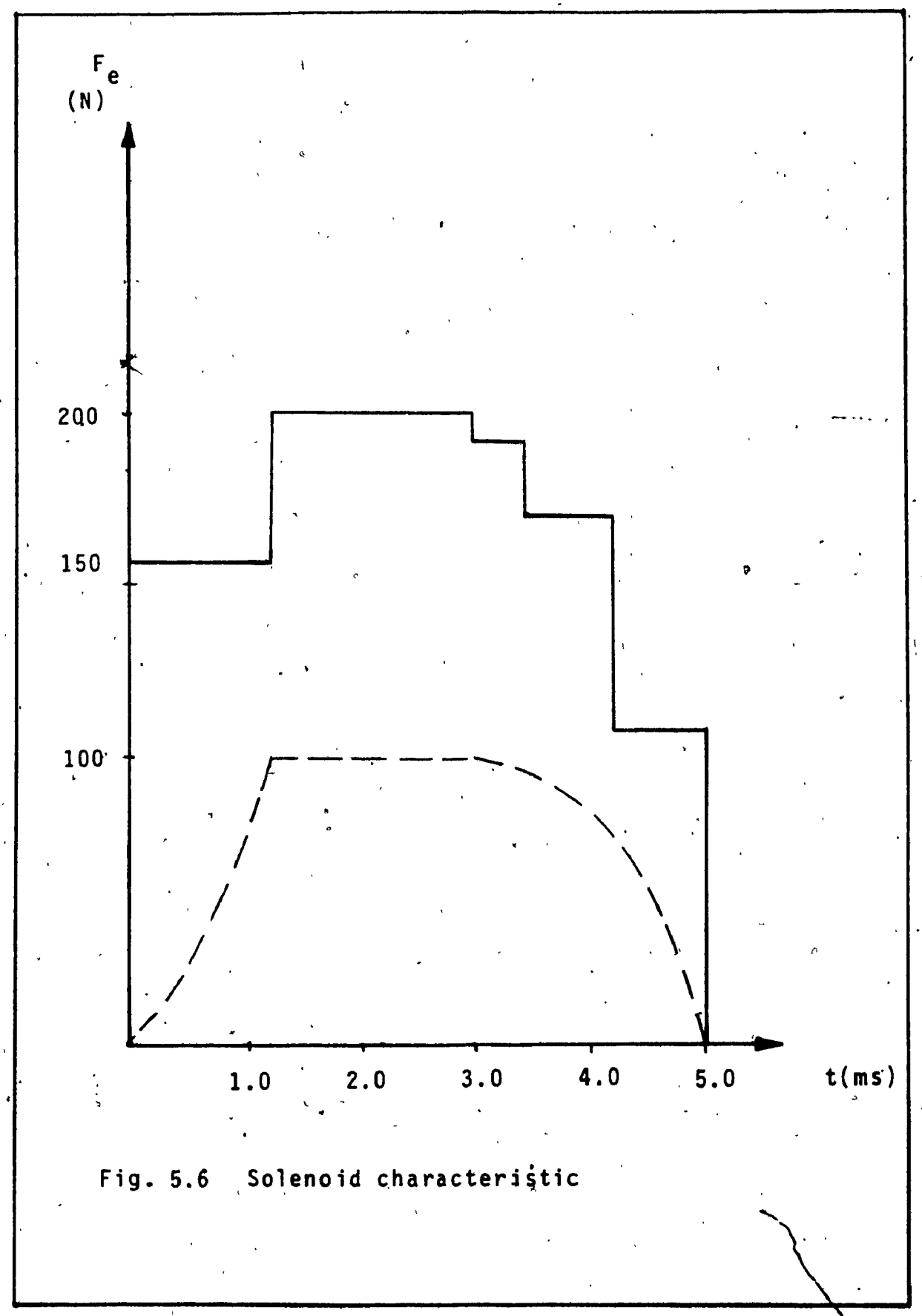

Fig. 5.6 Solenoid characteristic

was assumed to be 164 N in order to produce the same needle lift characteristic. This indicates that the initial effective force was 12 N. However, just after the needle started to move, there was an additional force of 84 N due to the gas pressure acting in the needle seat. Thus, the total effective force was 96 N. This force would ideally open the needle fully (.50 mm stroke) in 0.94 milliseconds. Therefore, the 1.20 ms opening time, as computed and as found experimentally, took into account damping and frictional forces as well as pressure variations.

2. When the needle had opened fully, the additional force required to hold it at that position was found to be F_e = 218 N. Thus, when the needle reached its maximum lift, it was assumed that the solenoid provided this force.

3. In order to close the injector, the solenoid force should be cancelled so that the energy stored in the spring would be able to return the needle to its seat. However, during the tests, it was found that the deenergizing process in the solenoid played an important role in increasing the injector's closing time. The solenoid force, generated during the injector's opening, did not disappear instantly after the current was cut-off. This resulted in delaying

the nozzle closing. Therefore, in the valve closing process, the solenoid force was assumed to decrease in four steps while the needle was closing instead of one that was assumed for the opening process. In each step, the force was assumed to drop a certain percentage of the maximum (holding) force. These percentages are:

1st step: 4%

2nd step: 15%

3rd step: 42%

4th step: 100%

The pressure drop in the injector was obtained by assuming a restriction with constant flow area at the inlet of the injector. This restriction represented all losses in the injector's ducting system. As it can be seen from figure 5.7, the calculated pressure in the injector almost coincides with the pressure signal obtained experimentally.

Another factor which was taken into consideration in evaluating the accuracy of the predicted results was

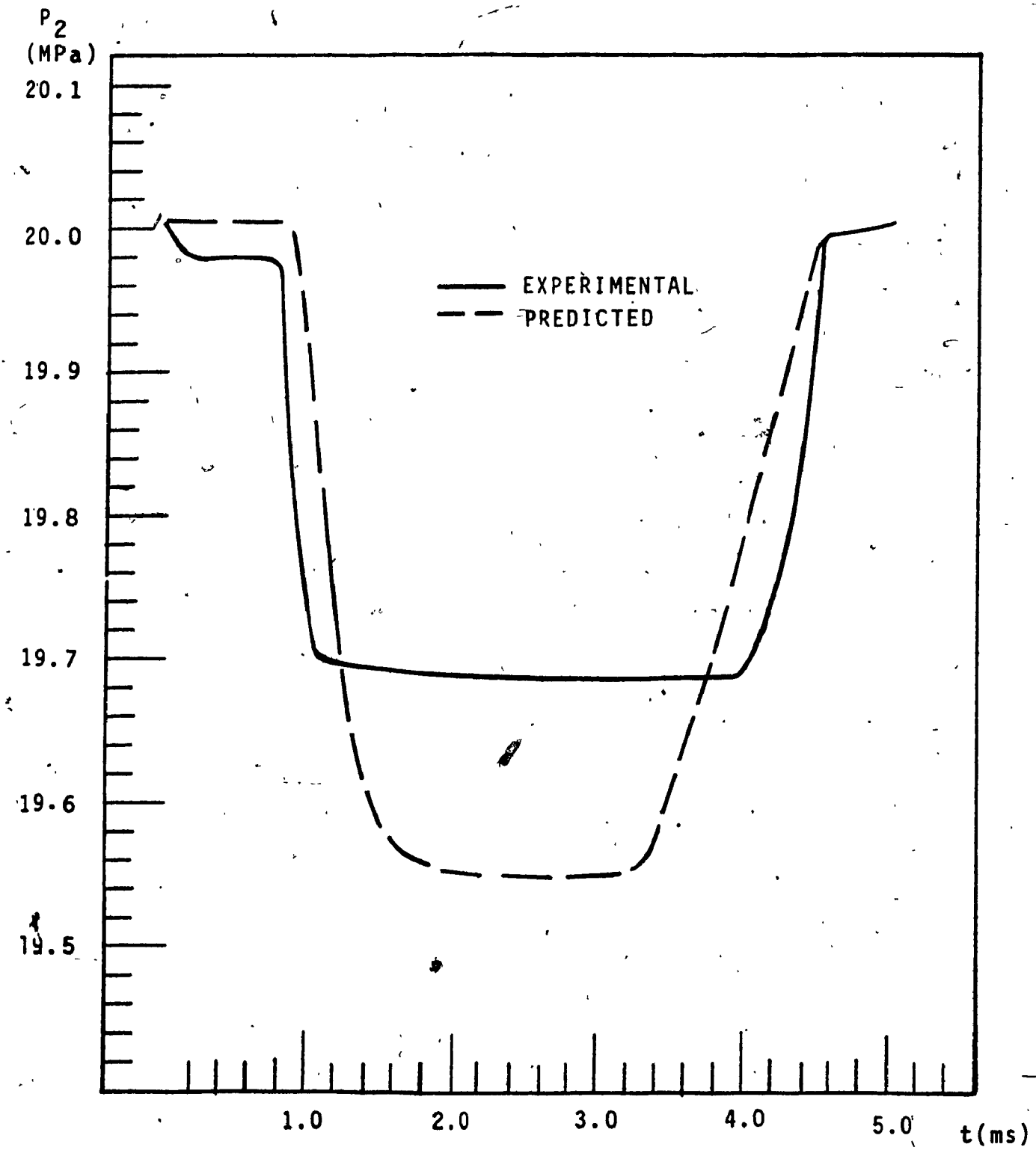

Fig. 5.7 Injector pressure characteristic

the total fuel dose per injection. In order to calculate the fuel dose, an average fuel discharge coefficient of 0.75 was assumed. Actually, as is discussed in the literature, the discharge coefficient in a nozzle injector can be assumed to be between 0.60 and 0.90 for approximate calculations. For more accurate calculations, it has to be determined experimentally for each particular injector.

The predicted fuel dose was found to be 11.06 mg (132.45 mL) whereas the measured fuel dose was 11.10 mg (133 mL). This result reveals that the mathematical model can simulate the gas injection process correctly. More reliable results would be obtained only if the actual discharge coefficient of the nozzle were known and if a much more elaborated apparatus could be made which would be able to collect all the gas without leakage.

Finally, the average mass flow rate, calculated as well as obtained experimentally, can also be considered for the assessment of the mathematical model. In chapter 4, it was found that the average mass flow rate of hydrogen $\dot{m}_{avg}$ = 2.31 mg/ms. On the other hand, the average mass flow rate calculated by the computer is

$$\dot{m}_{c,avg} = (11.06 \text{ mg})/(4.9 \text{ ms}) = 2.26 \text{ mg/ms}$$

The difference between these two values is 2.2 percent. Hence, the correctness of the simulation has been

confirmed once more.

Since the needle lift, the injector pressure, the total fuel dose and the average mass flow rate were predicted so closely, it may be concluded that the proposed mathematical model gives correct results. Based on this conclusion, it can also be expected that other variables, such as instantaneous mass flow rate, needle velocity and pressure under the needle seat, can be predicted with similar accuracy. These results are shown in figures 5.8,5.9,5.10 and 5.11. Figure 5.8 verifies the assumption of constant pressure under the needle seat once the needle has started to open. Figure 5.9 shows that the velocity characteristic of the needle in the closing phase must be greatly improved. The last two figures, namely 5.10 and 5.11, reveal information on the fuel injection process. Figure 5.10 shows the shape of the hydrogen mass discharge rate characteristic whereas figure 5.11 shows how the fuel accumulates in the engine cylinder with respect to time.

Therefore, the mathematical model could be used to optimize the design of the gas injector, especially of the gas mass flow rate characteristic, by changing the parameters of the nozzle flow area according to the requirements of the engine.

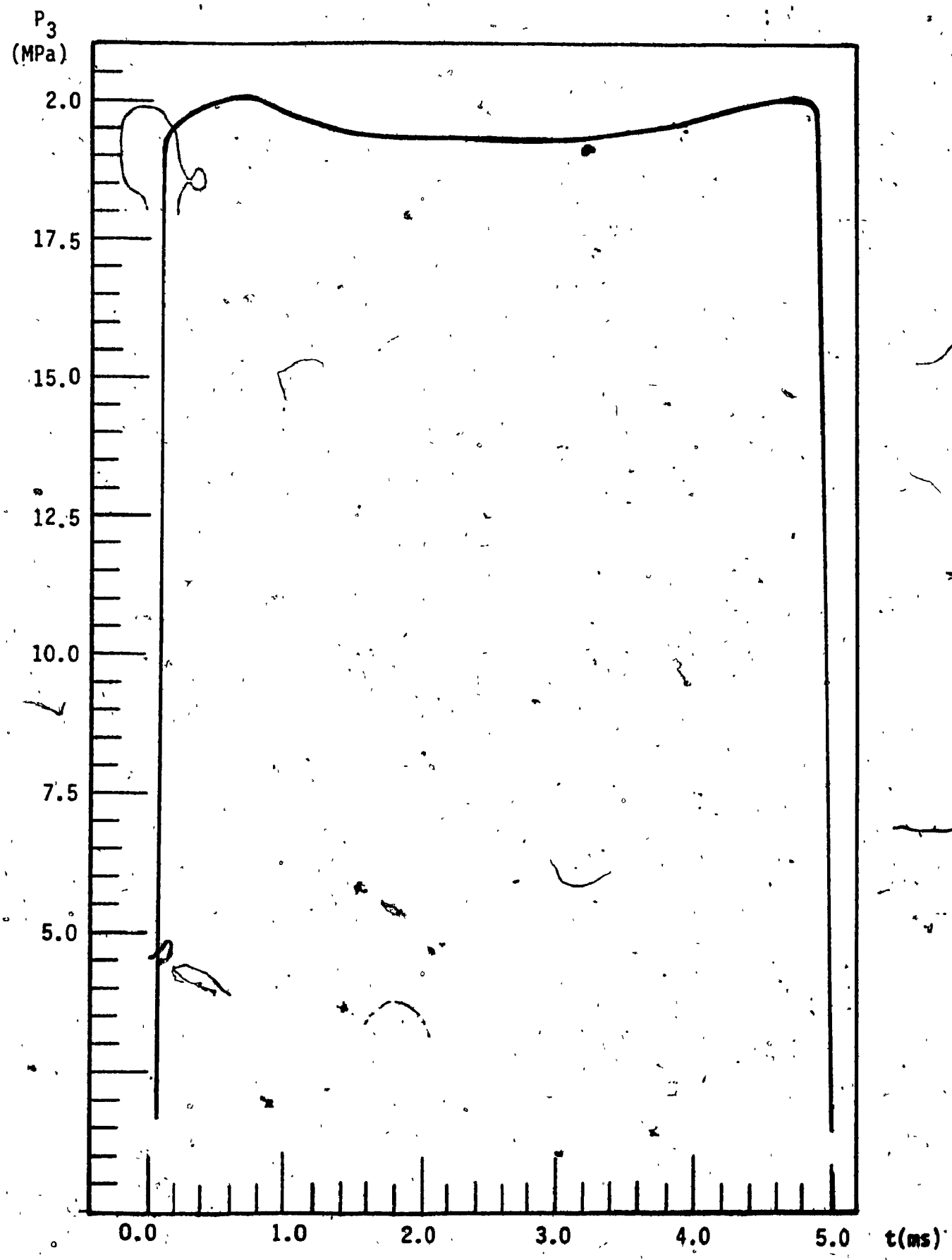

Fig. 5.8 Predicted pressure under needle seat

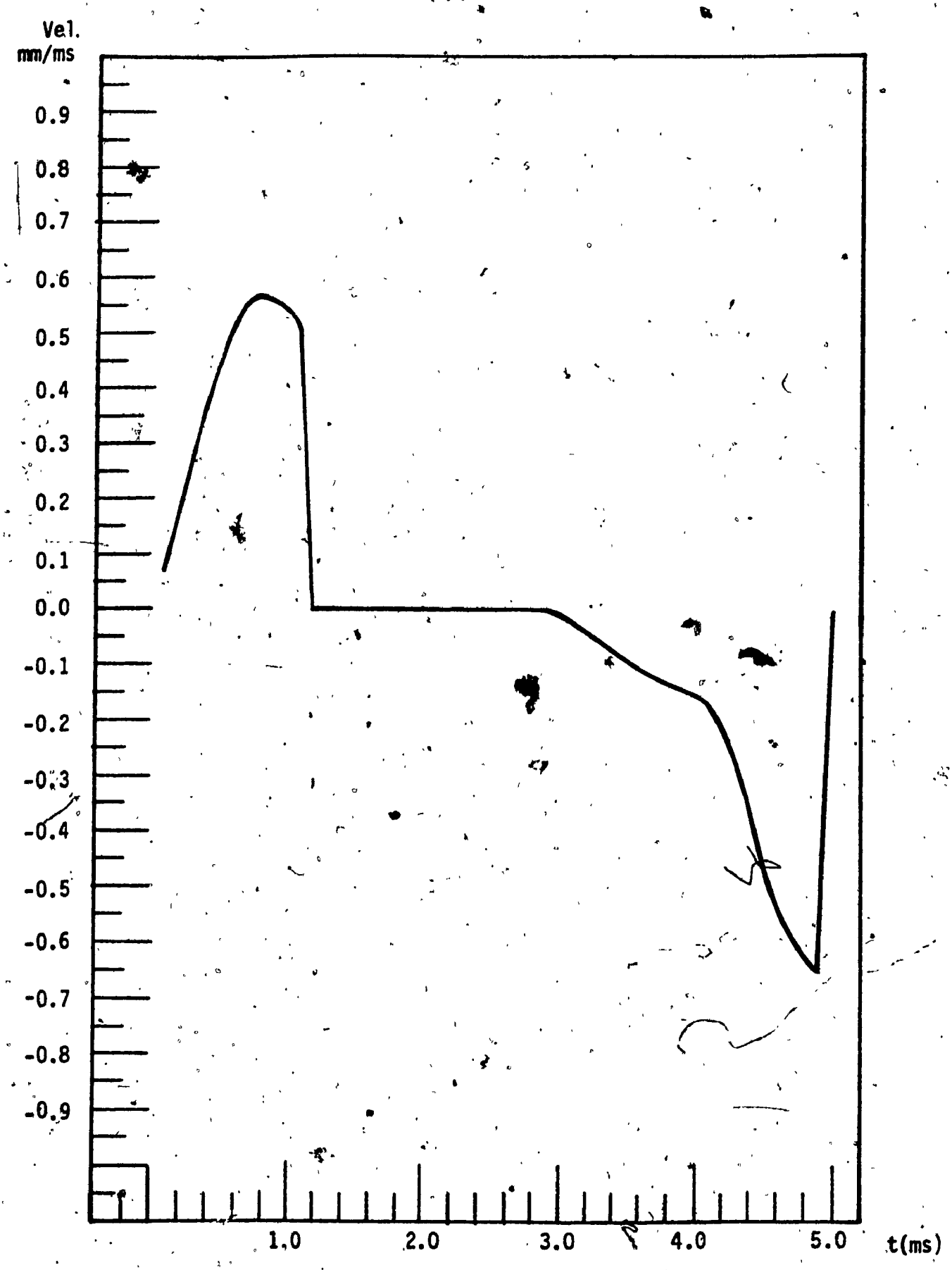

Fig. 5.9 Predicted needle velocity

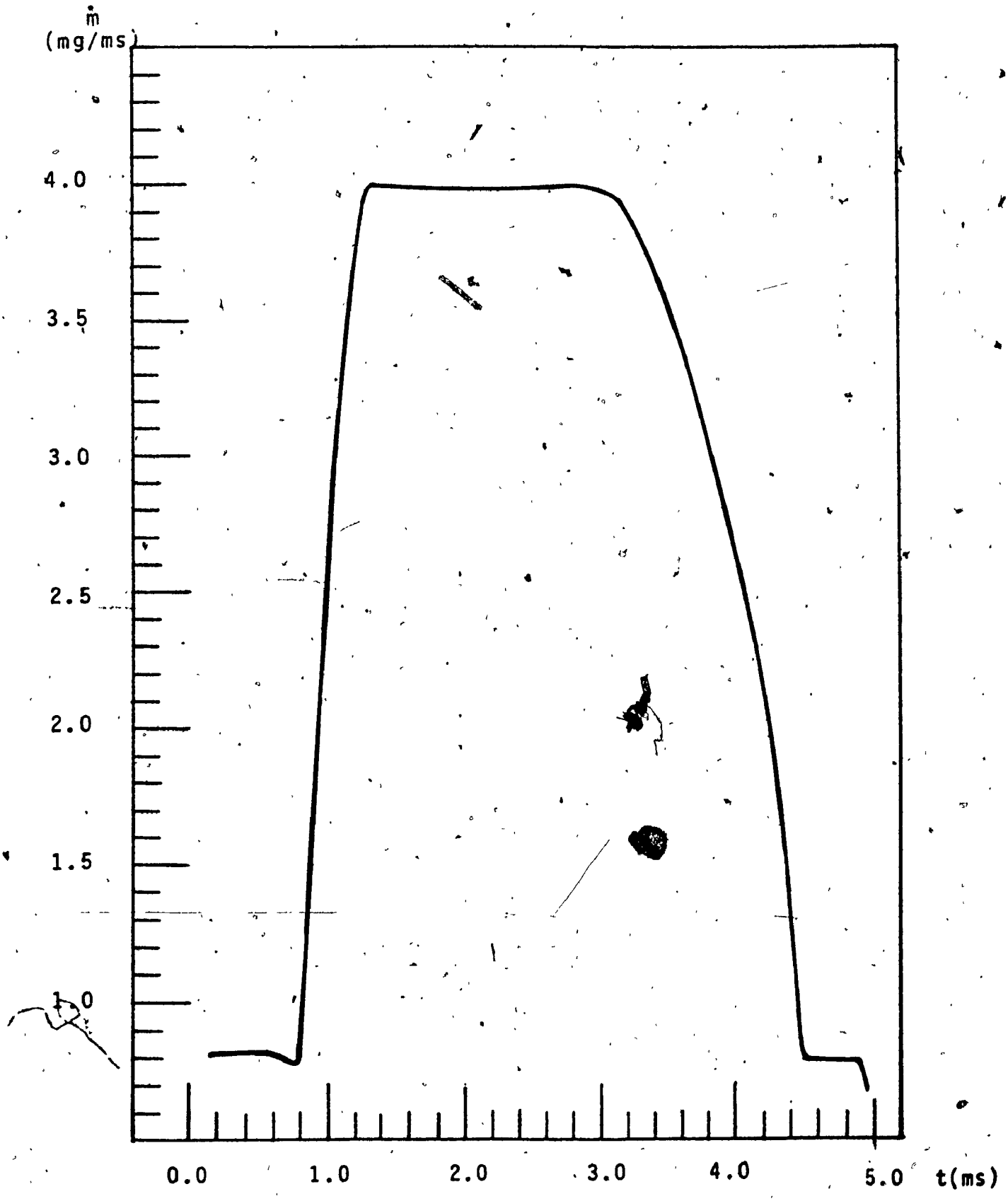

Fig. 5.10 Predicted mass flow rate characteristic

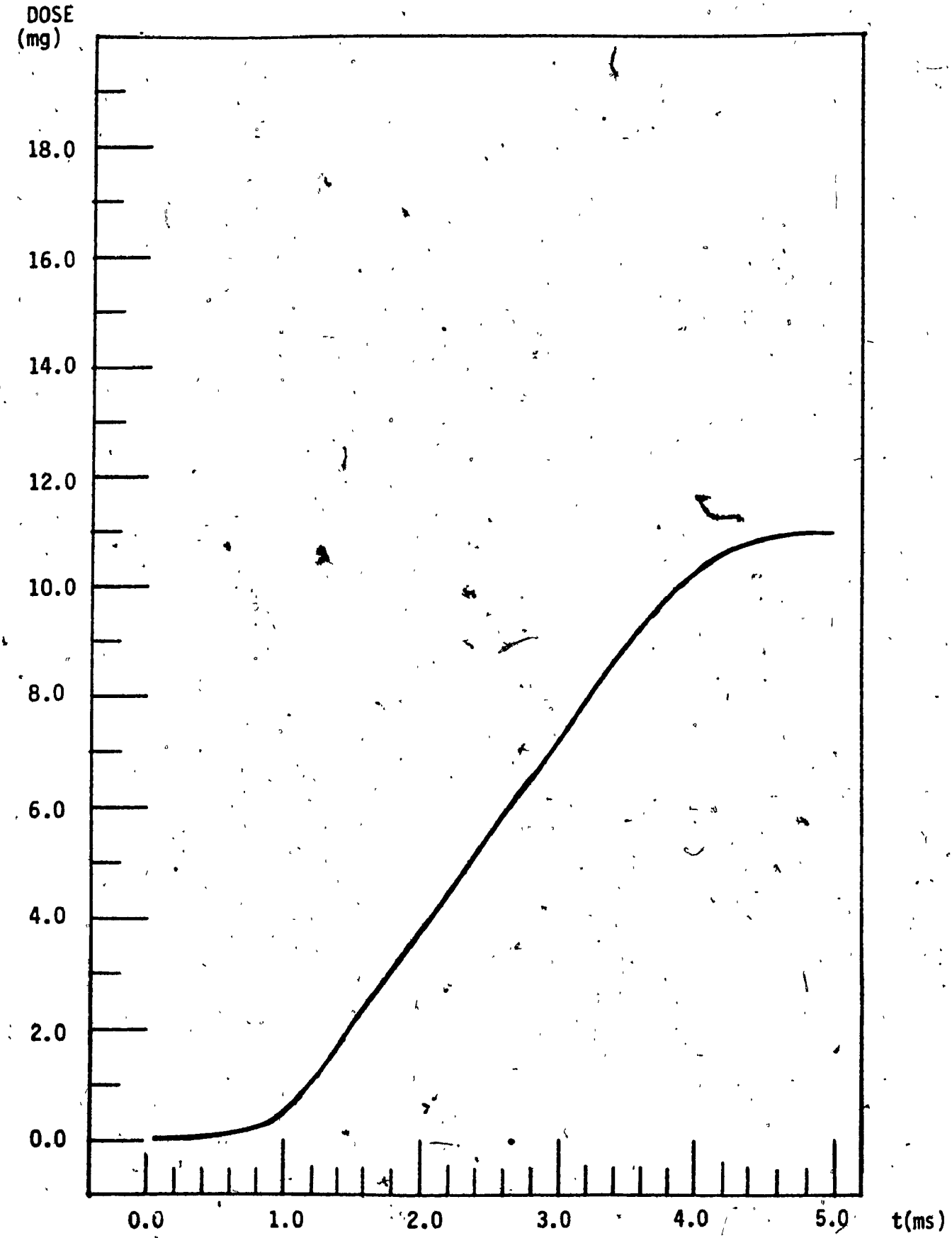

Fig. 5.11 Accumulation of fuel injected vs. injection time

CHAPTER 6

HYDROGEN INJECTION IN A DIESEL ENGINE

6.1 DISCUSSION ON THE FEASIBILITY TESTS

Some tests have been made with hydrogen gas injection into the combustion chamber of a diesel engine by using the developed prototype of the electronically controlled injector. The hydrogen injector was installed in the first cylinder of a 4-cylinder Peugeot diesel engine (plates 6.1 and 6.2). The remaining three cylinders were supplied with diesel fuel by the conventional fuel injection pump. In order to obtain the correct timing of the hydrogen injector with the other three diesel injectors, the microprocessor was controlled by interrupt signals. The control signals were obtained from a magnetic pick-up installed on the end of the crank shaft of the engine.

However, since the Z-80 microprocessor requires the interrupt signal to be a logic zero pulse of approximately 200 ns, a special circuit was built to produce the interrupting pulse when triggered by the magnetic pick-up as shown in figure 6.1. In addition, the circuit included a modulus 2 counter because the microprocessor had to be interrupted every second revolution only.

As expected, the hydrogen did not ignite well when injected into the compressed air. The use of a home made glow plug (plate 6.3) improved ignition but because high

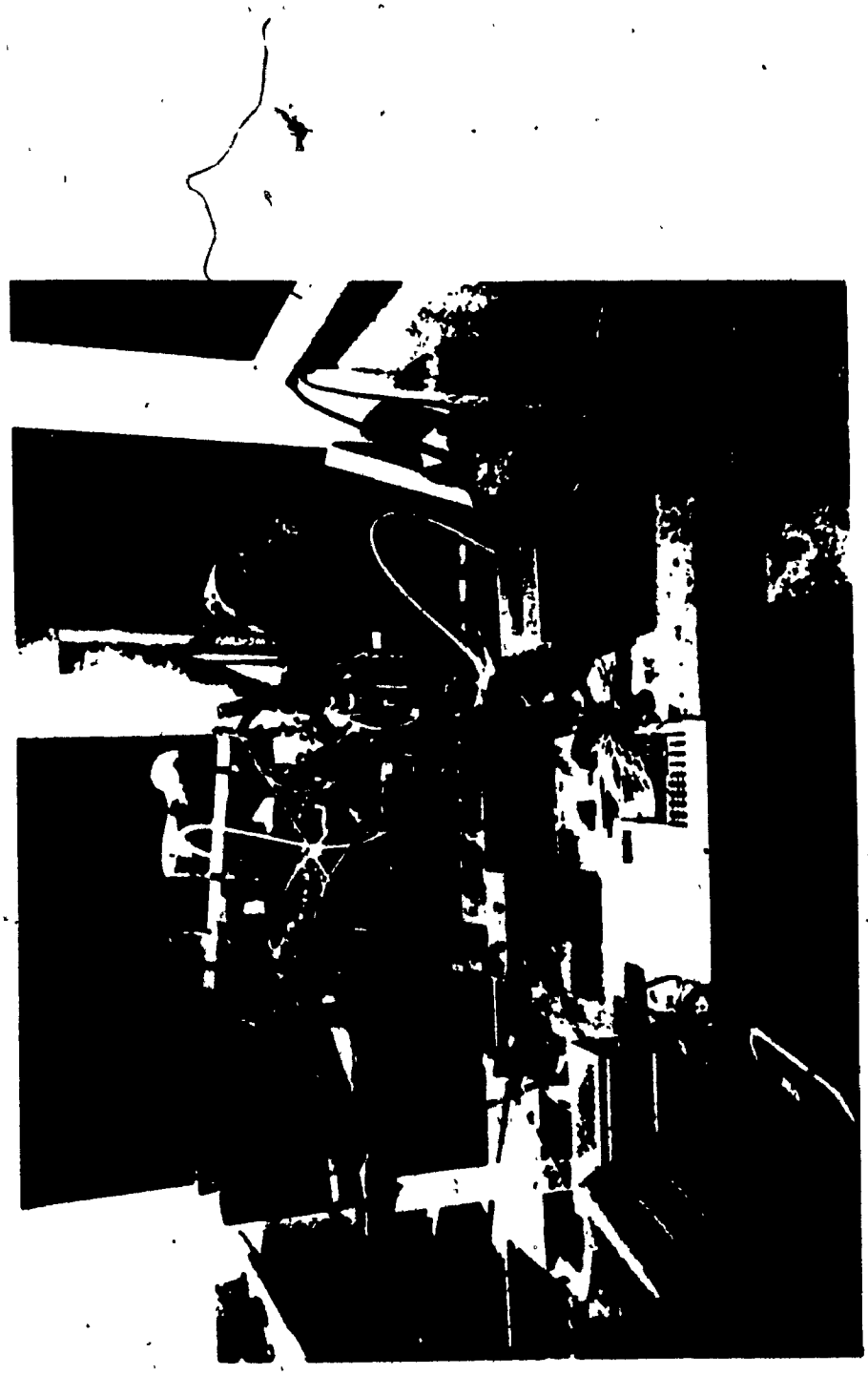

Plate 6.1 Installation of injection system on the diesel engine

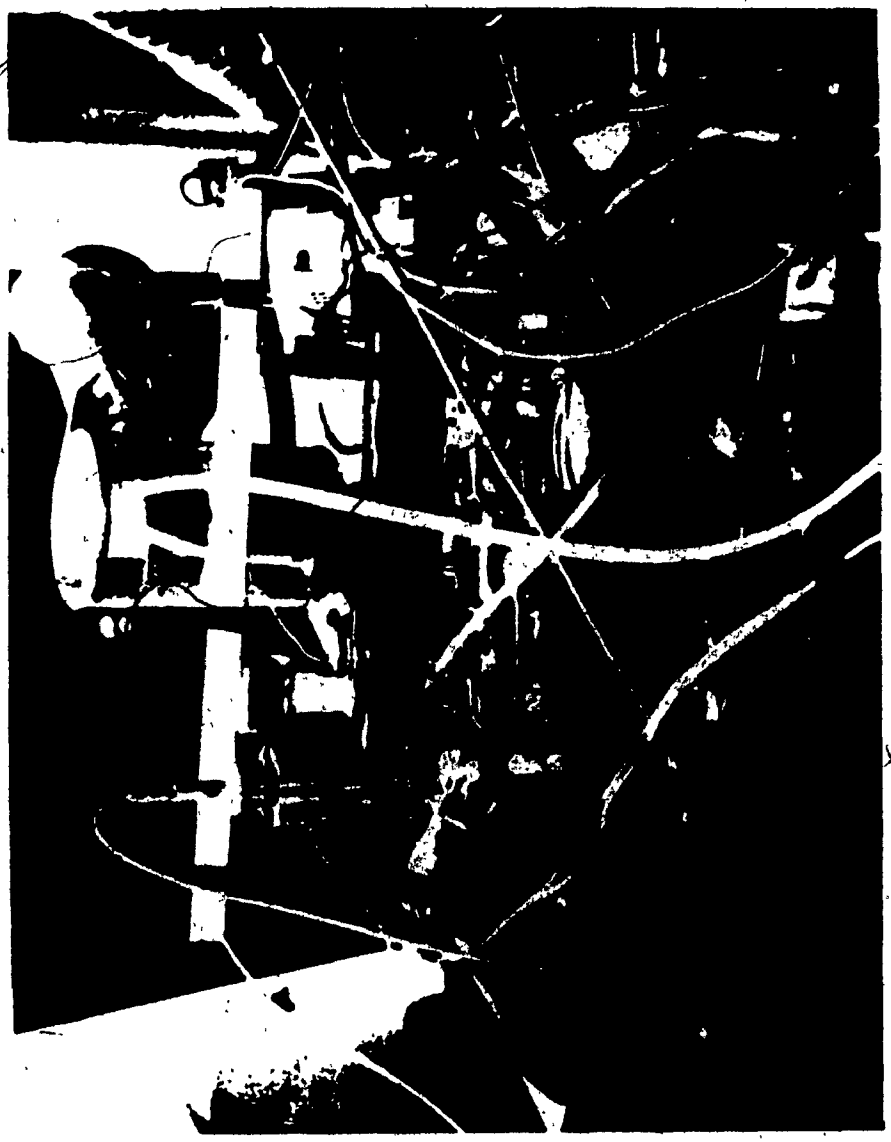

Plate 6.2 Close view of injector installation on the engine

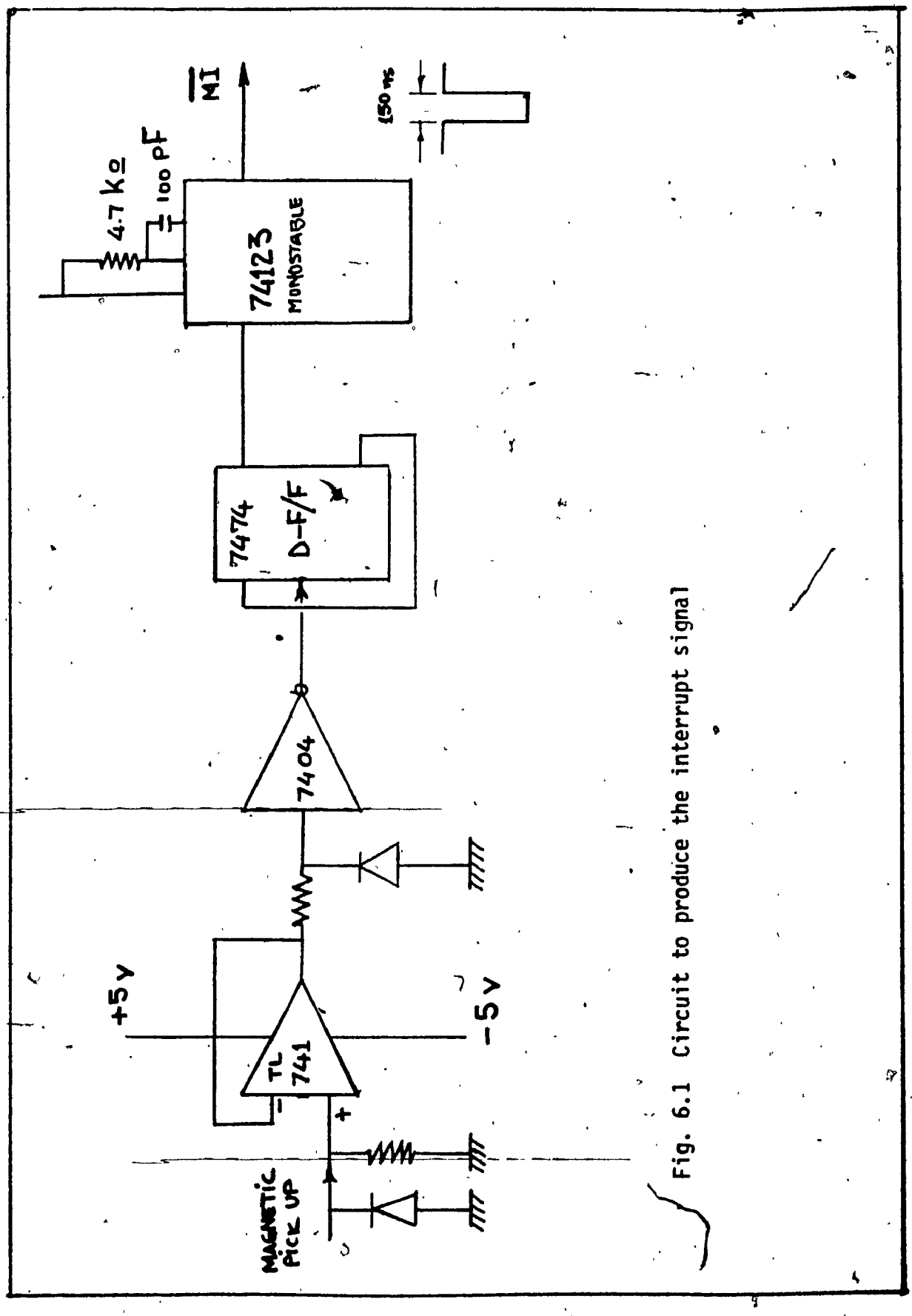

Fig. 6.1 Circuit to produce the interrupt signal

Plate 6.3 Glow plug used in engine tests

advance angle for injection was needed, the high pressure increase rate during combustion was found to be unacceptable. Furuhama [50] conducted extensive research on hydrogen combustion in diesel engines and has recommended a glow plug made with platinum wire, which seemed to have some catalitic effect, as necessary means to assist hydrogen ignition. However, in this research, a platinum wire glow plug was not tested because the effort was concentrated on the spark plug method for ignition support for the following reasons:

1. A spark ignition system based on modern electronic circuit is presently so inexpensive that it can be recommended for ignition support in hydrogen-fuelled compression ignition engines.

2. The ignition point in hydrogen combustion can be much better controlled by a spark plug than by a glow plug, assuming that the spark could be produced after only part of hydrogen would be injected. This would result in the reduction of the excessive pressure increase and in the elimination of the "diesel hammer" phenomenon.

A special spark plug was made (plate 6.4) and it

Plate 6.4 Spark plug used in engine tests

proved to be effective in providing a well controlled ignition of hydrogen-air mixture according to the initial feasibility tests. Several runs have been made with the first cylinder of the engine working on hydrogen. Figure 6.2 shows the spark timing as compared to the fuel injection timing obtained during the runs.

No other conclusions were drawn at this time about the engine performance because serious difficulties were encountered concerning the electronic control during the use of the spark ignition. The voltage required for spark penetration in the high density air, when compressed in a diesel engine, became detrimental to the microprocessor controlling the electronic injector. This interfered in the testing procedure and finally required to place the microprocessor far from the engine to assure its correct operation. Special means seem to be necessary to shield and to protect the CPU against the impact resulting from high intensity sparks which are much stronger than those produced in a spark ignition gasoline engine. Predicting such impact of these sparks on the microcomputers with which the contemporary vehicles are being equipped, the use of the glow plugs initiated successfully by Furuhama might still be a valuable option.

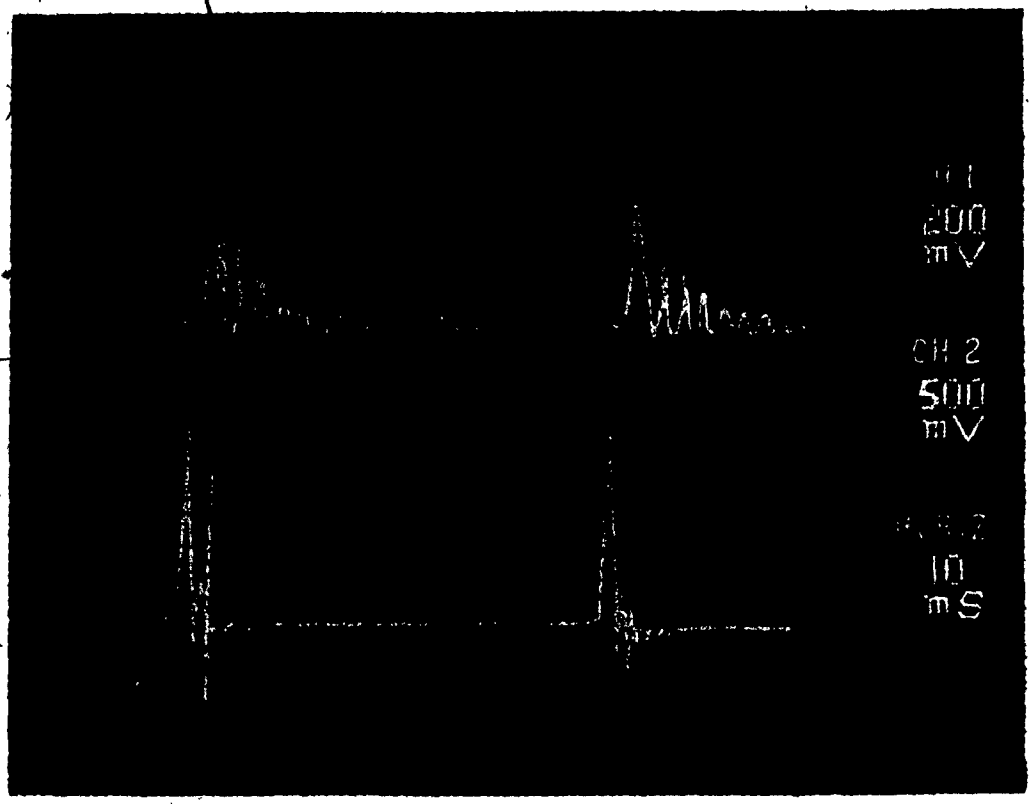

Fig. 6.2 Spark timing in the cylinder provided with hydrogen injection

CHAPTER 7

RECOMMENDATIONS FOR FUTURE WORK

7.1 PROPOSED GAS INJECTION SYSTEM

The results obtained from the presented feasibility study are very encouraging and they have indicated that a gas injection system with electronic control can offer several opportunities. Some of the major advantages that can be achieved are the following:

1. High flexibility in controlling the fuel dose.

2. High reliability due to simple mechanical components.

3. Compact size.

4. Low weight.

5. Low manufacturing cost due to simple hardware.

6. Very limited gas leakage (for the proposed injector).

The objective of this chapter is to propose a modified gas injection system which would be able to fullfil the above requirements. Among the three options tested in this project, the gas injector system with the

metering valve is recommended for further development. However, in the proposed system the metering valve should be provided with a digital actuator in order to control its flow area (fig. 7.1). Thus, the metering valve would perform two functions:

1. It would control the pressure drop in the injector at the end of every injection period.

2. It would be able to change the dose of the gas injected during the opening time period of injector.

The impact of the metering valve on the pressure inside the injector is shown in the oscillograms of figure 7.2. In figure 7.2a the metering valve is fully open, therefore the pressure drop in the injector during the gas discharge is very small. When the metering valve is at this position, the system corresponds to the Injector Only System (IOS) option and can supply the maximum fuel dose. In the other oscillogram, fig. 7.2b, the pressure drop is large due to the throttling effect of the partly open metering valve. The lowering of pressure at the end of each gas injection has four advantages:

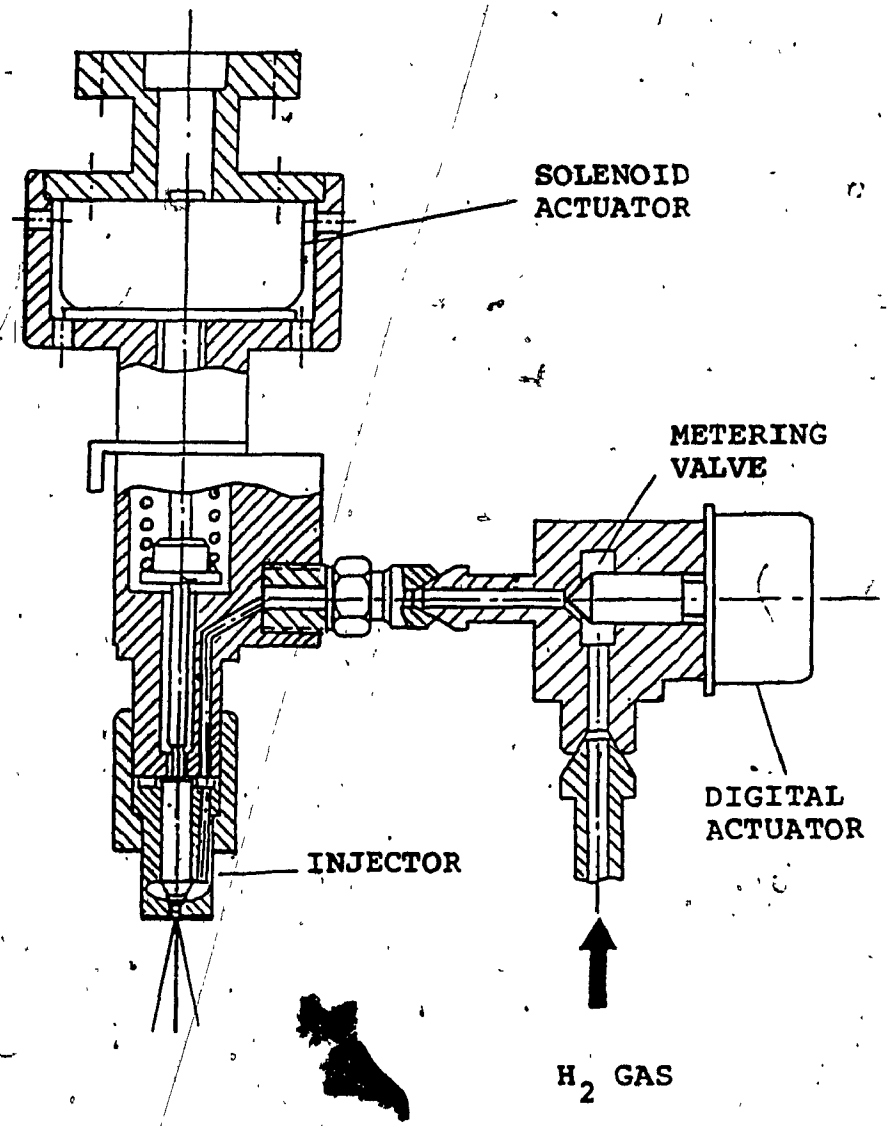

Fig. 7.1 Proposed hydrogen injector with digitally controlled metering valve

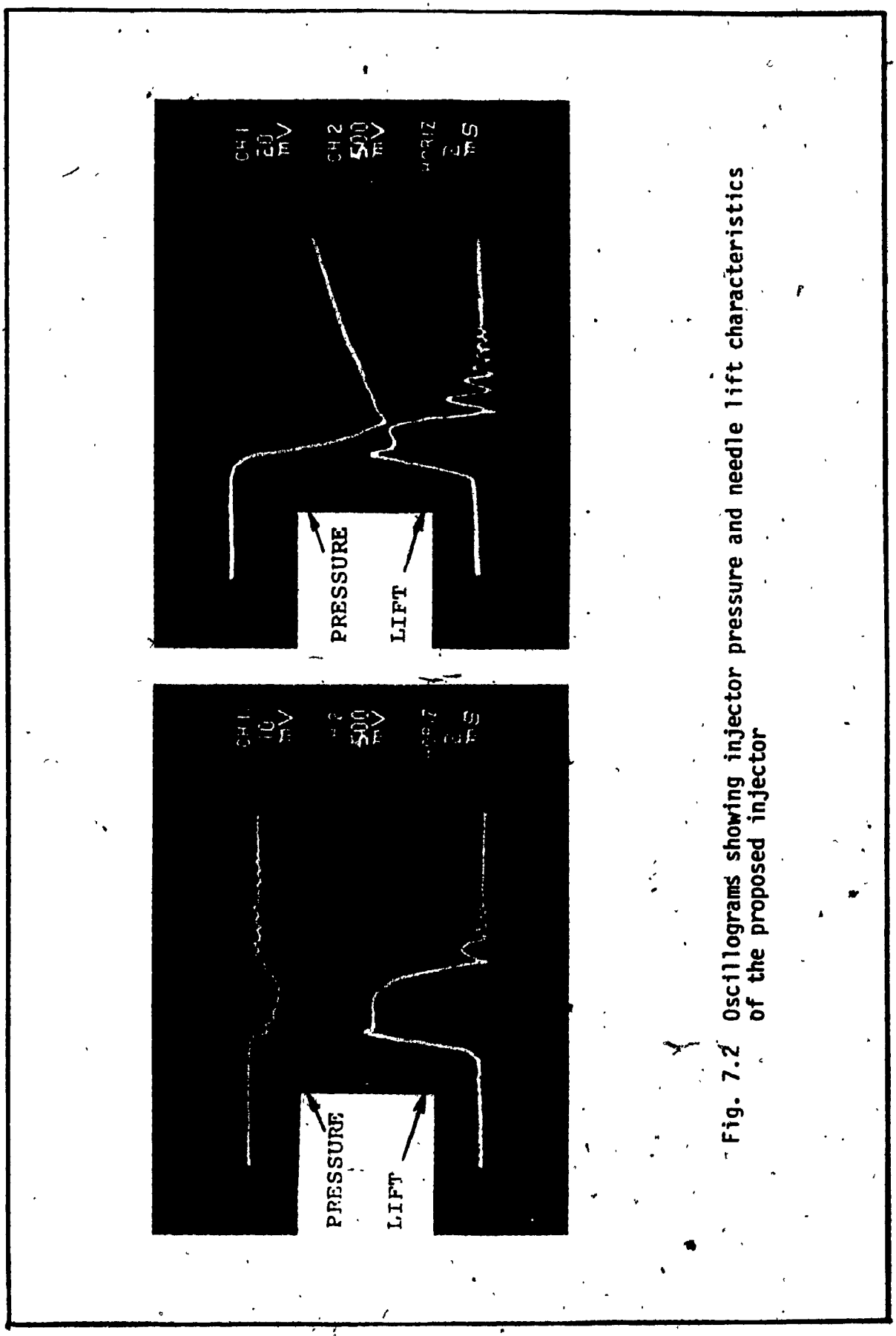

Fig. 7.2 Oscillograms showing injector pressure and needle lift characteristics of the proposed injector

1. It helps in the closing of the injector and avoids post-injection.

2. It reduces the gas leakage from the valve seat, especially right after the end of the injection when the needle is not yet well settled in its seat.

3. It reduces the gas leakage through the needle guide because the mean pressure in the injector is lowered during the part of time between injections.

4. It can control the required fuel dose.

The metering valve would be controlled by a digital actuator (stepper motor) and the degree of opening of the valve would depend on the resolution of the motor, the pitch of the screw and the geometry of the valve needle. Both, the digital actuator and the solenoid actuator will be under the management of a microprocessor which would be part of an on-board microcomputer. The CPU controls the maximum torque characteristic of the engine and acts as a speed governor. Then, the opening time of the injector as well as the degree of opening of the metering valve can be changed so that the fuel dose characteristic is shaped according to the required characteristic of the

compression ignition engine. Such fuel delivery characteristic of a diesel engine is shown in figure 7.3. The dashed lines indicate the possible changes of the characteristic which can be easily introduced due to the electronic control.

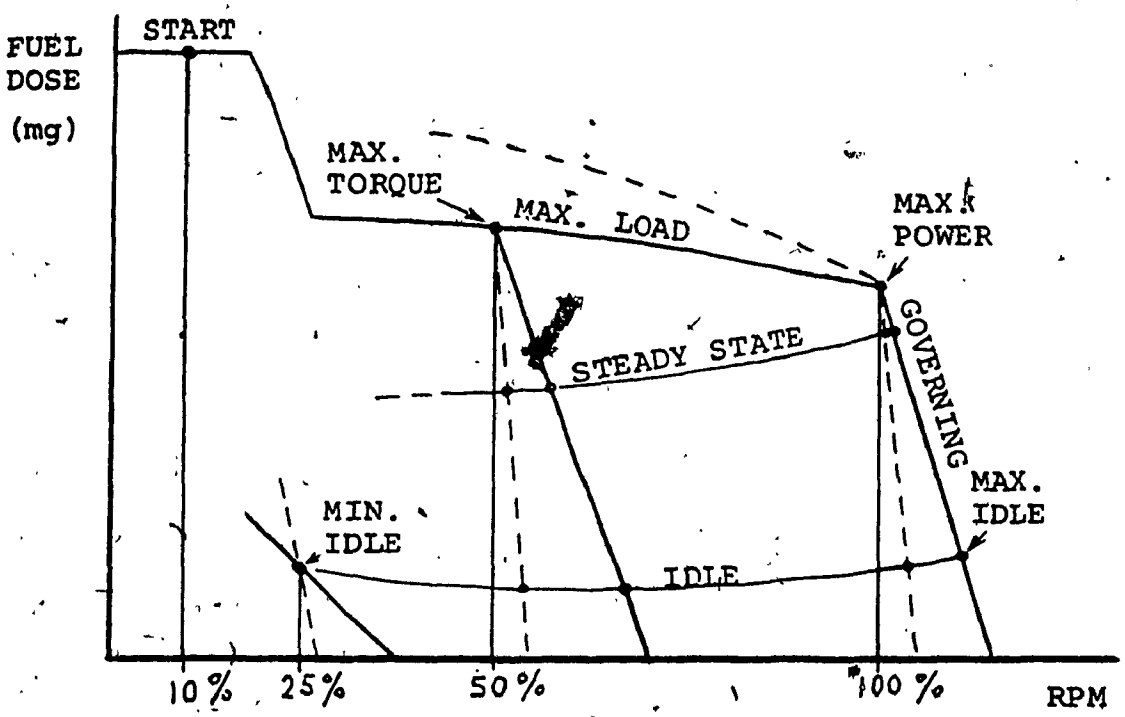

Fig. 7.3 Fuel dose characteristics of a diesel engine operating with the proposed hydrogen injector.

7.2 IMPROVED INJECTOR DESIGN

The large size and weight of the solenoid actuator used in the prototype injector during this feasibility study seem to challenge the rational design of the injector. However, this is not detrimental for this project due to the fact that much more powerful, smaller and lighter solenoids are already available on the market and they are recommended for the proposed prototype system [36,37]. It is believed that the employment of such solenoids will dramatically improve the performance of the proposed injection system which in its present state is already performing well. Two new injector designs are considered: one employing a "HELENOID" actuator (Fig. 7.4a) and one employing a "COLENOID" actuator (Fig. 7.4b) both of which can be designed to be leak proof. However, it is rather recommended to use the double acting COLENOID actuator. This type of actuator offers a unique advantage over the other type: it enables to eliminate the use of springs with high spring rates. In such a case, a spring would be required mainly to hold the needle in the seat when the injector is closed by a relatively small preload force.

The developed injector prototype has the option of controlling the nozzle orifice flow area depending on the needle lift due to the pintle type nozzle used. The

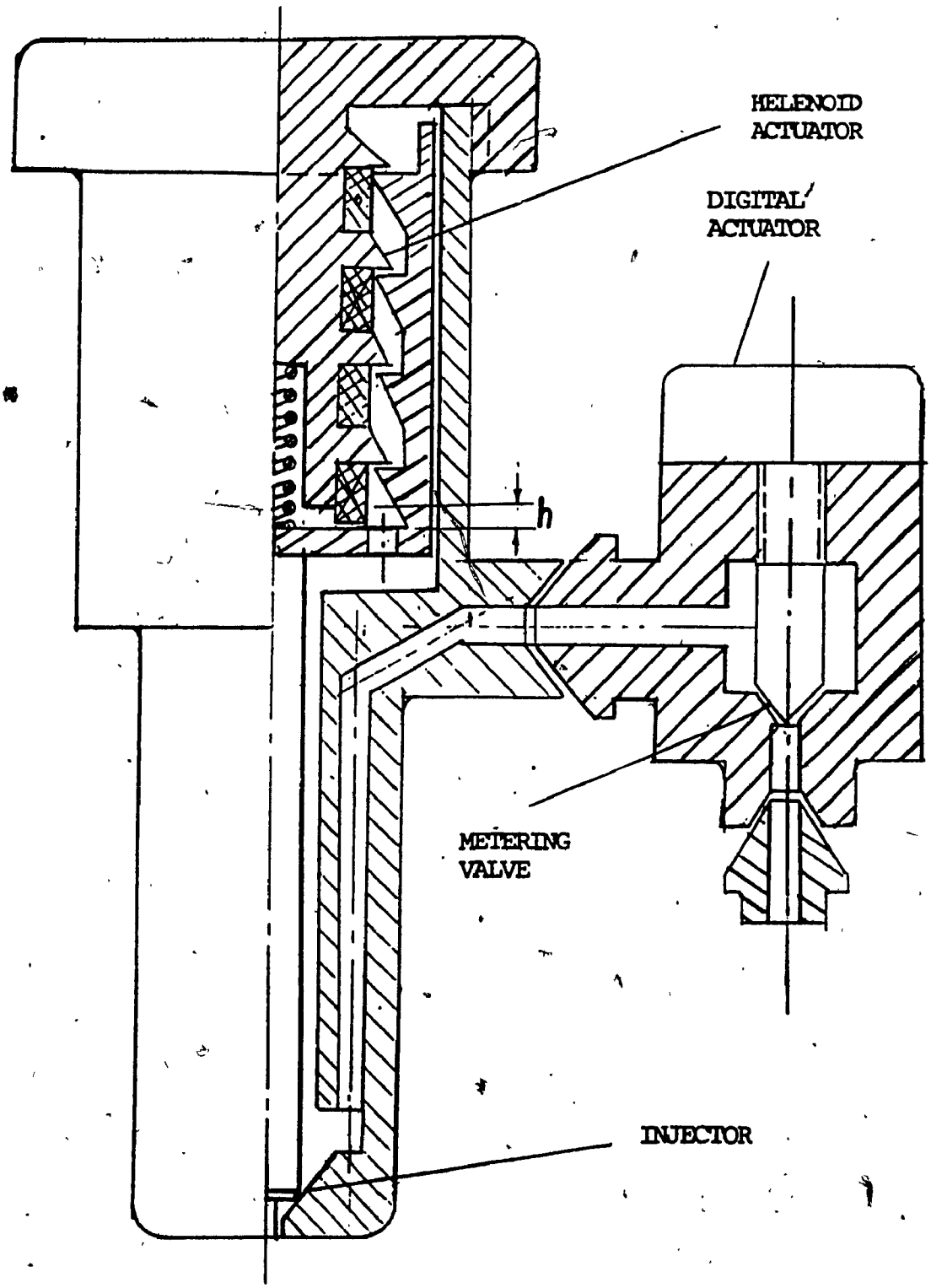

Fig. 7.4(a) Proposed hydrogen injector equipped with a HELENOID actuator

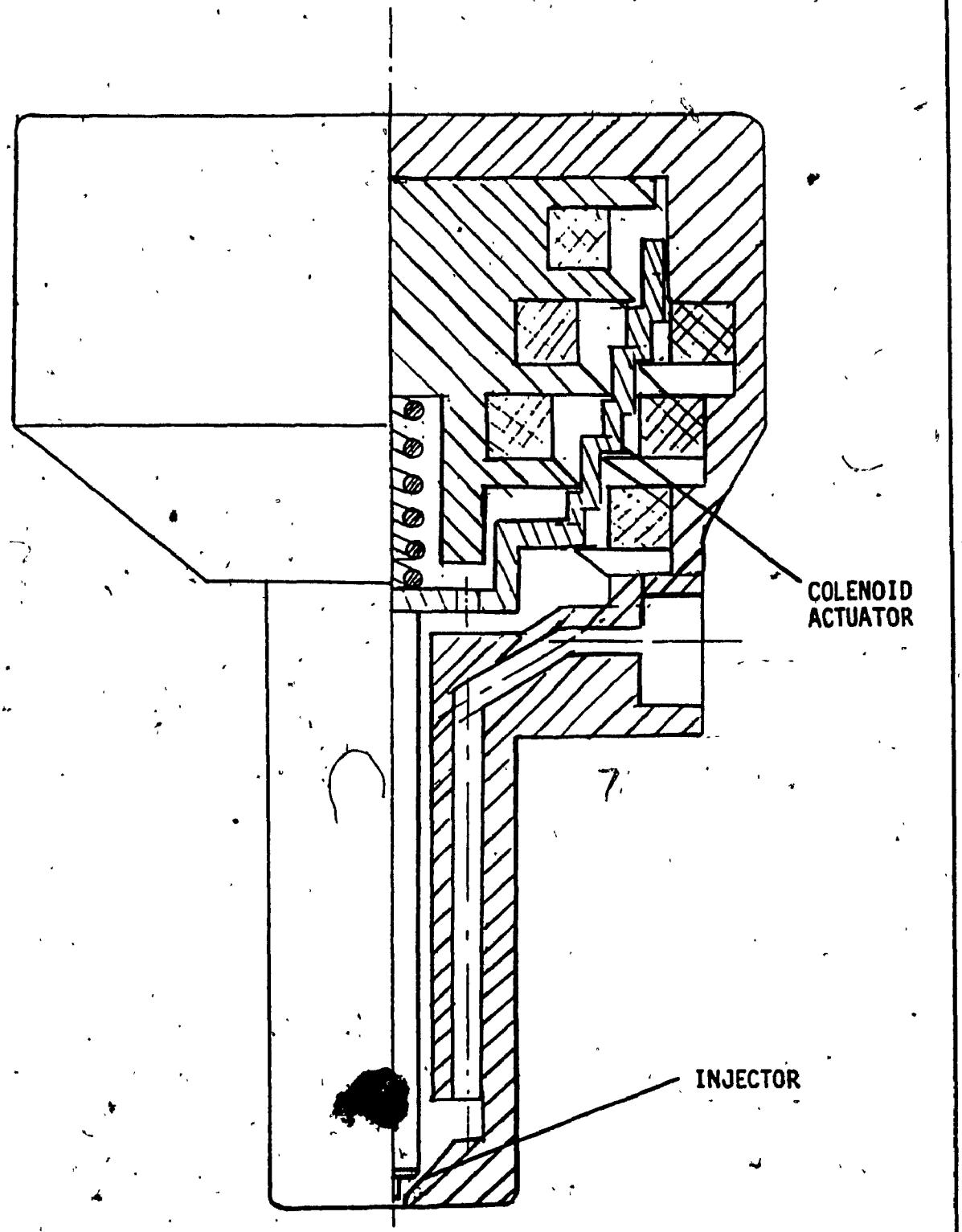

Fig. 7.4(b) Proposed injector equipped with a double acting COLENOID actuator

proposed injector design maintains this feature because it is particularly convenient for hydrogen gas injection due to the long ignition delay inherent in this fuel. It does not allow the accumulation of a large amount of fuel in the combustion chamber before ignition and hence, it limits the rapid pressure increase following the start of combustion. Therefore, it reduces the effect of "hammering", a well known phenomenon in diesel engines running on low cetane number fuel. The design of the flow areas should be based on the information provided in chapter 3. However, it is suggested to shape the pintle as shown in figure 7.5 to obtain a better fuel discharge coefficient. The equation (3-3) applies to such pintle shape as well, and the corresponding equations for the constants a_2, a_1, a_0 are given in appendix 1.

The use of the pintle type nozzle is considered as one of the best means available in shaping the discharge rate characteristic in gas fuelled diesel engines. This is the reason why the pintle nozzle is strongly recommended for the gas injector design in further research.

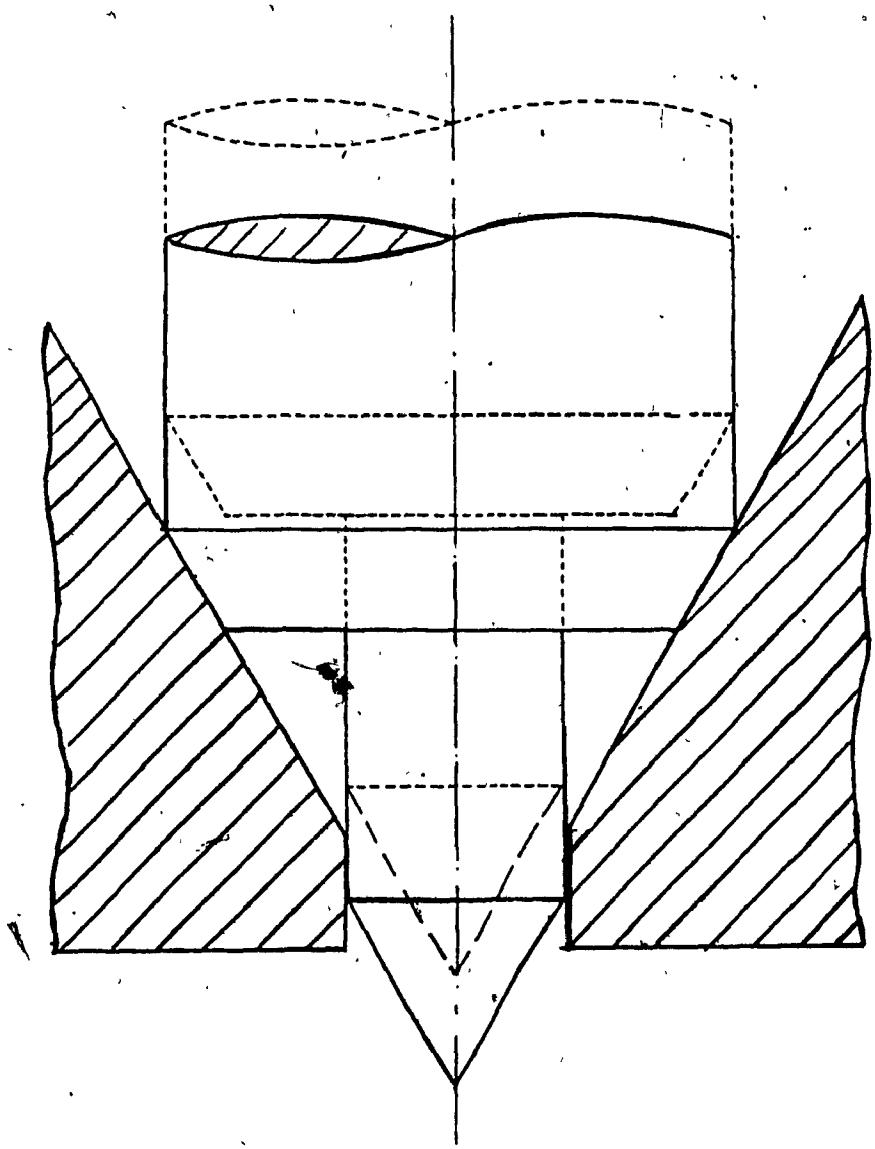

Fig. 7.5 Proposed pintle shape

7.3 IMPROVEMENTS IN ELECTRONIC CONTROL

The electronic circuit used in this feasibility study performed quite satisfactorily in terms of being able to open and close the injector within the required narrow time limits. However, because such a system consumes a lot of electric power, it would be very incovenient when installed and operated on an actual engine. Therefore, the electrical part of the system should be substantially improved before a claim can be made on the reliability of this system. The objective of this section is to make a few suggestions on how to improve the electrical characteristics of the circuit.

A basic problem which is encountered in the design of the electrical system is to overcome the "electrical inertia" of the circuit. Just as force is required to overcome the mechanical inertia, voltage is required to overcome the inductance or, as it is usually referred to, the "electrical inertia". Therefore, for a given supply voltage, the inductance should be made as low as possible when compared to the maximum power input permissible during the armature movement. This problem is part of the solenoid actuator design and will not be discussed further here. It is sufficient to say that the HELENOID and the COLENOID actuators seem to be ideally suited for use in fuel injectors.

Another problem to be solved is to find the best way to deliver the high peak power into the actuator. The magnetic flux rise in the working face areas must be as fast as possible in order to generate the required actuator force and this depends upon the rate of the electric current rise. Once the armature has closed its air gap, far lower power is required to hold it in this position. Therefore, the best method would be to supply high current initially and when the injector has opened, the current would be lowered in order to provide only a holding force. This can easily be done in this application by the D.C. supply from a car battery and a transistor circuit under microprocessor control. To improve the efficiency of the actuator, Seilly [37] suggests to limit the peak current and to maintain it at a certain level while the armature is moving (fig. 7.6). He claims that in this way, the current can be driven into the circuit extremely fast without wasting power in I^2R losses by overdriving the current. This idea seems reliable and should be tested because the holding force should be expected to be small due to small preload force and low spring rate.

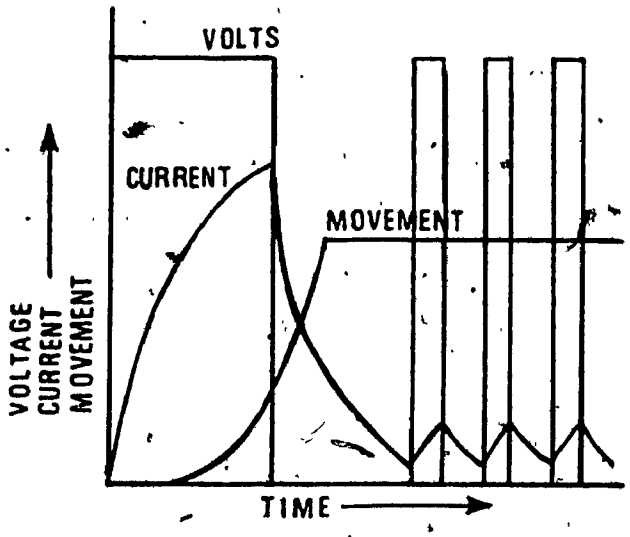

Fig. 7.6 Electrical characteristics with respect to needle motion, for low power control (Courtesy of Seilly (37))

CHAPTER 8.0

SUMMARY

8.1 CONCLUSIONS

A new hydrogen gas injection system was proposed for high speed compression ignition engines. The system was controlled by a microprocessor using solenoid actuators and it was designed to inject hydrogen gas under high pressure directly into the cylinder of a diesel engine. The design of this system included three versions: Injector Only System, Metering-Valve Injector System and Control-Valve Injector System. Furthermore, a mathematical model was developed in order to simulate the dynamic response of the fuel gas injector which would enable the design of a nozzle having the optimum gas flow rate characteristic.

The laboratory tests performed on the prototype of the hydrogen injection system enabled the investigation of the major design problems and established the basis for their solution. The objective of high operating frequency of the injector's needle was achieved in all three options. Yet, it can be concluded that the mathematical model simulated successfully the dynamic response of the injector since many calculated characteristics, such as needle lift, injector pressure, fuel dose, and average fuel flow rate, followed closely the actual ones which were found experimentally. According to the test results, it can be concluded that

such a simple microprocessor controlled gas injection system is feasible and could be used for hydrogen fuelled diesel engines. The fuel mass flow rate as well as the fuel delivery characteristic, can be very effectively controlled. Therefore, the optimization of the engine's power characteristic and of the combustion process from the point of view of fuel consumption can be done easier due to the flexibility of the electronic injection control.

However, there are many areas for improvements in such gas injection system with electronic control in order to become reliable and practical for actual engine use. Such improvements include the use of more powerful and more compact solenoids, the redesign of nozzle for better fuel discharge characteristics, better integration of timing control (solenoid) with metering area control (stepper motor), optimization of the gas pressure and other design parameters. Fuel leakage and possible needle seizure should also be investigated in order to be minimized. A new injector design that takes into consideration the above problems has been proposed and, if properly developed, it could greatly improve the performance of the gas injection system.

The most important improvement from the side of the diesel engine would be in hydrogen ignition. This should be investigated by using not only spark and glow plugs, but also pilot injection which in this

electronically controlled system is easy to obtain. Finally, entirely new ignition possibilities should be developed and tested to fully solve the ignition problem for all alternative fuels for which this remains still the most serious limitation.

REFERENCES

1. Dahlberg, R., "Replacement of Fossil Fuels by Hydrogen", Int. J. Hydrogen Energy, Vol.7, No. 2, 1982, pp.121-142.

2. "Nonpetroleum Vehicular Fuels", Symposium Papers Sponsored by Institute of Gas Technology and Presented at Arlington, Virginia, Feb., 11-13, 1980.

3. Encyclopedia of Energy, edited by Lapedes, D.N., McGrow Hill Book Company, New York, N.Y., 1981, pp. 373- 377.

4. Erren, R.A. and Cambell, N.H. "Hydrogen: A Commercial Fuel for Internal Combustion Engines and Other Purposes", J. Inst. Fuel, 6, 1933, pp. 277-290.

5. Carpetis, C., "Comparison of the Expenses Required for On-Board Fuel Storage Systems for Hydrogen Powered Vehicles", Int. J. Hydrogen Energy, Vol. 7, No. 1, 1982, pp. 61-77.

6. Carpetis, C., "Hydrogen Storage and Transport", Proc. 2nd International Symposium on Hydrogen Produced from Renewable Energy, Cocoa Beach, Florida, 1985, pp. 3-9.

7. Peschka, W., "Operating Characteristics of a LH_2 -refuelling Station", Int. J. Hydrogen Energy, Vol. 7, No. 8, 1982, pp. 661-669.

8. Homan, S. H., De Boer, P.C.T. and McLean, W.J., "The Effect of Fuel Injection on NOx Emissions and Undesirable Combustion for Hydrogen-Fuelled Piston Engines", Int. J. Hydrogen Energy, Vol. 8, No. 2, 1983, pp. 131-146.

9. Lucas, G.G., McLean, D. and Adcock, P., "Microprocessor Controlled Fuel Injection for Automotive Diesel Engines", SAE Paper No. 830576, 1983.

10. Miyagi, H., Nagase, M., Nakano, J. and Kobashi, M. "TOYOTA Electronic Control System for a Diesel Engine", SAE Paper No. 830862 (P. 139), 1983.

11. Eisele, H. and Bosch, R., "Electronic Control of Diesel Passenger Cars", SAE Paper No. 800167, 1980.

12. Trenne, U.M. and Ives, P.A., "Closed Loop Design

for Electronic Diesel Injection Systems", SAE Paper No. 820447, 1982.

13. Ricardo, H.R., "Further Note on Fuel Research", Empire Motor Fuels Committee Rep., Proc. Inst. Auto. Engrs, 18, 1923, p. 327.

14. Burstall, A.F., "Experiments on the Behaviour of Various Fuels in a High-Speed Internal Combustion Engine", Proc. Inst. Auto. Engrs. 22, 1927. p. 358.

15. Allen, N., "A Primer on the Fuels/Air Pollution Problem" Proc. 5th World Hydrogen Energy Conf., Toronto, Ontario, 1984.

16. Varde, K.S, and Lucas, G.G., "Hydrogen as a fuel for Vehicle Propulsion", Proc. Inst. Mech. Engrs, Vol. 188, No. 26, 1974.

17. Stewart, W.F. and Edeskuty, F.J., "Liquid Hydrogen as a Vehicular Fuel: An Evaluation", Mechanical Engineering, May, 1981.

18. Kukkonen, C.A., "Hydrogen as an Alternative Automotive Fuel", SAE Paper No. 810349, 1981.

19. Krepec, T., Tebelis, T. and Kwok, C., "Fuel Control Systems for Hydrogen-Fuelled Automotive Combustion Engines - A Prognosis", Int. J. Hydrogen Energy, Vol. 9, No. 1/2, 1984, pp. 109-114.

20. Lichty, C.L., Internal Combustion Engines, Sixth Ed., McGraw-Hill Book Company, New York, N.Y., 1951.

21. Burman, G.P. and DeLuca, F., "Fuel Injection and Controls for Internal Combustion Engines", The Technical Press Ltd., London, G.B., 1962.

22. Judge, W.A., High Speed Diesel Engines, 5th Edition, Champan and Hall Ltd., London, England, 1957, pp. 301-340.

23. Polson, A.J., Internal Combustion Engines, Second Ed., John Wiley and Sons, Inc., New York, N.Y., 1942, pp. 437-454.

24. Taylor, F.C., The Internal Combustion Engine in Theory and Practice, Vol. 2: Combustion, Fuels, Materials, Design, The M.I.T. Press, Cambridge, Mass., 1978, pp. 214-239.

25. Passenger Car Diesels: Progress in Technology, series No. 24, Selected Papers through 1981, SAE

PT-24, 1982.

26. Fuel Economy and Emissions of Lean Burn Engines, Proc. The Institution of Mechanical Engineers, London, 1979.

27. Amann, C.A., Monoghan, M.L. and Uyehara, O.A., "Why Passenger-Car Diesels?", Passenger Car Diesels, SAE PT-24, 1982.

28. May, H. and Schultz, H., "New Distributing Injection System and its Potential for Improving Exhaust Gas Emissions", SAE Paper No. 680043, 1968.

29. LaMasters, D.G., "Fuel Injection-Another Tool for Emission Control", SAE Paper No. 720679, 1972.

30. Glockler, O., Knapp, H. and Manger, H., "Present Status and Future Development of Gasoline Fuel Injection Systems for Passenger Cars", SAE Paper No. 800467, 1980.

31. Bowler, L.L. "Throttle Body Fuel Injection (TBI) An Integrated Engine Control System", SAE Paper No. 800164, 1980.

32. Bowler, L.L., "Electronic Fuel Management - Fundamentals", SAE Paper No. 800539, 1980.

33. Beck, J., "High Pressure Fuel Injection", Diesel Progress, April 1983, pp. 16-18.

34. Komiyama, K., Okazaki, T., Togashi K., Hashimoto H., and Takaya K., "Electronically Controlled High Pressure Injection System for Heavy Duty Diesel Engine -KOMPICS" SAE Paper No. 810997, 1981.

35. Cross, R.K., Lakra P. and C.G. O' Neill, Electronic Fuel Injection Equipment for Controlled Combustion Diesel Engines", SAE Paper 810258, 1981.

36. Seilly, A.H., "HELENOID Actuators A New Concept in Extremely Fast Acting Solenoids" SAE Paper No. 790119, 1979.

37. Seilly, A.H., "COLENOID Actuators-Further Developments in Extremely Fast Acting Solenoids", SAE Paper No. 810462, 1981.

38. Schechter, M.M., "Fast Response Multipole Solenoids", SAE Paper No. 820203 (SP-511), 1982.

39. Hood, B.R., "Sensors, Displays and Signal Conditioning", SAE Paper No. 740015 (SP-388), 1974.

40. Berger, F., "Actuating Devices for Electronic Controlled Systems", SAE Paper No. 740016 (SP-388), 1974.

41. Binder, K. and Withalm, G., "Mixture Formation and Combustion in a Hydrogen Engine Using Hydrogen Storage Technology", Int. J. Hydrogen Energy, Vol. 7, No. 8, 1982, pp. 651-659.

42. Buchner, H. and Povel, R., "The Daimler-Benz Hydride Vehicle Project", Int. J. Hydrogen Energy, Vol. 7, No. 3, 1982, pp. 259-266.

43. Suda, S., "Recent Development of Hydride Energy Systems in Japan", Proceedings of the 5th World Hydrogen Energy Conference, Toronto, Canada, 1984.

44. Alcock, C.B., Hewitt, J.S., Khatamian, D., Manchester, F.D., McLean, A., Ward, C.A. and Weatherly G.C., "Research in Hydrogen Storage Alloys and their Uses", Proceedings of 5th World Hydrogen Energy Conference, Toronto, Canada, 1984.

45. Northwood, D.O. and Ivey, D.G., "Storing Hydrogen as a Metal Hydride: A Review of Potential Materials with Special Emphasis on Zirconium Intermetallics", Proceedings of the Second International Symposium on Hydrogen Produced from Renewable Energy, Cocoa Beach, Florida, U.S.A., 1985, pp. 199-210.

46. Furuhama, S. and Kobayashi, Y., "A Liquid Hydrogen Car with a Two-Stroke Direct Injection Engine and LH2-Pump", Int. J. Hydrogen Energy, Vol. 7, No. 10, 1982, pp. 809-820.

47. Furuhama, S. and Kobayashi, Y., "Development of a Hot-Surface-Ignition Hydrogen Injection Two-Stroke Engine", Int. J. Hydrogen Energy, Vol. 9, No. 3, 1984, pp. 205-213.

48. Furuhama, S. and Fukuma, T., "High Output Power Hydrogen Engine with High Pressure Fuel Injection, Hot Surface Ignition and Turbo-Charging" Proceedings of the 5th World Hydrogen Energy Conference, Toronto, Canada, 1984.

49. Furuhama, S. and Fukuma, T., "New Liquid Hydrogen Car with High Pressure Hydrogen Injection, Hot Surface Ignition Turbocharging Engine", Presented at the 5th World Hydrogen Energy Conference, Toronto, Canada, 1984.

50. DeBoer, P.C.T., McLean, W.J. and Homan, H.S., "The Performance and Emissions of Hydrogen Fuelled

Internal Combustion Engines", Int. J. Hydrogen Energy, Vol. 1, 1976, p. 153.

51. Karim, G.A., Rashidi, M. and Taylor, M., "An Analytical Study of the Compression Ignition Characteristics of H_2-O_2-N_2 mixtures in a Reciprocating Engine", J. Mech. Eng. Science, Vol. 16, No. 2, 1974, pp. 88-94.

52. Karim, G.A. and Klat S.K., "Experimental and Analytical Studies of Hydrogen as a Fuel in Compression Ignition Engines", ASME Paper No. 75, DGP-9, 1975.

53. Takahashi, S., "An Experiment on the Ignition of Hydrogen Injected into a High Temperature Oxidizer", Int. J. Hydrogen Energy, Vol. 7, No. 7, 1982, pp. 589-596.

54. Ikegami, M., Miwa K. and Shiogi M., "A Study of Hydrogen Fuelled Compression Ignition Engines", Int. J. Hydrogen Energy, Vol. 7, No. 4, 1982, pp. 341-353.

55. Tebelis, T. and Krepec, T., "A Concept of Electronically Controlled Hydrogen-Gas Injector for High Speed Compression Ignition Engines", Proceedings of the Second International Symposium on Hydrogen Produced for Renewable Energy, Cocoa Beach, Florida, 1985, pp. 397-408.

56. Giannacopoulos, T., Krepec, T. and Lisio, C., "Preliminary Investigation of Microprocessor Controlled Hydrogen Injector with a Help of Computers", Proceedings of ASME International Computers in Engineering Conference, Chicago, Illinois, July 1986.

57. Krepec, T., Giannacopoulos, T. and Miele, D., "New Electronically Controlled Hydrogen-Gas Injector Development and Testing", Accepted for presentation at the Sixth World Hydrogen Energy Conference, Vienna, Austria, July 1986.

58. Wark, K., Thermodynamics, Third Edition, McGrow-Hill Book Co., New York, N.Y., 1977.

59. Thompson, A.P., Compressible Fluid Dynamics, McGraw-Hill Inc., New York, N. Y., 1972, pp. 137-146.

60. Neitz, A. and D'Alfonso, N., "The M.A.N. Combustion System with Controlled Direct Injection for Passenger Car Diesel Engines", SAE Paper No.

810479, 1981.

61. McCloy, D. and Martin, H.R., The Control of Fluid Power, Longman Group Limited, London, England, 1973.

62. Andersen, B.W., The Analysis and Design of Pneumatic Systems, John Wiley and Sons Inc., New York, N.Y., 1967.

63. Zacks, R., Programming the Z-80, Third Edition, SYNBEX Inc., 1982.

64. Nichols, C.J., Nichols, A.E. and Rony, R.P., Z-80 Microprocessor Programming and Interfacing, Book 2, Howard W. Sams and Co. Inc., Indianapolis, Indiana, 1979.

65. Match, W.L., Electromagnetics and Electromechanical Machines, 2nd Edition, Horper and Row Publishers, New York, N.Y., 1977.

66. Zalmanzon, A.L., Components for Pneumatic Control Instruments, Translated by Hardbottle, R., Pergam Press Ltd., Oxford, England, 1965.

67. Bosch, W., "Der Einspritzgesetz-Indikator, Ein neues Messgerat zur directen Bestimmung des Einspritzgesetzes von Einzeleinspritzungen", Motor technische Zeitschrift, 25/7, 1965, pp. 268-282.

68. Pischinger, A., Bewegungsgleichungen fur die Veranderliche Stomung in der Einspritzleitung und deren Losung: In H. List (Ed.), Gemischbildung und Verbrennung in Dieselmotor, Springer Verlag, Vienna, Austria, 1957, pp. 89-91.

69. Tanabe, H., Ohnishi, M., Fujimoto, H. and Sato, G. T., Experimental Study of the Transient Hydrogen Jet Using a Fast Response Probe", Int. J. Hydrogen Energy, Vol. 7, No. 12, 1982, pp. 967-976.

70. Allievi, L., "Allgemeine Theorie uber die veranderliche Bewegung des Wassers in Leitungen", Springer Verlag, Berlin, 1909.

71. Smith, H.D. and Spinweber, A.D., "A General Model for Solenoid Fuel Injector Dynamics", SAE Paper No. 800508, 1980.

72. Tse, S.F., Morse E.I and Hinkle, T.R., Mechanical Vibrations: Theory and Applications, 2nd Ed., Allyn and Bacon Inc., Boston, Mass., 1978.

73. Shingley, J.E., Simulation of Mechanical Systems,

McGraw-Hill Co., New York, N.Y., 1967.

74. Lapidus, L. and Schiesser, W.E., Numerical Methods for Differential Systems: Recent Developments in Algorithms, Software and Applications, Academic Press Inc., New York, N., 1976.

75. Jordan, D.W. and Smith, S., Nonlinear Ordinary Differential Equations, Clarendon Press, Oxford, G.B., 1977.

76. Huntley, I. and Johnson, R.M., Linear and Nonlinear Differential Equations, Ellis Horwood Ltd., Chichester, England, 1983.

77. Baker, C.T.H. and Philips C., Editors , "The numerical Solution of Nonlinear Problems, Clarendon Press, Oxford, G. B., 1981.

78. Hull, T.E. Enright, W.H., Fellen B.M. and Sedgewk, A.E., "Comparing Numerical Methods for Ordinaty Differential Equations", SIAM Journal of Numerical Analysis, 9, No. 4, 1972, pp. 603-637.

79. Enright, W.H., Hull, T.E. and Lindeberg, "Comparing Numerical Methods for Stiff Systems of O.D.E.'s", BIT, 15, 1975, pp. 10-48.

80. Shampine, L.F. and Gear, C.W., "A User's View of Solving Stiff Ordinary Differential Equations", SIAM Review, 21, No. 1, 1979, pp. 1-17.

81. Lapidus, L. and Seinfeld, J.H., Numerical Solution of Ordinary Differential Equations, Academic Press, New York, N.Y., 1971,

82. Lambert, J.D., Computational Methods in Ordinary Differential Equations, John Wiley and Sons Ltd., London, G.B., 1973.

83. Hull, T.E., Enright, W.H. and Jackson, K.R., IMSL Library, Vol. 1, Chapter D, p. DVERK-7.

84. Yuan, W.S., Foundations of Fluid Mechanics, Prentice-Hall Inc.,Englewood,N.J., 1967.

APPENDICES

APPENDIX 1

DERIVATION OF PINTLE NOZZLE FLOW AREAS

The overall shapes of both the original and the modified pintle geometries are shown in figure A.1 including the nomenclature used in the flow area equations.

1. Flow area at needle seat, A_{23}.

The minimum seat flow area is in section AB (fig. A.2), and is given by:

$$A_{23} = \pi RY - \pi r_{so}(Y - y) \qquad \text{(A1-1)}$$

To eliminate R, Y and y note that

$$\cos\theta = R/Y = r_{so}/(Y-y) \qquad \text{(A1-2)}$$

$$\sin\theta = y/h \qquad \text{(A1-3)}$$

Substituting equations (A1-2) and (A1-3) into (A1-1) and rearranging, the flow area at the seat can be expressed as:

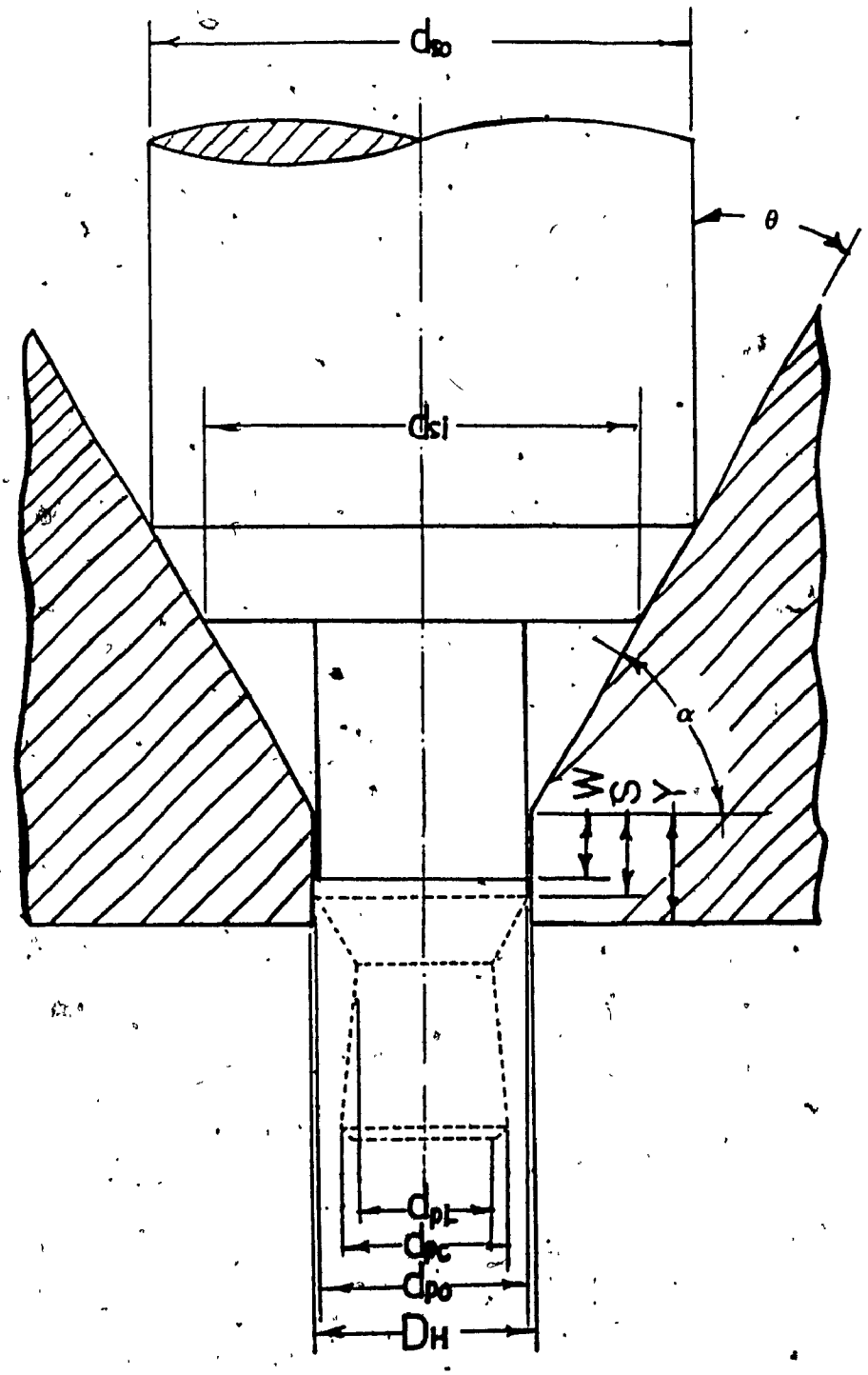

Fig. A.1 Original and modified pintle geometries

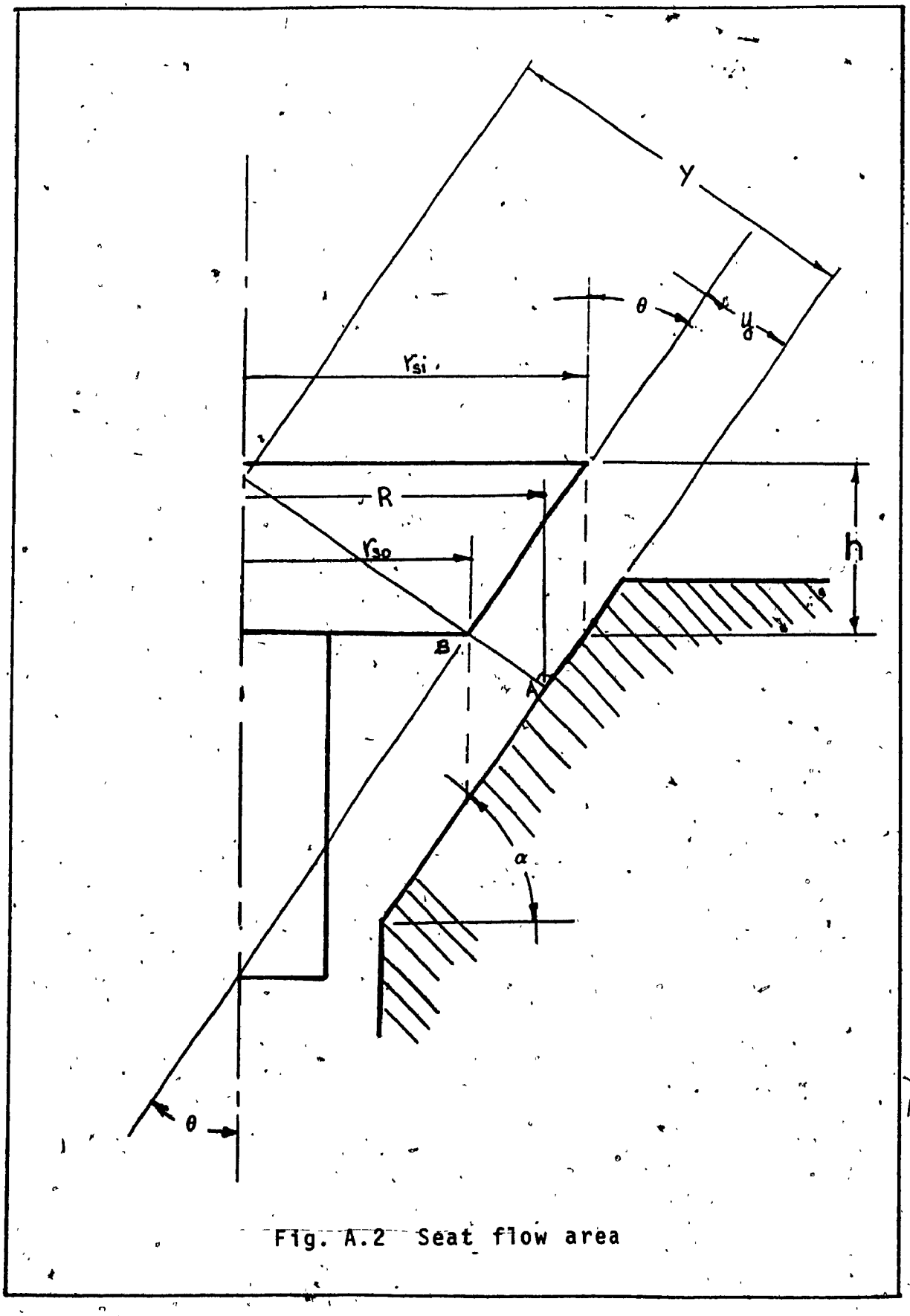

Fig. A.2 Seat flow area

$$A_{23} = a_2 h_1^2 + a_1 h_1 + a_o \qquad \text{(A1-4)}$$

where $h_1 = h$,

and the constants a_2, a_1, a_o are given by:

$$a_2 = \pi \sin^2\theta \cos\theta$$

$$a_1 = \pi d_{so} \sin\theta$$

$$a_o = 0$$

2. Flow area between pintle and nozzle hole, A_{34}.

This flow area becomes critical at three different sections during the needle motion (fig. A.3). The general form of the equation is the same as in equation (A1-4).

Namely;

$$A_{34} = a_2 h_2^2 + a_1 h_2 + a_o \qquad \text{(A1-5)}$$

However, the constants in equation (A1-5) differ for each section. In equation (A1-5), the relative lift, h_2 is related to the actual lift h, by:

$$h_2 = h - (S + y_o) \qquad \text{(A1-6)}$$

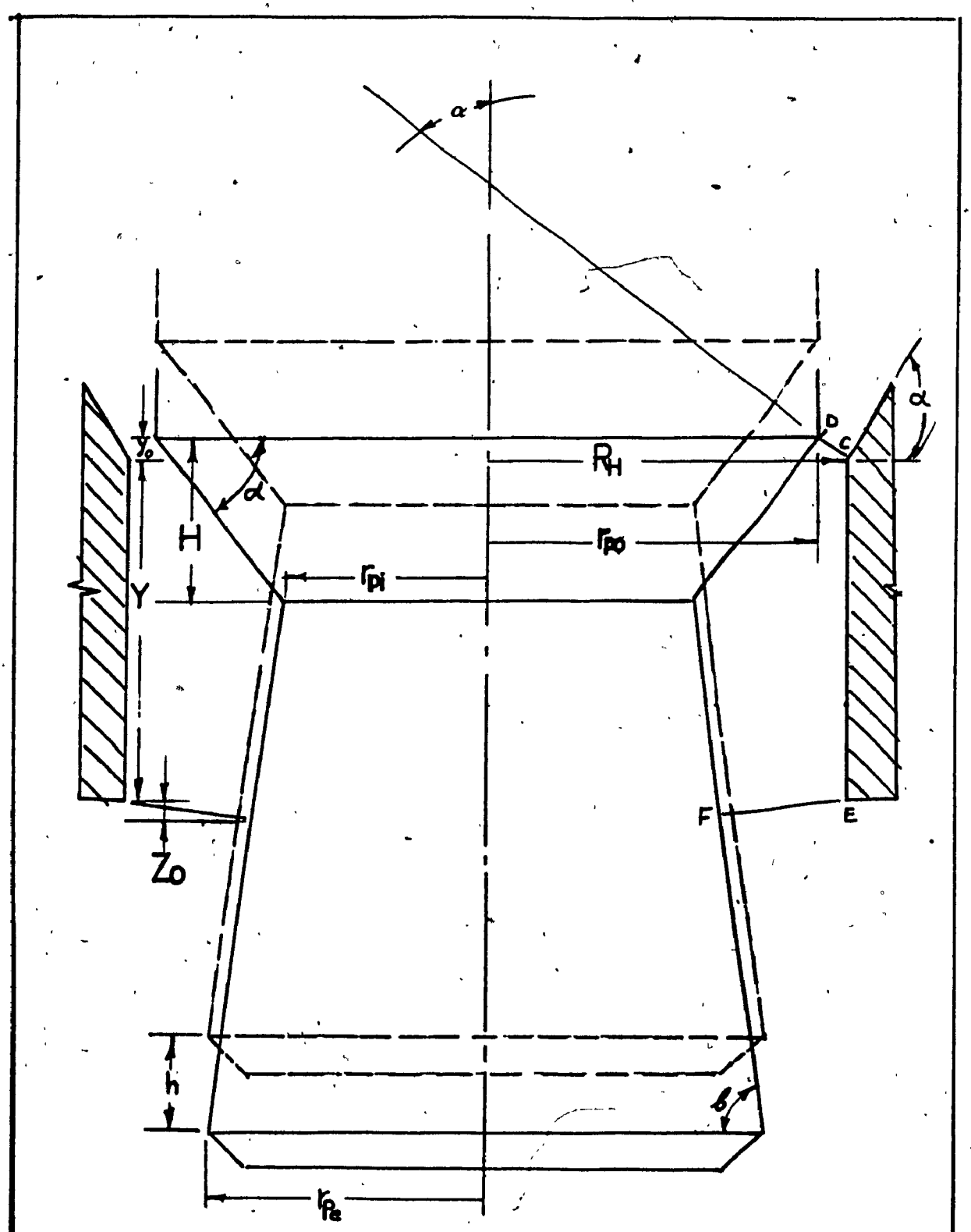

Fig. A.3 Sections of critical flow areas

A.1 ORIGINAL PINTLE GEOMETRY

(i) Flow area at annulus.

$$a_2 = a_1 = 0$$

$$a_0 = \pi(D_H^2 - d_{po}^2)/4$$

(ii) Flow area at nozzle hole inlet section CD.

$$a_2 = -\pi \sin\alpha \cos^2\alpha$$

$$a_1 = \pi d_{po} \cos\alpha$$

$$a_0 = \frac{\pi}{4\sin\alpha}(D_H^2 - d_{po}^2)$$

(iii) Flow area at nozzle hole exit section EF.

$$a_2 = -\pi \cos^2\beta \sin^2\beta$$

$$a_1 = \pi \cos\beta(2Z_0 \tan\beta - D_H)$$

$$a_0 = \frac{\pi Z_0}{\cos\beta}(D_H - Z_0 \tan\beta)$$

$$Z_0 = \frac{1}{2\tan\beta}\left[(D_H - d_{pi}) - \frac{(D_H - d_{po}) + 2(Y-H)\tan\alpha}{\tan\alpha \tan\beta}\right]$$

NOZZLE DATA FOR THE ORIGINAL PINTLE GEOMETRY

d_{si} = 2.52 mm

d_{so} = 2.00 mm

d_{po} = 0.97 mm

d_{pi} = 0.62 mm

d_{pe} = 0.76 mm

D_H = 0.99 mm

S = 0.40 mm

Y = 0.50 mm

H = 0.30 mm

A.2 MODIFIED PINTLE GEOMETRY

The flow area equations for the modified pintle geometry (fig. A.1) is given by equations (A1-4) and (A1-5). Also, the constants for the needle seat and the annulus are the same. For the nozzle hole, the constants are as follows (see fig. A.4):

(i) Flow area at nozzle hole inlet section CD.

$$a_2 = \pi \sin^2\alpha \cos^2\alpha$$

$$a_1 = \pi D_H \cos\alpha$$

$$a_0 = \frac{\pi}{4\sin\alpha}(D_H^2 - d_p^2) \; ; \quad \text{where } h_2 = h - (W + y_0)$$

(ii) Flow area at nozzle hole.

$$a_2 = a_1 = 0$$

$$a_0 = \frac{\pi}{4} D_H^2$$

All data is the same as in the original nozzle except W, which is 0.29 mm.

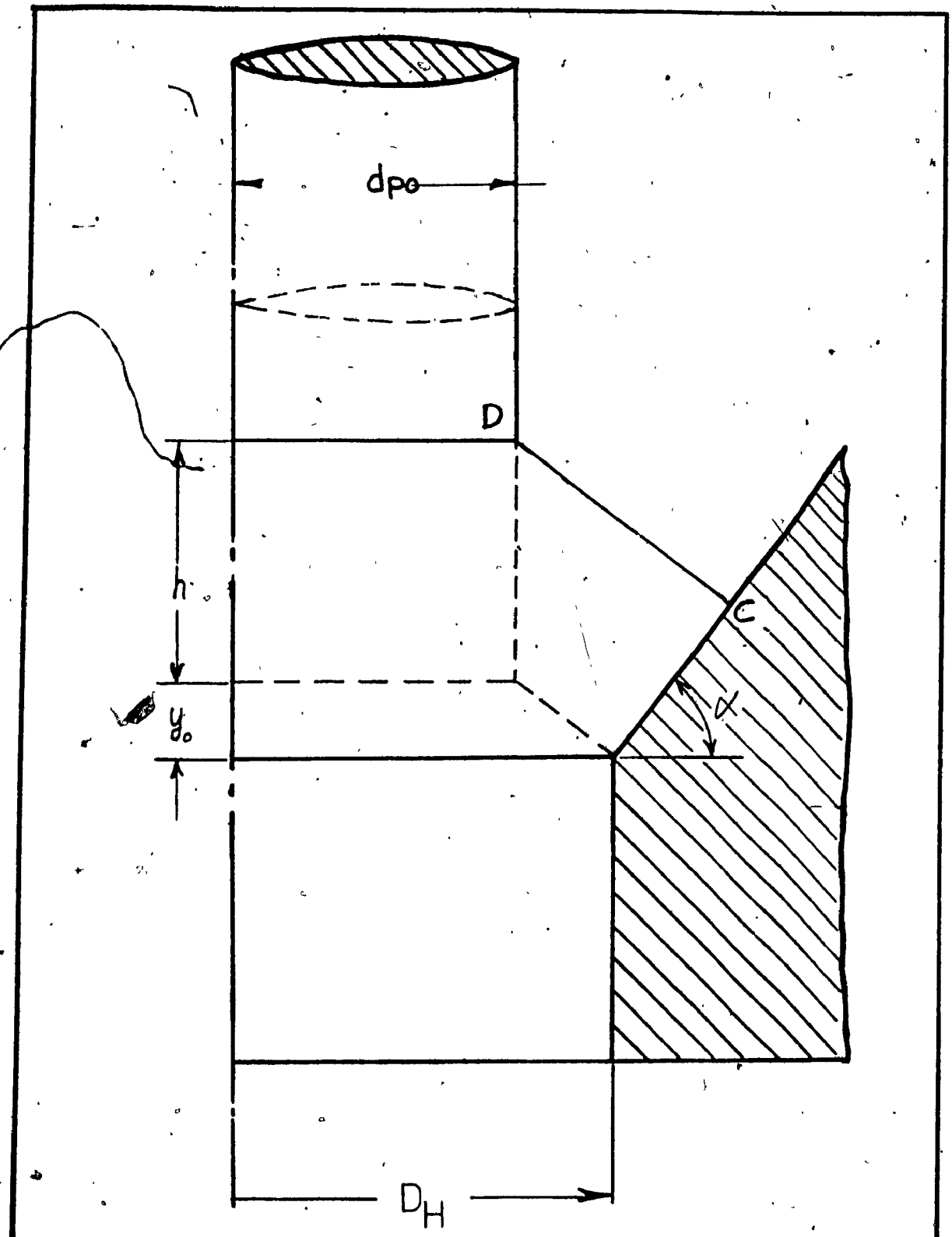

Fig. A.4 Critical flow area of modified pintle nozzle

A.3 PROPOSED PINTLE GEOMETRY

The constants for the proposed pintle geometry shown in figure A.5 are the following:

$$a_2 = \pi \sin^2\theta \cos\theta$$

$$a_1 = \pi d_{po} \sin\theta$$

$$a_0 = \frac{\pi d_{po}^2}{4\cos\theta}$$

The relative lift h_2 is also given by equation (A1-6) for this geometry

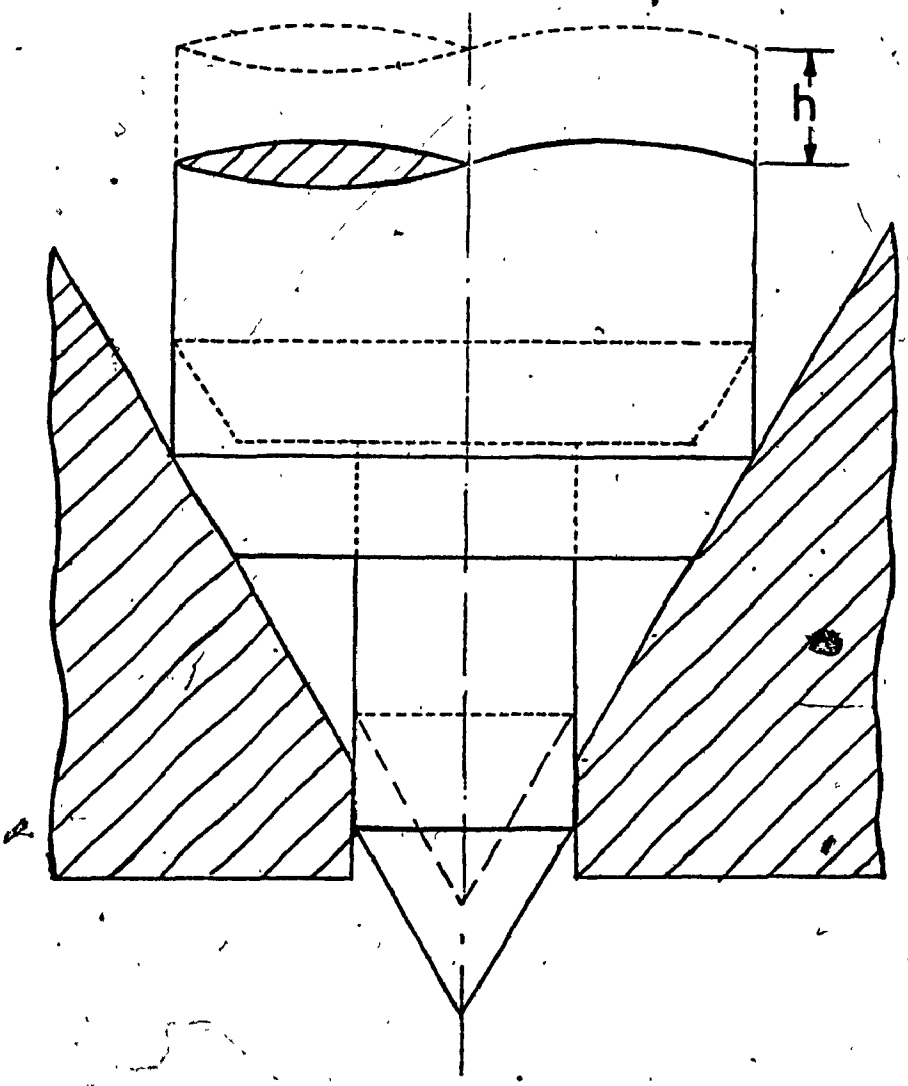

Fig. A.5 Proposed shape of pintle nozzle

APPENDIX 2

DERIVATION OF VISCOUS DAMPING FORCE

The viscous damping force is determined on the basis of the COUETTE flow theory (84), and is given by:

$$F_d = -\pi d_i \int_0^L \tau_{yx}\, dx \qquad \text{(A2-1)}$$

where

$$\tau_{yx} = \frac{\mu U}{\delta}\left[1 + \alpha\left(1 - \frac{2y}{\delta}\right)\right]$$

and

$$\alpha = \frac{\delta}{2\mu U_\delta}\left(-\frac{dP}{dx}\right) \doteq \frac{-\delta^2 (P_e - P_1)}{2\,\mu UL}$$

Integration of equation (A2-1) yields:

$$F_d = -D_f U \qquad \text{(A2-2)}$$

where

$$D_f = \left(\frac{\pi d_i L \mu}{\delta}\right)(1 - \alpha)$$

Since α is dependent on the needle velocity, the drag coefficient D_f is not constant. However, it can be shown that, for this injection system, the damping force is practically constant. If equation (A2-2) is rearranged, the damping force can be expressed as:

$$F_d = -C_1 U + C_2 \qquad \text{(A2-3)}$$

where

$$C_1 = \frac{\pi d_i \mu L}{\delta}$$

and

$$C_2 = \frac{\pi d_i}{2} (P_1 - P_e)$$

It was found experimentally that the maximum needle velocity is approximately 0.50 m/s. Moreover, considering the order of magnitude of both terms of equation (A2-3), it can be seen that the first term is of order 10^{-5}, whereas the second is of order 10^{4}. Then, the first term can be neglected and equation (A2-3) becomes:

$$F_d = \frac{\pi d_i}{2} (P_1 - P_e) \qquad \text{(A2-4)}$$

Therefore, the damping force is constant and depends only on the needle diameter and the pressure difference.

APPENDIX 3

CALIBRATION OF NEEDLE LIFT AND PRESSURE TRANSDUCERS

The calibration of a transducer consists of the precise determination of its output voltage in response to a known input. Three transducers were used in the testing of the hydrogen injection system: one linear displacement transducer and two pressure transducers. The calibration procedure for each transducer is as follows:

A3.1 LINEAR DISPLACEMENT TRANSDUCER

This transducer was used to measure the needle lift. In order to calibrate the displacement transducer, the needle was adjusted to open 0.50 mm. Then, the valve was opened by the microprocessor and the needle movement was recorded by an oscilloscope, as shown in figures 4.9, 4.10 and 4.11. As seen from these oscillograms, the needle reaches the maximum lift in the I.O.S.

option (fig. 4.9). Knowing the maximum lift and reading the output voltage in the oscilloscope, then the calibration of the displacement transducer S_n, is given by:

$$S_n = \frac{0.50 \text{ mm}}{1.4 \text{ V}} = 0.35714 \text{ mm/V}$$

A3.2 PRESSURE TRANSDUCERS

Both pressure transducers were calibrated using a pressure gauge to measure the pressure directly, and an oscilloscope to measure the output voltage produced by the transducers. Hydrogen gas was used, which was available from a high pressure bottle. The calibration curves for the Kistler and Validyne pressure transducers are given in figures A.6 and A.7 respectively.

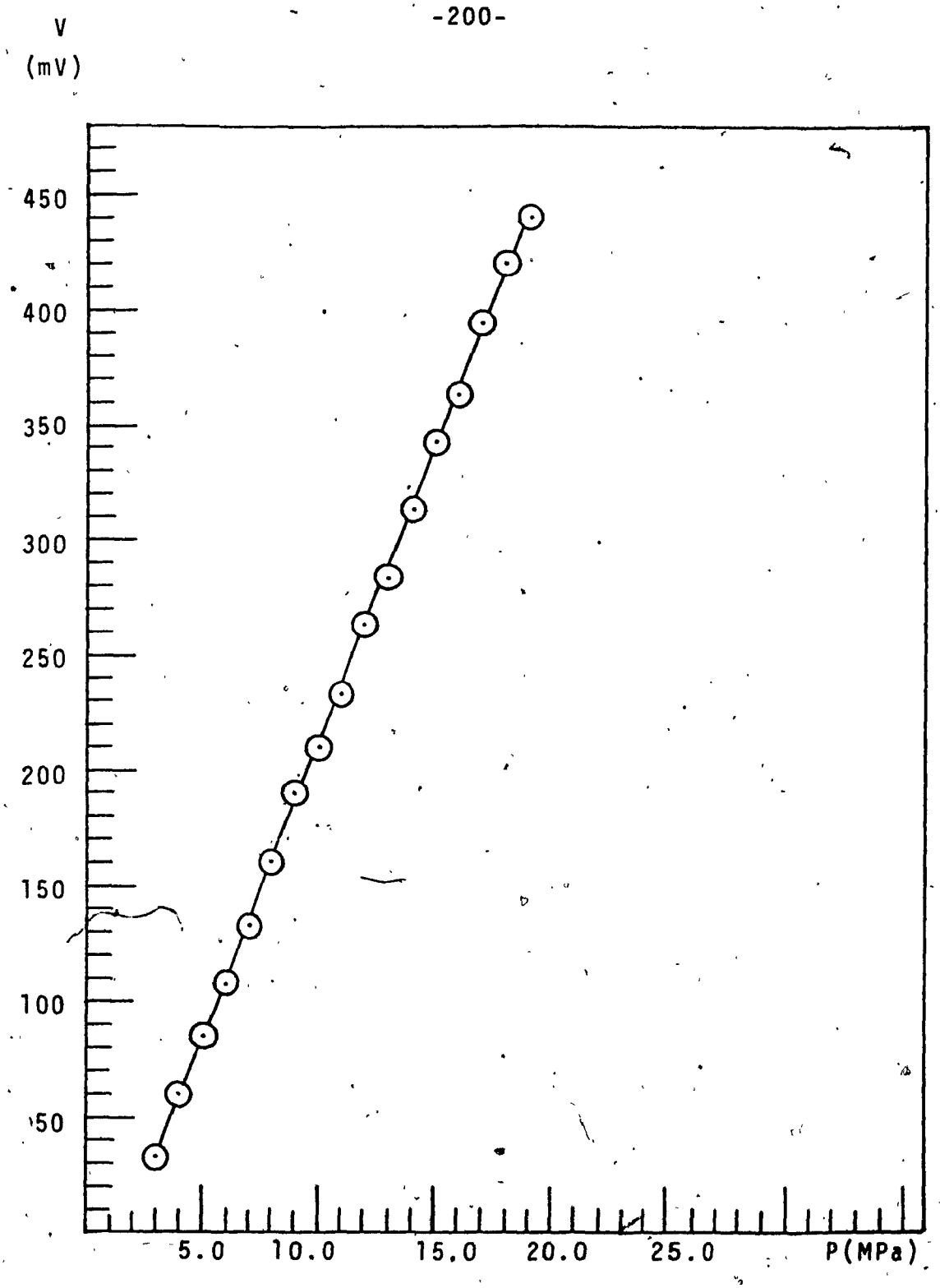

Fig. A.6 Calibration of Kistler, model 60382, pressure transducer (charge amplifier setting:0.5mV/pcb)

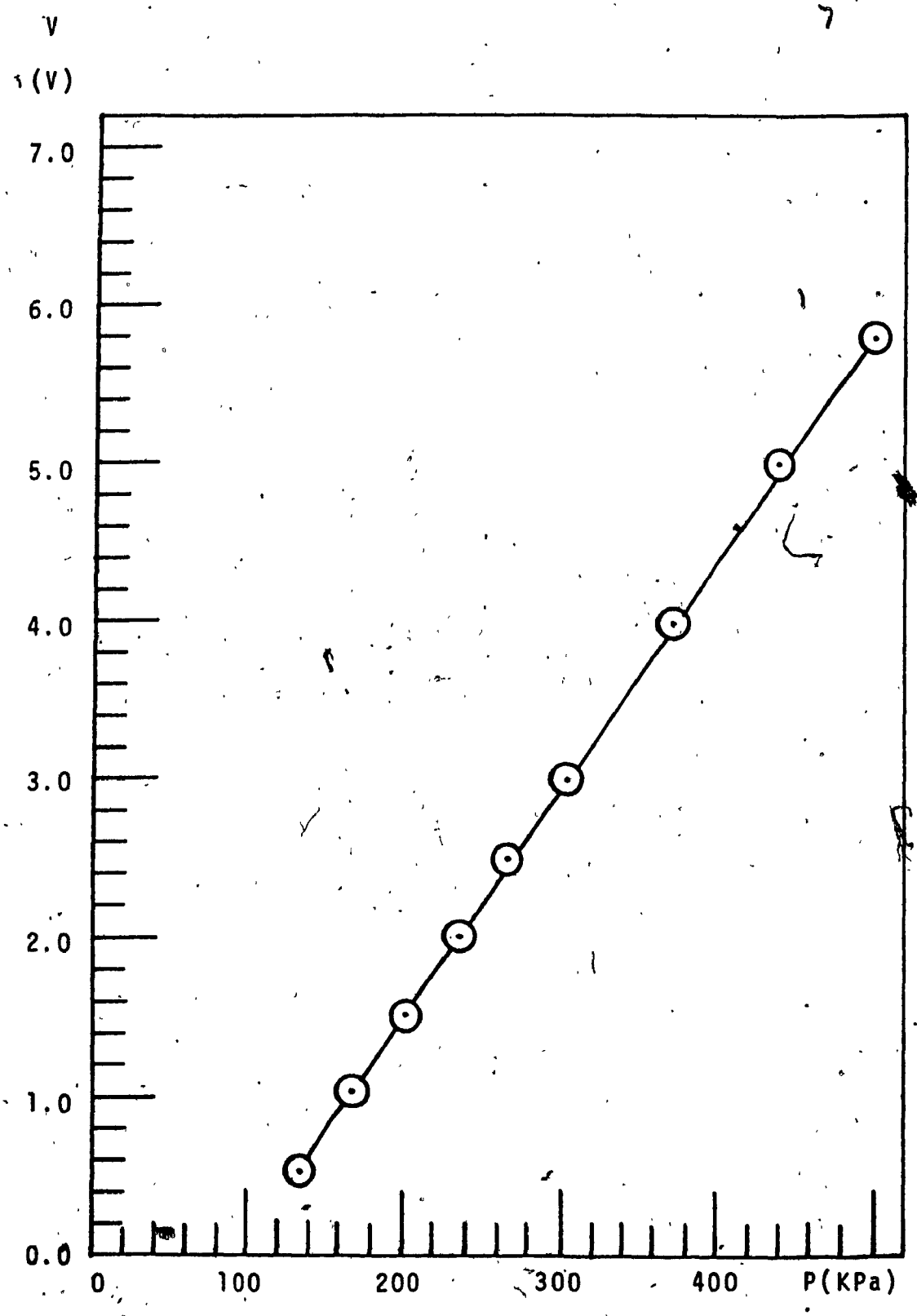

Fig. A.7 Calculation of Validyne, model KP-15, pressure transducer (100 psi diaphragm)

APPENDIX 4

LISTING OF THE MICROPROCESSOR PROGRAMS USED TO CONTROL THE HYDROGEN INJECTION SYSTEM

```
AVOCET SYSTEMS Z80 ASSEMBLER -  VERSION 1.03M  SERIAL #00132

SOURCE FILE NAME: THEOPG2.ASM

                ; THIS PROGRAM IS USED TO OPERATE THE INJECTOR FOR A
                ; DEFINATE NUMBER OF TIMES IN ORDER TO CALCULATE THE
                ; AVERAGE FUEL DOSE PER INJECTION.  SUBROUTINE "MVIS"
                ; IS CALLED FOR OPENING AND CLOSING THE INJECTOR.
                ;
1830                    ORG     1830H
                ;
1830 218018             LD HL, DATA1 ;THE CONTENTS OF THIS ADDRESS
1833                                 ;ARE INPUT TO THE DELAY
1833                                 ;SUBROUTINE.
1833 CDE018             CALL DELAY   ;A DELAY BEFORE COUNTING BEGINS
1836 218218             LD HL, DATA2 ;ADDRESS CONTAINING NUMBER
1839                                 ;OF INJECTION REQUIRED, N
1839 56                 LD D, (HL)   ;PUT N IN REGISTER D
                ;
183A 15         BEGIN:  DEC D
183B C23F18             JP NZ, SERVE ; IF D>0 GO TO SERVE
183E FF                 RST 038H     ; ELSE STOP
                ;
183F CD0018     SERVE:  CALL CONTROL ; CALL "CONTROL" FOR ONE INJECTION
1842 C33A18             JP BEGIN
1845 FF                 RST 038H
                ;
1880                    ORG 1880H
1880 00         DATA1   DEFB 00H
1881 FF                 DEFB 0FFH
1882 FF         DATA2   DEFB 0FFH
1883 06                 DEFB 06H
1884 BB                 DEFB 0BBH
1885 03                 DEFB 03H
1886 BC                 DEFB 0BCH
1887 1A                 DEFB 1AH
1888 CC                 DEFB 0CCH
                ;
1800            CONTROL EQU     1800H
18E0            DELAY   EQU     18E0H
0000                    END

AVOCET SYSTEMS Z80 ASSEMBLER -  VERSION 1.03M  SERIAL #00132

SOURCE FILE NAME: THEOPG2.ASM
 ---- SYMBOL TABLE ----

BEGIN    183A          DATA1    1880          DELAY    18E0
CONTROL  1800          DATA2    1882          SERVE    183F

***** NO ERRORS DETECTED *****
```

AVOCET SYSTEMS Z80 ASSEMBLER - VERSION 1.03M SERIAL #00132

SOURCE FILE NAME: THEOPG6.ASM

```
                        ; PROGRAM FOR CONTROL VALVE AND INJECTOR SYSTEM
                        ;
                        ; THIS PROGRAM OPERATES THE CONTROL VALVE AND THE
                        ; INJECTOR. FOR EXPLANATION OF SYMBOLS SEE FIGURE
                        ; A-3.1.
                        ;
                        ;
18A0                            ORG 18A0H
                        ;
18A0 3E01               BEGIN:  LD A, 01H
18A2 D304                       OUT (04H), A        ; OPEN CONTROL VALVE
                        ;
18A4 219118                     LD HL, DATA         ; LOAD FIRST ADDRESS OF DATA
                        ;
18A7 CDE018                     CALL DELAY          ; DELAY D1
                        ;
18AA 3E04                       LD A, 04H
18AC D305                       OUT (05), A         ; OPEN INJECTOR
                        ;
18AE CDE018                     CALL DELAY          ; DELAY D2
                        ;
18B1 3E02                       LD A, 02H
18B3 D304                       OUT (04H), A        ; REVERSE THE CURRENT
18B5 3E03                       LD A, 03H           ; DIRECTION IN THE
18B7 D304                       OUT (04), A         ; SOLENOID OF CONTROL VALVE
                        ;
18B9 CDE018                     CALL DELAY          ; DEENERGIZE THE CONTROL
18BC                                                ; VALVE SOLENOID
                        ;
18BC 3E02                       LD A, 02H
18BE D305                       OUT (05), A         ; CLOSE CONTROL VALVE
                        ;
18C0 CDE018                     CALL DELAY          ; DELAY D3
                        ;
18C3 3E08                       LD A , 08H
18C5 D305                       OUT (05), A         ; REVERSE CURRENT DIRECTION
18C7 3E0C                       LD A, 0CH           ; IN THE SOLENOID OF INJECTOR
18C9 D305                       OUT (05H), A
                        ;
18CB CDE018                     CALL DELAY          ; DEENERGIZE THE INJECTOR
18CE                                                ; SOLENOID
                        ;
18CE 3E08                       LD A , 08H
18D0 D305                       OUT (05H), A        ; CLOSE INJECTOR
                        ;
18D2 CDE018                     CALL DELAY          ; FREQUENCY ADJUSTMENT
```

```
18D5 C3A018          JP BEGIN
18D8 FF              RST 38H

1891                 ORG 1891H

AVOCET SYSTEMS Z80 ASSEMBLER -  VERSION 1.03M  SERIAL #00132

SOURCE FILE NAME: THEOPG6.ASM


1891 04         DATA    DEFB    04H
1892 C8                 DEFB    0C8H
1893 05                 DEFB    05H
1894 BA                 DEFB    0BAH
1895 03                 DEFB    03H
1896 BC                 DEFB    0BCH
1897 01                 DEFB    01H
1898 20                 DEFB    20H
1899 03                 DEFB    03H
189A BC                 DEFB    0BCH
189B 18                 DEFB    18H
189C C8                 DEFB    0C8H

18E0            DELAY   EQU     18E0H
0000                    END

AVOCET SYSTEMS Z80 ASSEMBLER -  VERSION 1.03M  SERIAL #00132

SOURCE FILE NAME: THEOPG6.ASM
---- SYMBOL TABLE ----

BEGIN    18A0           DATA     1891           DELAY    18E0

***** NO ERRORS DETECTED *****
```

```
AVOCET SYSTEMS Z80 ASSEMBLER -  VERSION 1.03M  SERIAL #00132

SOURCE FILE NAME:  THEOPG5.ASM

                ;  INTERUPT CONTROL
                ;
                ;
                ;  THIS PROGRAM, WITH INTERUPT CONTROL, IS USED FOR THE
                ;  SYNCHRONIZATION OF THE TEST ENGINE.  THE INTERUPT
                ;  SIGNAL IS OBTAINED FROM A MAGNETIC PICK-UP MOUNTED
                ;  ON THE ENGINE'S CRANK SHAFT.
                ;
                ;
1900                    ORG 1900H
                ;
1900 3E1B               LD A, 1BH
1902 ED47               LD I, A         ; LOAD INDEX REG WITH HIGH
1904                                    ;  ADDRESS BYTE.
1904 3EDD               LD A , 0DDH
1906 D300               OUT (CTC0), A   ; SET CTC TO COUNTER MODE
1908 3E01               LD A , 01H
190A D300               OUT (CTC0), A   ; SET COUNTER TO 1
190C 3EA8               LD A , 0A8H
190E D300               OUT (CTC0), A   ; LOAD CTC WITH LOW BYTE
                ;
                ;
1910 210018             LD HL, CONTROL  ; START OF SERVICE ROUTINE
1913 22A81B             LD (1BA8H), HL  ; STORE ADDRESS OF SERVICE
1916                                    ; ROUTINE AT A SPECIFIED
1916                                    ; MEMORY ADDRESS
1916 ED5E               IM2             ; INTERUPT MODE 2
1918 FB                 EI              ; ENABLE INTERUPT
                ;
1919 06FE       MAIN:   LD B, 0FEH      ; THIS IS AN INDEFINATE LOOP
191B                                    ; USED TO OCCUPY THE MICRO-
191B                                    ; PROCESSOR UNTILL AN INTER-
191B                                    ; UPT SIGNAL OCCURS.
191B 0EFE       B2:     LD C, 0FEH
191D 0D         B1:     DEC C
191E C21D19             JP NZ, B1
1921 05                 DEC B
1922 C21B19             JP NZ, B2
1925 C31919             JP MAIN
1928 FF                 RST 38H
                ;
0000            CTC0    EQU     0000H
1800            CONTROL EQU     1800H
                ;
0000                    END
```

```
AVOCET SYSTEMS Z80 ASSEMBLER -  VERSION 1.03M  SERIAL #00132

SOURCE FILE NAME: THEOPG5.ASM
---- SYMBOL TABLE ----

B1        191D     B2    191B     CONTROL  1800     CTCO     0000

***** NO ERRORS DETECTED *****
```

```
AVOCET SYSTEMS Z80 ASSEMBLER -  VERSION 1.03M  SERIAL #00132

SOURCE FILE NAME: THEOPG3.ASM

                ; SUBROUTINE "CONTROL"
                ;
                ;
                ; THIS SUBROUTINE CONTROLS THE OPENING AND CLOSING
                ; OF THE INJECTOR.
                ;
1800                    ORG 1800H
                ;
1800 219018     BEGIN:  LD HL, DATA
1803 3E04               LD A,  04H      ; SET ACCUMULATOR
1805 D305               OUT (05H), A    ; OPEN Q1
                ;
1807 CDE018             CALL DELAY      ; INJECTOR ON PERIOD
                ;
180A 3E08               LD A , 08H      ; CLOSE Q1
180C D305               OUT (05H), A
180E 3E0C               LD A , 0CH
1810 D305               OUT (05H), A    ; OPEN Q3
                ;
1812 CDE018             CALL DELAY      ; DEENERGIZE SOLENOID
                ;
1815 3E08               LD A , 08H
1817 D305               OUT (05H), A    ; CLOSE Q3
                ;
1819 CDE018             CALL DELAY      ; FREQUENCY ADJUSTMENT
                ;
181C 00                  NOP            ;OR EI (USED WITH INTERUPT CONTROL
181D 00                  NOP            ; RETI
181E C9                  RET
                ;
18E0            DELAY   EQU 18E0H
1890            DATA    EQU 1890H
181F 06BB03BC           DB  06H,0BBH,03H,0BCH,1AH,0CCH
0000                    END


AVOCET SYSTEMS Z80 ASSEMBLER -  VERSION 1.03M  SERIAL #00132

SOURCE FILE NAME: THEOPG3.ASM
 ---- SYMBOL TABLE ----

BEGIN    1800           DATA     1890           DELAY    18E0

***** NO ERRORS DETECTED *****
```

```
AVOCET SYSTEMS Z80 ASSEMBLER -  VERSION 1.03M  SERIAL #00132

SOURCE FILE NAME: THEOPG4.ASM

                ; SUBROUTINE "DELAY"
                ;
                ;
                ; THIS SUBROUTINE PROVIDES A DELAY TIME ACCORDING
                ; TO THE PARAMETERS STORED IN REGISTERS B AND C.
                ;
18E0                    ORG 18E0H
                ;
18E0 23                 INC HL
18E1 46                 LD B, (HL)    ; LOAD REG B WITH THE FIRST
18E2                                  ; DELAY PARAMETER STORED IN
18E2                                  ; MEMORY ADDRESS POINTED BY
18E2                                  ; THE HL PAIR.
18E2 23                 INC HL
18E3 4E         D2:     LD C, (HL)    ; LOAD REG C WITH THE SECOND
18E4                                  ; DELAY PARAMETER.
18E4 0D         D1:     DEC C
18E5 C2E418             JP NZ, D1
18E8 05                 DEC B
18E9 C2E318             JP NZ, D2
18EC C9                 RET
0000                    END

AVOCET SYSTEMS Z80 ASSEMBLER -  VERSION 1.03M  SERIAL #00132

SOURCE FILE NAME: THEOPG4.ASM
---- SYMBOL TABLE ----

D1          18E4            D2          18E3

***** NO ERRORS DETECTED *****
```

APPENDIX 5

NUMERICAL DATA FOR THE COMPUTER CALCULATIONS

A5.1 CONSTANTS

M_α	=	0.057	kg
M_n	=	0.027	kg
μ	=	8.8×10^{-6}	$N.S/m^2$
d_i	=	5.99×10^{-3}	m
L	=	2.00×10^{-2}	m
K_s	=	3.0×10^{5}	N/m
F_{ps}	=	618.0	N
F_r	=	0.5	N
F_e	=	164.0	N
d_{so}	=	2.5×10^{-3}	m
d_{si}	=	2.0×10^{-3}	m
d_{po}	=	9.6×10^{-4}	m
R	=	4120.42	J/kg.K
T	=	290.0	K
V_2	=	1.0×10^{-6}	m^3
V_3	=	1.1×10^{-9}	m^3
h_{max}	=	5.0×10^{-4}	m
	=	1.41	
P_1	=	2.0×10^{7}	Pa
P_4	=	1.0×10^{5}	Pa
C_d	=	0.75	
δ	=	5.0×10^{-7}	m

A5.2 INITIAL CONDITIONS

$h = 0.0$

$A_{12} = 9.0 \times 10^{-7}$ m^2

$A_{23} = 0.0$ m^2

$A_{34} = 1.667 \times 10^{-7}$ m^2

$\dot{m}_f = 0.0$ kg/s

$P_2 = P_1$ Pa

VEL= 0.0 m/s

DOSE= 0.0 kg

$P_3 = P_4$ Pa

APPENDIX 6

COMPUTER PROGRAM LISTING USED IN THE SIMULATION OF THE GAS INJECTION PROCESS

```
      PROGRAM PRESR(INPUT,OUTPUT)

C                C O N C O R D I A   U N I V E R S I T Y
C
C                F A C U L T Y   O F   E N G I N E E R I N G
C                  DEPARTMENT OF MECHANICAL ENGINEERING
C

C          SIMULATION OF AN ELECTRONICALLY CONTROLLED HYDROGEN-GAS
C          INJECTOR FOR COMPRESSION IGNITION ENGINES

C                                BY

C                      THEODORE  GIANNACOPOULOS

C          THIS WORK WAS CARRIED OUT AS PART OF THE THESIS FOR THE
C           MASTER OF ENGINEERING(MECHANICAL)
```

```
C                    N O M E N C L A T U R E

C       A12     =  FLOW AREA AT THE INLET OF INJECTOR - ( M2 )
C       A23     =  FLOW AREA AT THE NEEDLE SEAT       - ( M2 )
C       A34     =  FLOW AREA AT THE EXIT OF NOZZLE    - ( M2 )
C       AP2     =  DIFF. AREA OF NEEDLE CORRESPONDING
C                  TO THE NOZZLE CHAMBER              - ( M2 )
C       AP3     =  DIFF. AREA AT NEEDLE SEAT          - ( M2 )
C       CD      =  COEFFICIENT OF FUEL DISCHARGE      - ( -  )
C       DI      =  LARGEST NEEDLE DIAMETER            - ( M  )
C       DPO     =  PINTLE DIAMETER                    - ( M  )
C       DSO     =  NEEDLE DIAMETER AT SEAT            - ( M  )
C       DV      =  DAMPING FACTOR                     - (
C       FE      =  ELECTRICAL FORCE EXCERTED BY SOL.  - ( N  )
C       FRATE   =  FUEL DISCHARGE FLOWRATE            - ( KG/SEC )
C       FRICT   =  FORCE DUE TO FRICTION              - ( N  )
C       FPV     =  SPRING PRELOAD FORCE               - ( N  )
C       HV      =  NEEDLE LIFT                        - ( M  )
C       MV      =  MASS OF NEEDLE AND SPRING          - ( KG )
C       MS      =  MASS OF SOLENOID                   - ( KG )
C       G       =  RATIO OF SPECIFIC HEATS            - ( -  )
C       R       =  GAS CONSTANT FOR HYDROGEN          - ( J*M3/KG*K )
C       RF      =  INCEAMENT OF TIME STEP             - ( SEC )
C       P1      =  SUPPLY PRESSURE                    - ( KPA )
C       P2      =  PRESSURE IN NOZZLE CHAMBER         - ( KPA )
C       P3      =  PRESSURE UNDER NEEDLE SEAT         - ( KPA )
C       P4      =  PRESSURE IN ENGINE CYLINDER        - ( KPA )
C       T1      =  GAS TEMPERATURE                    - ( K  )
C       V2      =  VOLUME OF NOZZLE CHAMBER           - ( M3 )
C       V3      =  VOLUME BETWEEN SEAT AND PINTLE     - ( M3 )

C        DEFINE VARIABLES

        REAL            MS,MV,MT,KSV
        REAL            A2(600),A3(600),FM(600),DOSE(600)
        REAL            Z(4),C(24),W(4,9),X,TOL
        REAL            TIME(600),PR2(600),PR3(600),YV(600),VEL(600)
        COMMON/PARAM1/  PA,PB,PC,PD,T1,G,U,B,R,HV,HVI
        COMMON/PARAM2/  MT,DV,KSV,FPV,RV,FEV,CD,HMAX,W1,W2
        COMMON/PARAM3/  TON,TOL,IND,C,NW,IER,I1,I2,I3
        COMMON/PARAM4/  P2,P3,T2,V2,V3,RF,J,JJ,KK,M,MAX
        COMMON/AREA/    A12,A23,A34,AP2,AP3,FPO,FRATE
```

```
C       SET CONSTANTS

                FRICT = 0.05
                FE    = 164.00
                MS    = 0.0569657
                MV    = 0.0272206
                CD    = 0.75000
                MIU   = 0.00000880
                L     = 0.02000000
                DELTA = 0.00000050
                KSV   = 300000.0
                FPV   = 618.0
                RV    = FRICT
                FEV   = FE
                DI    = 0.005990
                DSO   = 0.002490
                DPO   = 0.000910
                PI    = 3.141592654
                T1    = 290.0
                MIN   = 100
                JK    = 1200
                JJ    = 400
                KK    = 1
                P1    = 20.0
                P4    = 0.10
                V2    = 1.00E-6
                V3    = 1.10E-9
                RF    = 0.000000025
                HVI   = 0.00012
                HMAX  = 0.50000
                HV    = HVI + 0.01988
                A12   = 0.0000009000
                A23   = 0.0
                A34   = 0.0000001667
                FRATE = 0.0
                N     = 4
                NW    = 4
                J     = 1
                X     = 0.0
                TON   = 0.0
                TOL   = 0.0001

C       INITIAL CONDITIONS

                T2    = T1
                P2    = P1
                P3    = P4
                PA    = 1000000.0*P1
                PB    = 1000000.0*P2
                PC    = 1000000.0*P3
```

```
            PD      = 1000000.0*P4

            MT      = MS + MV
            W1      = 0.0066240
            W2      = 14.2045
            FI      = PI*DI**2/4
            FSO     = PI*DSO**2/4
            FPO     = PI*DPO**2/4
            AP2     = FI - FSO
            AP3     = FSO - FPO

            Z(1)    = 0.0
            Z(2)    = HV/1000.0
            Z(3)    = PB*V2/T2
            Z( )    = PC*V3/T2

             R      = 4120.42
             G      = 1.41
      GCONST=(2/(G+1))**((G+1)/(G-1))
      BX =   (G/R)*GCONST
      B   = SQRT(BX)
          XU = (G-1)*GCONST/2
          U = SQRT(XU)
            M      = JK*MIN
            MAX    = 2*(M/JJ)
            A2(KK)  = 1000000.0*A23
            A3(KK)  = 1000000.0*A34

            TIME(KK)  = 1000.0*X
            PR2(KK)   = P2
            PR3(KK)   = P3
            YV(KK)     = HV
            FM(KK)     = 1000.0*FRATE
            DOSE(KK)   = 0.0
        PRINT 200
200     FORMAT(1H1)

            I1 = 0
            I2 = 0
            I3 = 0


C       SUBROUTINE VALVE IS CALLED TO SIMULATE THE OPENING
C       OF THE INJECTOR.

         CALL VALVE(N,X,Z,W,TIME,YV,VEL,PR2,PR3,A2,A3,FM,DOSE)
           IF(HV .GT. HMAX) THEN
               HV = HMAX
               Z(2) = HV/1000.0
            ELSE
            END IF
```

```
            MJK = 1000

C     PREPARE FOR CLOSING OF THE INJECTOR

            JKX = 320
            RV  = -1.00*FRICT
            FE  =  FE + 46.0

          DO 40 LL=1,3
           JK = LL*JKX
           IF(JK .GT. 900) THEN
             JK = JKX + 40
             FEV = 0.40*FE
           ELSE
            IF(LL .GT. 1) THEN
             JK  = JKX/2
              FEV = 0.89*FE
             ELSE
             JK  = JKX
              FEV = FE
            END IF
           END IF

            X = 0.0
            TON  = TIME(KK)
            M  = JK*MIN
            I1 = 0
            I2 = 0
            I3 = 2


C     SUBROUTINE VALVE IS NOW CALLED TO SIMULATE THE
C     CLOSING OF THE INJECTOR

          CALL VALVE(N,X,Z,W,TIME,YV,VEL,PR2,PR3,A2,A3,FM,DOSE)
 40         CONTINUE


C     FUEL  IS THE TOTAL FUEL DOSE INJECTED

            FUEL  = DOSE(KK)


C     PRINT RESULTS


            PRINT 21, P1,P2,P3,V2,V3
 21         FORMAT(1H0,/5X,'PROBLEM PARAMETERS:   P1 =',F7.3,' MPA',5X,
     + 'P2 =',F7.3,' MPA',3X,'P3 =',F7.3,' MPA'//27X,
```

```
     + 'V2 =',E9.3,' M3',5X,'V3 =',E9.3,' M3'
     +  /////25X,'R E S U L T S'//)
        PRINT 30
  30   FORMAT(1H0,2X,'TIME',4X,'PR2',5X,'PR3',5X,'HV',
     +  5X,'VEL',4X,'A2',5X,'A3',5X,'FLOW',4X,'DOSE'/2X,
     +  '(MSEC)',2X,'(MPA)',3X,'(MPA)',3X,'(MM)',2X,'(MM/MS)',
     +  1X,'(MM2)',2X,'(MM^)',1X,'(MGR/MS)',1X,'(MGR)')

        DO 500 II=1, KK
          PRINT 31, TIME(II),PR2(II),PR3(II),YV(II),VEL(II),
     + A2(II),A3(II),FM(II),DOSE(II)
  31    FORMAT(1H0,2X,F4.2,2X,F6.3,2X,F6.3,2X,F5.3,2X,F5.3,
     + 3X,F5.3,1X,F5.3,2X,F6.3,2X,F6.3)
  500   CONTINUE

        FLVOL  =  (FUEL*R*T1)/100000.0
            PRINT 32, FUEL, FLVOL
  32        FORMAT(1H0,/10X,'FUEL DOSE(MGRAMS)  =',F7.2//7X,
     + 'OR FUEL DOSE(MLITERS) =',F7.2)
          STOP
        END
```

```
      SUBROUTINE VALVE(N,X,Z,W,TIME,YV,VEL,PR2,PR3,A2,A3,FM,DOSE)

C     THIS SUBROUTINE SIMULATES THE OPENING AND CLOSING
C     OF THE INJECTOR. THE SOLUTION OF THE SYSTEM OF
C     EQUATIONS IS PERFORMED BY A FIRST ORDER DIFFERANTIAL
C     EQUATION SOLVER, CALLED DVERK, WHICH IS AVAILABLE FROM THE
C     INTERNATIONAL MATHEMATICAL AND STATISTICAL LIBRARY (IMSL).
C     THIS SOLVER CONSISTS OF A PAIR OF A FIFTH AND SIXTH
C     ORDER RUNGE-KUTTA FORMULAS.


      EXTERNAL FCN

        REAL            A2(MAX),A3(MAX),FM(MAX),DOSE(MAX)
        REAL            Z(N),C(24),W(N,9),X,TOL,XEND
        REAL            TIME(MAX),PR2(MAX),PR3(MAX),YV(MAX),VEL(MAX)
        COMMON/PARAM1/  PA,PB,PC,PD,T1,G,U,B,R,HV,HVI
        COMMON/PARAM /  TON,TOL,IND,C,NW,IER,I1,I2,I3
        COMMON/PARAM4/  P2,P3,T2,V2,V3,RF,J,JJ,KK,M,MAX
        COMMON/AREA/    A12,A23,A34,AP2,AP3,FPO,FRATE

          IER = 0
          IND = 2
          DO 5 I=1,N
             DO 6 II=1,9
               W(I,II) = 0.0
               C(II)   = 0.0
6            CONTINUE
5         CONTINUE
          C(1) = 1.0
        DO 10 K=1, M
        XEND = RF*FLOAT(K)

        IF(I1 .GT. 0 .AND. I2 .GT. 0) THEN

            X = XEND
        ELSE
      CALL DVERK(N,FCN,X,Z,XEND,TOL,IND,C,NW,W,IER)
          IF(IND .LT. 0 .OR. IER .GT. 0) GO TO 50
        PB = (T2*Z(3))/V2
        PC = (T2*Z(4))/V3
        P2 = PB/1000.0
        P3 = PC/1000.0
        END IF
           IF(J .LT. JJ) THEN
              J = J + 1
           ELSE
            L          = KK
            KK         = KK + 1
            TIME(KK)   = 1000.0*X + TON
```

```
            PR2(KK)   = P2/1000.0
            PR3(KK)   = P3/1000.0
            YV(KK)     = HV
            VEL(KK)   = Z(1)
            A2(KK) = 1000000.0*A23
            A3(KK) = 1000000.0*A34
            FM(KK) = 1000.0*FRATE
      DOSE(KK) = DOSE(L)+(FM(KK)+FM(L))*(TIME(KK)-TIME(L))/2.0
         J = 1

       IF(I3 .LT. 1) THEN

        DVEL = ABS(VEL(KK) - VEL(L))
        DPR2 = ABS(PR2(KK) - PR2(L))
          IF(DVEL .LT. TOL) THEN
            I1 = 1
          ELSE
            I1 = 0
          END IF

          IF(DPR2 .LT. 0.001) THEN
            I2 = 1
          ELSE
            I2 = 0
          END IF

       ELSE
         I1 = 0
         I2 = 0
       END IF

       END IF
 10    CONTINUE
       GO TO 100
50     CONTINUE
       PRINT 40, IND,IER,XEND
40   FORMAT(1H0,5X,'ERROR: IND.LT. OR IER.GT.0   IND =',I2,
    65X,'IER =',I3,5X,F8.5)
       PRINT 41, Z(K), W(1,K), X
41   FORMAT(1H0,3X,'Z=',F6.2,3X,'W=',F10.8,3X,'X=',F4.1)
       STOP

 100   CONTINUE
       RETURN
       END
```

```
      SUBROUTINE FGN(N,X,Z,ZPRIME)

C     THIS SUBROUTINE CONTAINS THE SYSTEM OF THE
C     DIFFERENTIAL EQUATIONS WHICH DESCRIBE THE
C     MATHEMATICAL MODEL AND IT IS CALLED BY DVERK
C     EVERY TIME A NEW APPROXIMATION IS REQUIRED TO
C     BE CALCILATED.

      INTEGER N
      REAL Z(N),ZPRIME(N),X,N12,N23,N34,C23,C34
      REAL MT,KSV
      COMMON/PARAM1/ PA,PB,PC,PD,T1,G,U,B,R,HV,HVI
      COMMON/PARAM2/ MT,DV,KSV,FPV,RV,FEV,CD,HMAX,W1,W2
      COMMON/AREA/   A12,A23,A34,AP2,AP3,FPO,FRATE

C     CALCULATION PARAMETERS N12,N23,N34,C23 AND C34

      I = 1
        PRATIO = PA/PB
      N12 = PARN(PRATIO,G,U,PB,I)
      I = 2
        PRATIO = PB/PC
      N23 = PARN(PRATIO,G,U,PB,I)
      C23 = PRATIO*N23
      I = 3
        PRATIO = PC/PD
      N34 = PARN(PRATIO,G,U,PC,I)
      C34 = PRATIO*N34
      HV  = 1000.0*Z(2)

C     CALCULATION OF FLOW AREAS

      A23 = CD*(0.[illegible]*HV**2 + 3.14159*HV)/1000000.0
      IF(HV .LT. 0.29000) THEN
          A34 = 0.00000003234*CD
        ELSE
          C1 = 0.68017
          C2 = 1.55509
          C3 = 0.03555
          S  = 0.29580

      A34 = CD*(C1*(HV-S)**2+C2*(HV-S)+C3)/1000000.0
      END IF
```

```
        F2 = PB*AP2 + PC*AP3 + PD*FPO

      IF(A23 .LT. 0.0) THEN
        PRINT 20, HV,A23,A34
20      FORMAT(1H0,2X,'ERROR IN FCN',2X,'HV=',E10.4,2X,
     + 'A23=',E10.4,2X,'A34=',E10.4)
        STOP
       ELSE
        IF(HV .GE. HVI  .AND.  HV .LE  HMAX) THEN
          F1 = KSV*Z(2) + FPV + RV
        ELSE
          F1   = KSV*Z(2) + FPV + RV
          Z(1) = 0.0
        END IF


C     CALCULATION OF THE DERIVATIVES


      ZPRIME(1) = (W1*(W2 - Z(1))-F1+FEV+F2)/MT
      ZPRIME(2) = Z(1)
      ZPRIME(3) = B*R*(PA*A12*N12-PC*A23*C23)/(SQRT(T1))
      ZPRIME(4) = B*R*(PB*A23*N23-PD*A34*C34)/(SQRT(T1))

        END IF
        FRATE = (B*PC*A34*N34)/(SQRT(T1))
      RETURN
      END
```

```
      FUNCTION PARN(PRATIO,G,U,PB,I)

C     THIS FUNCTION DETERMINES WHETHER THE GAS FLOW
C     THROUGH THE INJECTOR ORIFICE IS "CHOKED" OR
C     "UNCHOCHED" ACCORDING TO THE DOWN STREAM TO
C     UP STREAM PRESSURE RATIO.

        PR = 1.0/PRATIO
        XPARN=(PR**(2/G)-PR**((G+1)/G))
      IF(XPARN .LT. 0.0) THEN
           PARN = 0.0
           PRINT 5, PRATIO,XPARN,PB,I
5     FORMAT(1H0,2X,'PRATIO=',E16.10,2X,'XP=',E9.3,
     6  2X,'PB=',E15.9,1X,'I=',I1)
        STOP
        ELSE
      IF(PRATIO .GT. 1.880) THEN
        PARN = 1.00
        ELSE
          PARN = (SQRT(XPARN))/U
        END IF
      END IF
        RETURN
        END
```